

## INFORMATION TO USERS

This dissertation was produced from a microfilm copy of the original document. While the most advanced technological means to photograph and reproduce this document have been used, the quality is heavily dependent upon the quality of the original submitted.

The following explanation of techniques is provided to help you understand markings or patterns which may appear on this reproduction.

1. The sign or "target" for pages apparently lacking from the document photographed is "Missing Page(s)". If it was possible to obtain the missing page(s) or section, they are spliced into the film along with adjacent pages. This may have necessitated cutting thru an image and duplicating adjacent pages to insure you complete continuity.
2. When an image on the film is obliterated with a large round black mark, it is an indication that the photographer suspected that the copy may have moved during exposure and thus cause a blurred image. You will find a good image of the page in the adjacent frame.
3. When a map, drawing or chart, etc., was part of the material being photographed the photographer followed a definite method in "sectioning" the material. It is customary to begin photoing at the upper left hand corner of a large sheet and to continue photoing from left to right in equal sections with a small overlap. If necessary, sectioning is continued again — beginning below the first row and continuing on until complete.
4. The majority of users indicate that the textual content is of greatest value, however, a somewhat higher quality reproduction could be made from "photographs" if essential to the understanding of the dissertation. Silver prints of "photographs" may be ordered at additional charge by writing the Order Department, giving the catalog number, title, author and specific pages you wish reproduced.

### **University Microfilms**

300 North Zeeb Road  
Ann Arbor, Michigan 48106

A Xerox Education Company

72-23,094

FISHER, Cary Andrew, 1941-  
DYNAMIC BUCKLING OF AN AXIALLY COMPRESSED  
CYLINDRICAL SHELL WITH DISCRETE RINGS AND  
STRINGERS.

The University of Oklahoma, Ph.D., 1972  
Engineering, mechanical

University Microfilms, A XEROX Company, Ann Arbor, Michigan

THE UNIVERSITY OF OKLAHOMA

GRADUATE COLLEGE

DYNAMIC BUCKLING OF AN AXIALLY COMPRESSED CYLINDRICAL  
SHELL WITH DISCRETE RINGS AND STRINGERS

A DISSERTATION

SUBMITTED TO THE GRADUATE FACULTY

in partial fulfillment of the requirements for the

degree of

DOCTOR OF PHILOSOPHY

BY

CARY A. FISHER

Norman, Oklahoma

1972

DYNAMIC BUCKLING OF AN AXIALLY COMPRESSED CYLINDRICAL  
SHELL WITH DISCRETE RINGS AND STRINGERS

APPROVED BY

*C. N. Bert*

*F. J. Appel*

*Wm. E. Gale*

*R. F. Thayer*

*David C. Kay*

DISSERTATION COMMITTEE

PLEASE NOTE:

Some pages may have

indistinct print.

Filmed as received.

University Microfilms, A Xerox Education Company

## ACKNOWLEDGMENT

Without the enthusiastic guidance of Dr. Charles W. Bert, this dissertation would not have become a reality. Dr. Bert suggested the original idea as a topic of practical as well as academic interest. Despite his very busy schedule, he was always available for advice and comment on every facet of this work. It has been a pleasure working under his guidance.

Dr. Davis M. Egle contributed many valuable suggestions concerning the writing of the computer program, particularly the use of the coefficient algorithm documented in Section 2.6.

Dr. Richard F. Maye was instrumental in demonstrating the mathematical "idiosyncrasies" of the Dirac delta function. In addition, his general suggestions were of great value, especially during the derivation of the governing equations contained in Appendix A.

Dr. Franklin J. Appl contributed many valuable suggestions regarding the buckling of structures in general, and the use of the Galerkin procedure in studying buckling of columns.

As the committee member from the Department of Mathematics, Dr. David C. Kay provided valuable criticism on the reading and final copies of this dissertation.

Special thanks goes to Professor Karl Bergey, who provided insights into how light aircraft are actually constructed. He was instrumental in obtaining aircraft production drawings, and in arranging

several meetings with FAA personnel on the subject of crashworthiness.

The personnel of the various aircraft companies which were contacted also deserve special thanks. They provided detailed aircraft production drawings which were used as a basis for modeling a representative aircraft structure. They are:

Mr. Fred Strickland	Piper Aircraft Corporation
Mr. Don P. Zurfluh	Lock Haven, Pennsylvania
Mr. Jack Simmonds	Piper Aircraft Corporation
	Vero Beach, Florida
Mr. Jerry Gerteis	Cessna Aircraft Corporation
Mr. A. L. Asher	Wichita, Kansas
Mr. Chet Rembleske	Beech Aircraft Corporation
	Wichita, Kansas
Mr. R. D. Christian	Aero Commander
Mr. T. W. Lindsay	Bethany, Oklahoma

Finally, this work is dedicated to my wife, Betsy. Her constant encouragement, patience, and enthusiasm have been extraordinary, especially after editing and typing numerous manuscript drafts for this dissertation.

## TABLE OF CONTENTS

	Page
ACKNOWLEDGMENT . . . . .	iii
LIST OF TABLES . . . . .	vii
LIST OF ILLUSTRATIONS. . . . .	viii
LIST OF SYMBOLS. . . . .	ix
CHAPTER	
I. INTRODUCTION . . . . .	1
1.1 Survey of Shell Buckling. . . . .	1
1.2 Research Objectives . . . . .	10
II. FORMULATION OF THEORY. . . . .	12
2.1 Method of Analysis. . . . .	12
2.2 Hypotheses. . . . .	13
2.3 Prebuckling Equations . . . . .	15
2.4 Buckling Equations. . . . .	16
2.5 Application of Galerkin's Method. . . . .	17
2.6 Numerical Solution. . . . .	21
III. EVALUATION OF THEORY . . . . .	25
3.1 Comparison with Static Buckling . . . . .	25
3.2 Comparison with Dynamic Buckling. . . . .	27
IV. RESULTS. . . . .	31
4.1 Representative Aircraft Structure . . . . .	31
4.2 Dynamic Considerations. . . . .	38
4.3 Geometric Considerations. . . . .	42
4.4 Discreteness Considerations . . . . .	53
V. CLOSURE. . . . .	58
REFERENCES . . . . .	60

TABLE OF CONTENTS (Cont'd.)

APPENDICES

A.	DERIVATION OF KINETIC AND POTENTIAL ENERGIES OF A DISCRETELY STIFFENED CYLINDRICAL SHELL . . . . .	66
A.1	Nonlinear Strain Displacement Formulation. . . . .	66
A.2	Unstiffened Cylinder Strain Energy . . . . .	66
A.3	Ring Strain Energy . . . . .	69
A.4	Stringer Strain Energy . . . . .	70
A.5	External Load Potential Energy . . . . .	70
A.6	Total Potential Energy . . . . .	71
A.7	Total Kinetic Energy . . . . .	71
B.	APPLICATION OF HAMILTON'S PRINCIPLE TO DERIVE THE EQUATIONS OF MOTION. . . . .	72
C.	APPLICATION OF GALERKIN'S METHOD TO OBTAIN A SET OF ORDINARY NONLINEAR GOVERNING DIFFERENTIAL EQUATIONS. . . . .	78
D.	COMPUTER PROGRAM DOCUMENTATION. . . . .	88
E.	COMPUTER PROGRAM LISTING. . . . .	93

## LIST OF TABLES

Table	Page
2.1 Coefficient Algorithm. . . . .	24
3.1 Comparison of Smeared and Discrete Terms . . . . .	25
4.1 Representative Light Aircraft Geometry . . . . .	32
C.1 Integrated Terms from Axial Equation of Motion . . . . .	79
C.2 Integrated Terms from Circumferential Equation of Motion. . . . .	81
C.3 Unstiffened Cylinder Integrated Terms from Radial Equation of Motion. . . . .	82
C.4 Ring Integrated Terms from Radial Equation of Motion . .	84
C.5 Stringer Integrated Terms from Radial Equation of Motion. . . . .	85

## LIST OF ILLUSTRATIONS

Figure	Page
3.1 Static Buckling Comparison. . . . .	28
3.2 Dynamic Buckling Comparison, Unstiffened Shell. . . . .	30
4.1 General Aircraft Fuselage . . . . .	35
4.2 Comparison of Buckling Load for Different Cylinder Regions. . . . .	37
4.3 Maximum Radial Deflection Versus Time for Various End Loads, $n = 9$ . . . . .	41
4.4 Maximum Radial Deflection Versus Time for Various End Loads, $n = 10$ . . . . .	43
4.5 Buckling Load Versus Time Duration, $n = 9$ . . . . .	44
4.6 Axial Force Versus Wave Number with Increasing Number of Stringers . . . . .	45
4.7 Influence of Number of Stringers on Buckling Load . . .	46
4.8 Axial Force Versus Wave Number for Different Ring Spacing, Subshell III. . . . .	48
4.9 Axial Force Versus Wave Number for Different Ring Spacing, Subshell I. . . . .	49
4.10 Influence of Number of Rings on Buckling Load . . . . .	50
4.11 Influence of Stiffener Eccentricity on Buckling Load. .	52
4.12 Convergence of Solution, Subshell I . . . . .	55
4.13 Convergence of Solution, Subshell II. . . . .	56
A.1 Shell Geometry. . . . .	67
D.1 Computer Program Flow Chart . . . . .	92

## SYMBOLS

A	Stiffener cross-sectional area (in. <sup>2</sup> )
d	Stringer center-to-center spacing (in.)
D	Bending stiffness (in.-lb.)
$\bar{e}$	Distance from shell middle surface to line where $\hat{N}_x$ acts (in.)
E	Young's modulus (psi)
$\bar{F}$	Nondimensional buckling load, $\bar{F} = \hat{N}_x R / Eh^2$
g	Time step
G	Shear modulus (psi)
h	Unstiffened shell wall thickness (in.)
i	Integer
I	Moment of inertia of stiffener about its centroid (in. <sup>4</sup> )
$I_0$	Moment of inertia of stiffener about shell middle surface (in. <sup>4</sup> )
$I_i$	$\equiv im\pi/L$ (in. <sup>-1</sup> )
$I_j$	$\equiv im\pi j\ell/L$ (dimensionless)
$I_\zeta$	$\equiv \zeta m\pi j\ell/L$ (dimensionless)
j	Integer
J	Polar moment of inertia (in. <sup>4</sup> )
$J_j$	$\equiv jn/R$ (in. <sup>-1</sup> )
$J_k$	$\equiv jnk d/R$ (dimensionless)
$J_\xi$	$\equiv \xi nk d/R$ (dimensionless)
k	Integer

$\ell$	Ring center-to-center spacing (in.)
L	Shell length (in.)
m	Number of half-waves in axial direction
M	Number of stringers on cylinder
$M_x, M_y, M_{xy}$	Middle-surface moment resultants
n	Number of waves in circumferential direction
N	Number of rings on cylinder
$N_x, N_y, N_{xy}$	Middle-surface stress resultants
$\hat{N}_x$	Externally applied axial load resultant (positive in comp.)
Q	Galerkin "error functions"
r	Subscript referring to ring quantities
R	Radius of cylinder middle surface (in.)
s	Subscript referring to stringer quantities
t	Time (sec)
u,v,w	Displacements in axial, circumferential, and radial directions
U	Strain energy (in.-lb.)
W	Dependent variable used in Runge-Kutta algorithm
$\bar{W}$	Dimensionless radial deflection of shell middle surface, $\bar{W} = w/w_{\text{initial}}$
x,y,z	Circular cylindrical coordinates with origin lying in middle surface of shell and oriented in the axial, circumferential, and radial directions, respectively
$\bar{z}$	Distance from centroid of stiffener to shell middle surface (in.)
Z	Batdorf parameter, $Z = L^2(1-\nu^2)/(Rh)$
$\delta_{ij}$	Kroneker delta
$\delta(x-j\ell)$	Dirac delta function

$\Delta_1$	$\delta_{i\zeta} \delta_{j\xi}$ (Double Kroneker delta)
$\Delta_2$	$\delta_{i\zeta} \delta_{3j\xi}$
$\Delta_3$	$\delta_{3i\zeta} \delta_{j\xi}$
$\Delta_4$	$\delta_{3i\zeta} \delta_{3j\xi}$
$\Delta_5$	$\delta_{2i\zeta} \delta_{2j\xi}$
$\epsilon_x, \epsilon_y, \gamma_{xy}$	Axial, circumferential and shear strains of shell middle surface
$\zeta$	Integer
$\nu$	Poisson's ratio
$\xi$	Integer
$\rho$	Density (lb-sec <sup>2</sup> /in. <sup>4</sup> )
$\sigma_x, \sigma_y, \tau_{xy}$	Axial, circumferential and shear stresses
$\sum_j$	Indicates $\sum_{j=1}^N$
$\sum_k$	Indicates $\sum_{k=1}^M$
$\sum \sum$	Indicates $\sum_{i=1}^{\infty} \sum_{j=1}^{\infty}$

A subscript preceded by a comma indicates partial differentiation with respect to the subscript.

Primes indicate total derivatives with respect to x.

DYNAMIC BUCKLING OF AN AXIALLY COMPRESSED CYLINDRICAL  
SHELL WITH DISCRETE RINGS AND STRINGERS

CHAPTER I

INTRODUCTION

1.1 Survey of Cylindrical Shell Buckling

For the past decade, the aerospace and defense industry has been actively involved in studying the structural response of high-performance aircraft and missiles to blast-induced loadings. However, the structural response of a light aircraft (in the general aviation fleet) subjected to a crash loading has been largely ignored. Apparently, there are no current studies directed toward understanding the structural response of such aircraft to crash loadings. There are several reasons cited for this lack of analytical effort. These reasons are research cost, great variation in design of aircraft in the general aviation fleet, complexity of the crash-loading time-history delivered to the aircraft structure, and the lack of a procedure to treat the dynamic response of a complex structure.

The design of a more crashworthy aircraft will undoubtedly receive greater emphasis in the near future. In a recent article appearing in Time magazine [1], the high accident rate of the nation's 3,200 "third level" carriers was discussed. These include air taxis and commuter lines that usually fly smaller planes such as Cessna, Piper, Beechcraft and the like. According to Time, "last year 106

people died in third-level crashes. The accident death rate for every 100,000 hours flown is 1.31 for the third-levels, as compared with 0.09 for the nation's eleven first level trunk carriers and nine regionals." This high accident rate was further documented in a FAA report [2] which claimed that the death rate for general aviation is seven times that of automobiles. While many of these accidents could be avoided by improved procedures, many of the fatalities could probably have been avoided by an aircraft designed to withstand a certain level of crash loading.

At the present time, crash impact loading is not considered in the design of light aircraft. The problem is understandably complex, due to the great number of unknowns, and the lack of any controlled experimental data. However, the problem should be manageable if the structure is broken down into representative elements and if the crash loading is simplified. After the response of a representative element is correctly modeled and understood, a more rational design could perhaps be proposed to resist the effects of crash loading on the structure.

As a point of departure, the basic structural element of a light aircraft is assumed to be a thin cylinder, internally stiffened by both stringers and rings (bulkheads). One typical loading to be expected in a crash would be a suddenly applied axial compression loading of short to medium duration. If one could mathematically model the dynamic behavior of a stiffened cylinder to such a loading, one could then begin to rationally design a "crashworthy" aircraft.

Beginning first with the static axial buckling studies of unstiffened thin-walled cylinders, one is impressed by the incredible

number of papers written over the past several decades on this subject alone. This fact is due in large part to the serious discrepancies between theory and experiment. Two authors who have provided extensive bibliographies on this subject are Hoff [3] and Stein [4].

The so-called classical linear buckling theory was probably first formulated by Timoshenko [5]. In this theory, effects due to nonlinear prebuckling and initial imperfections are neglected. Unfortunately, experimental results range from twenty per cent to eighty per cent of the values predicted by this linear small deflection theory. Investigators have attempted to resolve this discrepancy by including in their analysis one or more of the following general effects: in-plane boundary conditions, nonlinear prebuckling, nonlinear postbuckling and initial imperfections.

Apparently, the first effects considered were initial imperfections and nonlinear postbuckling. In 1934 Donnell [6] proposed a nonlinear finite-deflection theory, together with a consideration of initial imperfections present in the thin-walled cylinder. This theory was modified and refined by numerous authors including von Kármán and Tsien [7], Kempner [8], and Almroth [9]. In order to answer questions of convergence of various solutions in the postbuckling range, Hoff [10] solved the large displacement equations using a radial displacement expression containing 1100 terms. It should be noted, however, that all authors have implicitly ignored exact satisfaction of some boundary conditions. This is partly due to the nonlinear terms in the boundary conditions arising from the nonlinear strain-displacement relations. Hoff [10] stated that the assumption of  $L/R > 1$  makes it possible

Filmed as received  
without page(s) 4.

UNIVERSITY MICROFILMS.

In-plane boundary conditions can play a significant role in obtaining theoretical buckling loads lower than the classical value. This has been pointed out by numerous authors [3,15-17]. Apparently, Hoff [3] was one of the first to document four different sets of boundary conditions which could be identified as "simple-support boundary conditions". Experiments performed in the ordinary tension-compression testing machine could be represented by several of these sets, depending upon the friction between testing machine and test specimen.

It is now generally agreed that, given a realistic set of boundary conditions, the main reason that theory and experiment did not agree in the past was due to initial imperfections in the test cylinder. The agreement obtained between theoretical (linear) results for a perfect shell with correct boundary conditions and experimental results from very nearly perfect specimens indicate the validity of the linear theory [19,20].

Theoretical buckling predictions for stiffened cylinders have not shown the wide disparity with experimental results that their unstiffened counterparts have shown. However, numerous authors have investigated the effects of in-plane boundary conditions, nonlinear prebuckling, and initial imperfections. Nonlinear prebuckling deformations have been shown to have only a small effect on the buckling load of stiffened cylinders [16,21-24]. The effect of in-plane boundary conditions on the buckling load of stiffened cylinders has also been investigated [16]. As before, the choice of in-plane simple support boundary conditions can make a difference on the magnitude of the buckling load.

However, as noted in reference [16], the influence of in-plane boundary conditions diminishes for internally stiffened shells with increasing values of stiffener eccentricity and area. Of course, a light-aircraft structure would have internally located stiffeners.

As in the unstiffened case, initial imperfections can make a considerable difference in the experimentally determined buckling load of stiffened cylinders. The bulk of this research has been conducted using the imperfection sensitivity concepts first introduced by Koiter [25] and expanded by numerous authors [26-30]. However, as pointed out by reference [24], the predicted regions of large imperfection sensitivity shift from one study to another, and have not been verified by experiment. Also, the predicted sensitivities appear to depend strongly on quantities such as torsional stiffness of stiffeners, which only slightly affect the classical buckling load [32]. Fortunately, the studies have shown that an internally stiffened shell is relatively imperfection insensitive, whereas an externally stiffened shell is imperfection sensitive [29,30].

The importance of two other effects, stiffener eccentricity and stiffener discreteness, have been explored by numerous investigators of stiffened shells. The stiffener eccentricity or one-sidedness has a significant effect on the buckling strength, as demonstrated in various ways by many authors [32-40]. Stiffener discreteness was shown by Block, *et al.* [21] to have a significant effect on the buckling load, even for structures with many stiffeners. Block [21] used a finite difference approach and considered discrete rings only. His conclusion is in direct contrast with Singer's concluding remark in reference [41]

that "in ring stiffened shells under axial compression, the discreteness effect is always very small." Singer used a linear Donnell theory, and treated the stiffeners as linear discontinuities represented by the Dirac delta function. Despite the disagreement as to the importance of stiffeners in most light-aircraft, both stiffener eccentricity and discreteness should be included.

Linear buckling theory has been used by nearly all investigators in their study of stiffened cylinder buckling, primarily because stiffeners are closely spaced in most aerospace applications. However, as demonstrated by reference [43], linear theory is only applicable when the stiffeners are closely spaced. Again, this will not be the case for the light-aircraft structure considered in this study.

This problem of static buckling of stiffened and unstiffened cylinders has been extensively researched over the past 60 years. By contrast, dynamic buckling of axially loaded cylinders has been studied only for the past 15-20 years, and the amount of published work is only a small fraction of its static buckling counterpart.

The first studies were primarily experimental and phenomenological in nature. Some of the earliest work was published by Schmidt [44] and Coppa [45]. Both experimenters considered only unstiffened cylinders.

One of the first analytical treatments of dynamic buckling is credited to Volmir [48]. In 1957, he investigated the buckling of a shallow circular cylindrical panel subjected to a rapidly applied axial load. He used the large deflection shell equations (generally attributed to Donnell) and reduced them to equations in time only, using a

Galerkin procedure. By making certain restrictions on the time-dependent coefficients of the assumed radial deflection function, the system of equations was reduced to a single equation, which was then solved numerically. The final results were presented in the form of dimensionless axial load versus time. A closely related study was one by Agamirov and Volmir [47]. As in all subsequent work, both the longitudinal and circumferential inertia were neglected.

In 1962, using essentially the same procedure as Volmir used, Coppa and Nash [48] studied the dynamically loaded thin cylinder. They used a two-term Galerkin procedure, in which the terms approximated the familiar diamond buckle shape. Rotatory and axial inertia terms were neglected. The assumed two-term solution contained a guess as to the axial and circumferential buckle wavelength. The procedure was repeated over a range of axial and circumferential wavelengths to find the combination that gave the lowest buckling load. A constant rate of axial end shortening was used as the dynamic loading mechanism. Only qualitative correlations with related experiments were made.

In 1964 Roth and Klosner [49] studied the same problem previously investigated by Coppa and Nash. Roth and Klosner constructed appropriate kinetic and potential energy relations. They used the middle-surface nonlinear strain-displacement relations for thin circular shells which was based on the work of Donnell [6]. Applying Hamilton's principle, they derived the equations of motion and appropriate boundary conditions. Next, they rewrote their governing equations of motion using an Airy-type stress function, and obtained the same equations as Coppa and Nash. Using a four-term radial-deflection function,

together with the Galerkin procedure, they reduced their problem to a set of four ordinary nonlinear differential equations. This final set was solved using Runge-Kutta procedures. As is the case with all prior large deflection theories, the assumed deflection modes did not exactly satisfy all of the boundary conditions. Also, no correlations with any experiments were made.

Lindberg [50] used a linear, small-deflection theory instead of a large deflection theory, to calculate the growth of normal modes of cylinders under axial impact. An inspection of Lindberg's experimental setup quickly reveals that he was using an impulsive rather than a step function loading. His shells were free at the end opposite the impact end. As a result, the compressive impact stress had a duration (at the impact end), which at most was equal to the transit time of the longitudinal stress wave up and down the shell.

In a recent dissertation, Howell [51] studied the transient response of stiffened cylinders to an impact load. He used a linear theory and smeared the effect of the stiffeners over the cylinder surface. However, he applied the impact to a point on the cylinder surface between stringers rather than to the ends of the cylinder. Also, his time duration of loading and subsequent transient response measurements indicate a wave propagation-type of study rather than a buckling analysis.

The amount of experimental data on the dynamic buckling of unstiffened shells, other than very early work [44,45], has been sparse. The most recent was that of Tennyson [52]. To date, no experimental data on the dynamic buckling of stiffened cylindrical shells have been found.

The influence of damping on the dynamic stability of shells has been investigated recently by several authors. Mescall and Tsui [53] found that damping always increased the critical dynamic buckling load for the thin cylinders, cones, and spheres considered in their analysis. Consequently, it should be expected that a dynamic buckling analysis that neglected damping would yield conservative results.

## 1.2 Research Objectives

The major objective of this research is to develop a dynamic buckling analysis capable of predicting the dynamic response and buckling load of a stiffened, thin, circular cylindrical shell under the action of a suddenly applied step axial-loading pulse. This pulse will be similar to that experienced by a light aircraft during a crash on take-off or landing. The cylinder will be stiffened with widely spaced rings and stringers, which will be representative of modern light-aircraft fuselage structures. The stiffeners will be considered as discrete elements with eccentricity due to their internal location.

In order to accomplish the research objectives it has been necessary to devise a number of new approaches and methods. The following specific original contributions are noted:

1. The first discretely stiffened cylinder buckling analysis in which nonlinear rather than linear strain-displacement relations are used.
2. The first cylinder buckling analysis to solve the resultant nonlinear algebraic and differential equations using a modified Gauss-Jordan technique in conjunction with a Runge-Kutta algorithm.

3. The first dynamic buckling analysis with the capability of handling any number of assumed deflection terms, limited only by the available computer capacity.
4. The first dynamic buckling analysis of a discretely stiffened cylinder.
5. The first dynamic analysis of any kind to use the Dirac delta function to account for stiffener discreteness.
6. The first dynamic buckling analysis to contain the effects of stiffener eccentricity or one-sidedness.

## CHAPTER II

### FORMULATION OF THEORY

#### 2.1 Method of Analysis

An energy approach is used to facilitate the writing of compatible governing equations for the unstiffened cylinder, stringers and rings, which all buckle as an unit. This procedure allows for treatment of stringers and rings as discrete elements, rather than the usual orthotropic "smeared" analysis. Appropriate expressions for the potential and kinetic energies of the unstiffened cylinder, stringers, and rings are formulated and presented in Appendix A. To allow for finite deflections of the cylinder during the buckling process, the appropriate nonlinear strain-displacement relations, as suggested by Donnell [6], are employed. Also, the strain-displacement relations for the rings and stringers are related to the mid-surface unstiffened shell displacements. Then, in Appendix B, Hamilton's principle is used to obtain the governing nonlinear differential equations of motion and the appropriate boundary conditions which govern the prebuckling and buckling of a stiffened cylinder. To obtain the prebuckling and buckling equations, the axial, circumferential and radial displacements of the shell ( $u, v$ , and  $w$ ) are assumed to be separable into two parts as follows:

$$u(x,y,t) = u_A(x) + u_B(x,y,t)$$

$$v(x,y,t) = v_A(x) + v_B(x,y,t)$$

$$w(x,y,t) = w_A(x) + w_B(x,y,t) \quad (2-1)$$

The subscript A denotes the axisymmetric prebuckling displacement; the subscript B denotes the time-varying unsymmetric buckling displacement.

The prebuckling equations and boundary conditions are obtained by substitution of the axisymmetric displacements in Equations (2-1) into Equations (B-10). In a like manner, the buckling equations and boundary conditions are obtained by substituting Equations (2-1) into Equations (B-11), and subtracting out the previously obtained prebuckling identities.

To solve the buckling equations, the prebuckling quantities (subscript A) are first determined directly. Galerkin's technique is then applied to the three buckling equations of motion. The result of this operation is a set of simultaneous, nonlinear, ordinary differential equations. The coupled equations are then solved by means of a Runge-Kutta technique with the aid of a digital computer.

## 2.2 Hypotheses

All of the following assumptions are implicit in the analysis:

1. The circular cylindrical shell and all stiffeners remain in the linear elastic range during buckling.
2. The cylinder undergoes a classical axisymmetric prebuckling deformation during axial loading.
3. Initial imperfections in the stiffened cylinder are neglected.
4. The Kirchoff-Love hypothesis is used for the shell; thus,

it is assumed to have a wall thickness which is small compared to its radius.

5. The Donnell shallow-shell assumptions [54] apply. The buckled cylinder contains at least several buckled circumferential wavelengths. See reference [55] for details.
6. The stiffeners are discretely located along the length and circumference of the cylinder, and the width of the stiffeners is small compared to the distance between them.
7. In-surface and rotatory inertia effects in the stiffened cylinder are neglected.
8. Stiffeners behave as beam elements, and displacements vary linearly across stiffener depth. This implies that the stiffener depth is small compared to the radius of the shell middle surface.
9. The total circumferential arc length of the ring is approximately the same as that of the middle surface of the shell.
10. The stiffeners are rigidly attached to the shell.
11. The stiffeners are symmetrical with respect to a normal from the shell middle surface passing through the stiffener centroid.
12. The boundary conditions at the shell ends are not necessarily satisfied exactly, as assumed by references [6,7,8,10,45,48,49].
13. The cylinder has the characteristic buckling behavior of

a "long" cylinder. Thus, the Batdorf parameter is greater than thirty.

14. Effects of axial-wave propagation do not influence the wavelengths at which the buckles form.
15. All material damping, thermal, and initial-stress effects are neglected.
16. The shell and stiffener materials are homogeneous and isotropic.

### 2.3 Prebuckling Equations

The general nonlinear equations of motion governing the stiffened cylinder buckling are derived in Appendices A and B. The appropriate equations of motion and boundary conditions governing the cylinder prebuckling are obtained by substituting the A-subscript portion of Equations (2-1) into Equations (B-10) and (B-11). Primes indicate total differentiation with respect to  $x$ . The prebuckling equations become

$$N'_{xA} = 0 \quad (2-2)$$

$$N'_{xyA} = 0 \quad (2-3)$$

$$-M''_{xA} + (N_{yA}/R) = 0 \quad (2-4)$$

The appropriate boundary conditions at the cylinder ends are:

$$N_{xA} + \hat{N}_x = 0 \quad \text{or} \quad u_A = 0 \quad (2-5)$$

$$N_{xyA} = 0 \quad \text{or} \quad v_A = 0 \quad (2-6)$$

$$M_{xA} + \hat{N}_x \bar{e} = 0 \quad \text{or} \quad w'_A = 0 \quad (2-7)$$

$$M'_{xA} = 0 \quad \text{or} \quad w_A = 0 \quad (2-8)$$

In the above equations the following definitions apply:

$$N_{xA} = \frac{E}{1-\nu^2} (u'_A + \nu R^{-1} w'_A) + \sum_k \delta(y-kd) E_{sA} u'_s \quad (2-9)$$

$$N_{yA} = \frac{E}{1-\nu^2} (R^{-1} w'_A + \nu u'_A) + \sum_j \delta(x-j\ell) E_{rA} R^{-1} w'_A \quad (2-10)$$

$$N_{xyA} = G v'_A \quad (2-11)$$

$$M_{xA} = - \sum_k \delta(y-kd) E_{sA} \bar{z}_s u'_s \quad (2-12)$$

Equations (2-2) and (2-5) require that  $N_{xA}$  must equal  $-\hat{N}_x$ . This condition satisfies boundary condition (2-5). In a similar manner, Equations (2-3) and (2-6) require that there be no applied shear. Thus, if  $N_{xy}$  is equated to zero, boundary condition (2-6) will be satisfied. To satisfy the third boundary condition (2-7),  $w_A$  is set equal to a constant. By making  $w_A$  equal to a constant, a classical prebuckling membrane state is assumed for the stiffened cylinder. Finally, the fourth boundary condition (2-8) is satisfied by setting  $M_{xA}$  equal to zero.

For later use in the formulation of the buckling equations, the following prebuckling identities will be used:

$$N_{yA} = 0 \quad (2-13)$$

$$N_{xA} = 0 \quad (2-14)$$

$$N_{xyA} = 0 \quad (2-15)$$

#### 2.4 Buckling Equations

The governing equations and boundary conditions of a stiffened cylinder with discrete rings and stringers can be obtained by substituting

Equations (2-1) into Equations (B-10) and (B-11), subtracting out identities (2-2) through (2-4) and making use of Equations (2-13) through (2-15). The buckling equations become:

$$N_{xB,x} + N_{xyB,y} = 0 \quad (2-16a)$$

$$N_{yB,y} + N_{xyB,x} = 0 \quad (2-16b)$$

$$\begin{aligned} & -M_{xB,xx} - 2M_{xyB,xy} - M_{yB,yy} + R^{-1}N_{yB} + \hat{N}_x w_{B,xx} - N_{xB} w_{B,xx} \\ & - N_{yB} w_{B,yy} - 2N_{xyB} w_{B,xy} + \rho h w_{B,tt} + \sum_j \rho_r A_r w_{B,tt} \delta(x-j\ell) \\ & + \sum_k \rho_s A_s w_{B,tt} \delta(y-kd) = 0 \end{aligned} \quad (2-16c)$$

The boundary conditions at the stiffened cylinder ends become

$$N_{xB} = 0 \quad \text{or} \quad u_B = 0 \quad (2-17a)$$

$$N_{xyB} = 0 \quad \text{or} \quad v_B = 0 \quad (2-17b)$$

$$M_{xB} = 0 \quad \text{or} \quad w_{B,x} = 0 \quad (2-17c)$$

$$M_{xB,x} + 2M_{xyB,y} - N_x w_{B,x} + N_{xB} w_{B,x} + N_{xyB} w_{B,x} = 0 \quad \text{or} \quad w_B = 0 \quad (2-17d)$$

The definitions for the various buckling terms may be found in Appendix B, Equations (B-4) through (B-9), where a subscript B is added to each term and displacement.

## 2.5 Application of Galerkin's Method

The buckling Equations (2-16) are a set of coupled, nonlinear partial differential equations. To reduce them to a set of ordinary differential equations, the Galerkin weighted average method will be used.

The Galerkin method is an approximate assumed-mode method similar to the Rayleigh-Ritz method when applied correctly [56]. The method should be applied only to the equations of motion which arise directly from application of either Hamilton's principle or Newton's second law. If the equations are escalated by differentiation and combined, the method often yields incorrect results [57].

To apply the Galerkin method, solutions are assumed for the unknown variables in the equations of motion. In general, the solutions will not satisfy the equations of motion exactly. In order to minimize the error, the assumed solutions are inserted into the equations of motion and a non-zero "error function" is generated. Each error function is then orthogonalized with respect to the assumed solution functions. This orthogonalization process will give rise to a set of equations which can be solved for the unknown solution function coefficients. The resulting set of equations can be either linear or nonlinear, algebraic or differential, depending on the equations of motion and the form of the assumed solution.

To apply Galerkin's method to the buckling equations, the following series of assumed modes will be used

$$u = \sum \sum u_{ij}(t) \sin(im\pi x/L) \cos(jny/R) \quad (2-18a)$$

$$v = \sum \sum v_{ij}(t) \cos(im\pi x/L) \sin(jny/R) \quad (2-18b)$$

$$w = \sum \sum w_{ij}(t) \cos(im\pi x/L) \cos(jny/R) \quad (2-18c)$$

Most researchers [6-9,45,48,49] who used a nonlinear shell theory to study buckling resorted to one or more terms of the above

series. As noted in Chapter I, these researchers were unable to satisfy all of the boundary conditions. In line with hypothesis 14, Equations (2-18) satisfy boundary conditions (B-11a), (B-11b), and (B-11c), but not boundary condition (B-11d).

Substitution of Equations (2-18) into the buckling Equations (2-16) yields a set of "error functions",  $Q_x$ ,  $Q_y$ ,  $Q_z$ , respectively. The orthogonalization process may be formulated as

$$\int_0^{2\pi R} \int_0^L Q_x(u,v,w) \sin(\zeta m \pi x/L) \cos(\xi n y/R) dx dy = 0 \quad \begin{array}{l} \zeta=1,2,3 \dots \\ \xi=1,2,3 \dots \end{array} \quad (2-19)$$

$$\int_0^{2\pi R} \int_0^L Q_y(u,v,w) \cos(\zeta m \pi x/L) \sin(\xi n y/R) dx dy = 0 \quad \begin{array}{l} \zeta=1,2,3 \dots \\ \xi=1,2,3 \dots \end{array} \quad (2-20)$$

$$\int_0^{2\pi R} \int_0^L Q_z(u,v,w) \cos(\zeta m \pi x/L) \cos(\xi n y/R) dx dy = 0 \quad \begin{array}{l} \zeta=1,2,3 \dots \\ \xi=1,2,3 \dots \end{array} \quad (2-21)$$

Because  $Q_x$  and  $Q_y$  are not dependent on time, Equations (2-19) and (2-20) will each yield a set of nonlinear algebraic equations. Since  $Q_z$  is dependent on time, Equation (2-21) will yield a set of nonlinear ordinary differential equations in time. The resultant equations after some simplification are listed below, and the details of the Galerkin method are found in Appendix C.

$$\begin{aligned} & \delta_{i\zeta} \Sigma \Sigma u_{ij} [I_i^2 \delta_{j\xi} + \frac{1}{2}(1-\nu) J_j^2 \delta_{j\xi} + (1-\nu^2) (\pi R E h)^{-1} I_k^2 \Sigma E_s A_s \cos J_k \cos J_\xi] \\ & + \Delta_1 \Sigma \Sigma v_{ij} \frac{1}{2}(1+\nu) I_i J_j + \delta_{i\zeta} \Sigma \Sigma w_{ij} [R^{-1} \nu I_i \delta_{j\xi} \\ & + (1-\nu^2) (\pi R E h)^{-1} I_k^3 \Sigma E_s A_s \bar{z}_s \cos J_k \cos J_\xi] - \delta_{2i\zeta} \Sigma \Sigma w_{ij}^2 [\frac{1}{2} I_i J_j^2 \delta_{2j\xi} + \frac{1}{2} I_i^3 \delta_{2j\xi} \\ & + (1-\nu^2) (2 E h \pi R)^{-1} I_k^3 \Sigma E_s A_s \cos^2 J_k \cos J_\xi] = 0 \end{aligned} \quad (C-1)$$

$$\begin{aligned}
& \Delta_1 \Sigma \Sigma u_{ij} \cdot \frac{1}{2} (1+\nu) I_i J_j + \delta_{j\xi} \Sigma \Sigma v_{ij} [J_j^2 \delta_{i\zeta} + \frac{1}{2} (1-\nu) I_i^2 \delta_{i\zeta}] \\
& + 2(1-\nu^2) (EhL)^{-1} J_j^2 \int_j E_r A_r \cos I_j \cos I_\zeta + \delta_{j\xi} \Sigma \Sigma w_{ij} [R^{-1} J_j \delta_{i\zeta} \\
& + 2(1-\nu^2) (EhL)^{-1} \int_j (R^{-1} J_j E_r A_r + J_j^3 E_r A_r \bar{z}_r) \cos I_j \cos I_\zeta] - \delta_{2j\xi} \Sigma \Sigma w_{ij}^2 [\frac{1}{2} J_j^3 \delta_{2i\zeta} \\
& + \frac{1}{2} I_i^2 J_j \delta_{2i\zeta} + (1-\nu^2) (EhL)^{-1} J_j^3 \int_j E_r A_r \cos^2 I_j \cos I_\zeta] = 0
\end{aligned} \tag{C-2}$$

$$\begin{aligned}
& Eh(1-\nu^2)^{-1} (1/32) \Sigma \Sigma w_{ij}^3 [I_i^4 (3\Delta_1 + \Delta_2 - 3\Delta_3 - \Delta_4) + 2I_i^2 J_j^2 (-\Delta_1 + \Delta_2 + \Delta_3 - \Delta_4 + 4\nu\Delta_1 \\
& - 2\nu\Delta_2 - 2\nu\Delta_3) + J_j^4 (3\Delta_1 - 3\Delta_2 + \Delta_3 - \Delta_4)] + (2/L) \Sigma \Sigma w_{ij}^3 (\delta_{j\xi} - \delta_{3j\xi}) \frac{1}{8} J_j^4 \int_j E_r A_r \cos^3 I_j \\
& \cdot \cos I_\zeta + (1/\pi R) \Sigma \Sigma w_{ij}^3 (\delta_{i\zeta} - \delta_{3i\zeta}) \frac{1}{8} I_i^4 \int_k E_s A_s \cos^3 J_k \cos J_\xi + \Delta_5 Eh(1-\nu^2)^{-1} (\nu/8R) \\
& \cdot \Sigma \Sigma w_{ij} (I_i^2 + J_j^2) + \delta_{2j\xi} (2/L) \Sigma \Sigma w_{ij}^2 (\frac{1}{2} R^{-1} J_j^2 - \frac{1}{2} J_j^4 \bar{z}_r) \int_j E_r A_r \cos^2 I_j \cos I_\zeta \\
& - \delta_{2i\zeta} (1/\pi R) \Sigma \Sigma w_{ij}^2 \frac{1}{2} I_i^4 \int_k E_s A_s \bar{z}_s \cos^2 J_k \cos J_\xi + \Delta_1 Eh(1-\nu^2)^{-1} \Sigma \Sigma w_{ij} [(h^2/12) I_i^4 \\
& + (h^2/6) I_i^2 J_j^2 + (h^2/12) J_j^4 + (1/R^2) - \hat{N}_x (1-\nu^2) I_i^2 (Eh)^{-1}] + \delta_{j\xi} (2/L) \Sigma \Sigma w_{ij} \\
& \cdot [J_j^4 E_r I_{or} + 2R^{-1} J_j^2 E_r A_r \bar{z}_r + (1/R^2) E_r A_r] \int_j \cos I_j \cos I_\zeta + \delta_{j\xi} (2/L) \Sigma \Sigma w_{ij} J_j^2 \\
& \cdot I_i \int_j G_{J_r r} \zeta_{m\pi L}^{-1} \sin I_j \sin I_\zeta + \delta_{i\zeta} (1/\pi R) \Sigma \Sigma w_{ij} I_i^4 \int_k E_s I_{os} \cos J_k \cos J_\xi \\
& + \delta_{i\zeta} (1/\pi R) \Sigma \Sigma w_{ij} I_i^2 J_j \int_k G_{J_s s} \xi_{nR}^{-1} \sin J_k \sin J_\xi + \Delta_1 Eh(1-\nu^2)^{-1} \nu R^{-1} \Sigma \Sigma u_{ij} I_i \\
& + \delta_{i\zeta} (1/\pi R) \Sigma \Sigma u_{ij} I_i^3 \int_k E_s A_s \bar{z}_s \cos J_k \cos J_\xi + \Delta_1 Eh(1-\nu^2)^{-1} R^{-1} \Sigma \Sigma v_{ij} J_j \\
& + \delta_{j\xi} (2/L) \Sigma \Sigma v_{ij} (J_j^3 \bar{z}_r + J_j R^{-1}) \int_j E_r A_r \cos I_j \cos I_\zeta + \Delta_5 \frac{1}{2} Eh(1-\nu^2)^{-1} \Sigma \Sigma u_{ij} w_{ij} (I_i^3 \\
& + I_i J_j^2) + \delta_{2i\zeta} (1/\pi R) \Sigma \Sigma u_{ij} w_{ij} \frac{1}{2} I_i^3 \int_k E_s A_s \cos^2 J_k \cos J_\xi + \Delta_5 Eh(1-\nu^2)^{-1}
\end{aligned}$$

$$\begin{aligned}
& \cdot \sum \sum v_{ij} w_{ij} (J_j^3 + I_i^2 J_j) + \delta_{2j\xi} L^{-1} \sum \sum v_{ij} w_{ij} J_j^3 \sum_r E_r A_r \cos^2 I_j \cos I_\zeta \\
& + \sum \sum \ddot{w}_{ij} [\Delta_1 \rho h + \delta_{j\xi} \rho_r A_r (2/L) \sum_j \cos I_j \cos I_\zeta + \delta_{i\zeta} \rho_s A_s (1/\pi R) \sum_k \cos J_k \cos J_\xi] = 0
\end{aligned}
\tag{C-3}$$

## 2.6 Numerical Solution

The buckling equations consist of a set of  $2k$  nonlinear algebraic equations and a set of  $k$  nonlinear differential equations, where  $k$  represents the number of terms used in the assumed modes. Because of the complex nature of these sets of equations, no closed form solution is known to exist. However, with given initial conditions, the above sets of equations should be numerically solvable if we use a Gauss-Jordan technique on the algebraic equations and a Runge-Kutta technique on the nonlinear differential equations. In addition to the initial conditions on the dependent variables, the solution of the equations depends also on the externally applied axial load resultant,  $\hat{N}_x$ , and the circumferential wave number  $n$ . Of course, it will be necessary to vary  $n$  over a range of values to find the minimum critical load, since this will be the true dynamic buckling load of the stiffened cylinder.

An inspection of the set of algebraic Equations (C-1) and (C-2) reveals that the nonlinearity is in the radial deflection terms,  $w_{ij}(t)$ . Thus, if  $w_{ij}(t)$  is specified initially, Equations (C-1) and (C-2) can be solved by a suitable technique for solving simultaneous linear equations. The results, together with the value of  $w_{ij}(t)$ , can be substituted into the set of nonlinear differential equations

(C-3). Using a fourth order Runge-Kutta algorithm and advancing it  $\frac{1}{4}$  step, a new set of  $w_{ij}(t)$  can be obtained. The new  $w_{ij}(t)$  set can be resubstituted into Equations (C-1) and (C-2) and the process repeated three times to yield one complete step.

Since most Runge-Kutta algorithms are written specifically for first-order differential equations, it is necessary to convert the  $k$  second-order differential equations into  $2k$  first-order equations by a simple change of variable. The following fourth-order algorithm attributed to Kutta is used in the analysis [58]:

$$w_{i+1} = w_i + (g/6)(k_1 + 2k_2 + 2k_3 + k_4)$$

where

$$k_1 = f(t_i, y_i)$$

$$k_2 = f(t_i + \frac{1}{2}g, y_i + \frac{1}{2}gk_1)$$

$$k_3 = f(t_i + \frac{1}{2}g, y_i + \frac{1}{2}gk_2)$$

$$k_4 = f(t_i + g, y_i + gk_3)$$

In order to begin the numerical procedure, it is necessary to choose representative initial values for the set of dependent variables,  $w_{ij}(t)$ . Physically, this corresponds to giving the shell a slight initial radial deflection or velocity. This procedure was first suggested by Roth and Klosner [49].

Finally, a criterion for identifying dynamic buckling must be established. An inspection of the representative buckling curves found in Chapters III and IV make it apparent that at some critical load the structure is diverging from its initial displacement rather than returning to its equilibrium (or zero displacement) position. Thus, as

suggested in references [49] and [59], the buckling load can be defined as the load at which a large increase in the amplitude of the deflection occurs. Of course, as mentioned earlier in this section, it will be necessary to plot the buckling load as a function of circumferential wave number,  $n$ , and then pick the lowest resultant load as the true buckling load.

Further details concerning the numerical techniques employed may be obtained by consulting Appendices IV and V. One particularly important technique, which allowed a general formulation of the governing equation coefficients independent of the number of assumed mode terms, will be illustrated here. It should be noted that the coefficients of the various terms in Equations (C-1) through (C-3) can be written as functions of the assumed mode subscripts  $i$ ,  $j$ ,  $\zeta$  and  $\xi$ . However, the identification of parameters by four rather than by two subscripts becomes very cumbersome when attempting to construct a general computer program. This problem was solved by making use of an algorithm suggested in reference [60]. The algorithm permits the rewriting of each coefficient in terms of only two subscripts  $P$  and  $Q$ , and then "decoding" the subscripts as necessary during the numerical procedure. If a typical coefficient is represented by  $A_{\zeta\xi ij}$ , the algorithm will convert it to  $A_{QP}$  as follows:

$$i = P - \left(\frac{P-1}{i^*}\right)_T i^*$$

$$j = 1 + \left(\frac{P+1}{i^*}\right)_T$$

$$\zeta = Q - \left(\frac{Q-1}{i^*}\right)_T i^*$$

$$\xi = 1 + \left(\frac{Q+1}{i^*}\right)_T$$

where  $i^*$  represents the maximum value of the  $i$  coefficient and the symbol  $( \quad )_T$  represents the operation of integer truncation. An example of this calculation for a four-term assumed deflection mode is shown in Table 2.1. The operation of this algorithm can be observed in Appendix V.

Table 2.1 Coefficient Algorithm

$\zeta$	$\xi$	$i :$	1	2	1	2
		$j :$	1	1	2	2
1	1		(Q=1,P=1)	(Q=1,P=2)	(Q=1,P=3)	(Q=1,P=4)
2	1		(Q=2,P=1)	(Q=2,P=2)	(Q=2,P=3)	(Q=2,P=4)
1	2		(Q=3,P=1)	(Q=3,P=2)	(Q=3,P=3)	(Q=3,P=4)
2	2		(Q=4,P=1)	(Q=4,P=2)	(Q=4,P=3)	(Q=4,P=4)

## CHAPTER III

### EVALUATION OF THEORY

#### 3.1 Comparison with Static Buckling

During the literature search no studies were found that dealt exclusively with sparsely stiffened cylinders. Consequently, most studies used a linear buckling theory in conjunction with a smeared stiffener analysis. In the smeared analysis, the stiffener properties are averaged over the appropriate dimension by dividing by the stiffener spacing. In the more exact analysis contained in this investigation, the stiffener properties are considered as discrete and a Dirac delta function is used to handle the discreteness in the analysis. In order to reduce the present discrete analysis to a smeared one for comparison, the typical results in Table 3.1 can be used.

Table 3.1 Comparison of Smeared and Discrete Terms

	SMEARED	DISCRETE
Typical Term	$E_s A_s u_{,xx}/d$	$\sum_k E_s A_s u_{,xx} \delta(y-kd)$
Result After Galerkin Procedure	$-\frac{1}{2} u_{ij} I_i^2 \pi R L E_s A_s / d$	$-\frac{1}{2} u_{ij} I_i^2 L E_s A_s \sum_k \cos J_k \cos J_\xi$
Equivalent Terms	$\pi R / d$	$\sum_k \cos J_k \cos J_\xi$

Block, *et al.* [38] used a linear smeared analysis and a one term assumed mode approach. This procedure reduced the static buckling problem to a single algebraic equation containing the applied axial load and the circumferential and axial wave numbers. In order to compare Block's final equation with the present results, Equations (C-1), (C-2) and (C-3) were linearized, the stiffeners were smeared using results analogous to those presented in Table 3.1, the inertia terms were removed, and only the first displacement terms were included. When the resulting equations were reduced, they compared exactly to final Equation (15) of reference [38].

In a later reference, Block [21] completed a linear classical buckling solution for a cylinder with smeared stringers and discrete rings. He used a Dirac delta approach to model the discrete rings. His assumed modes consisted of a single circumferential term together with a large number of axial terms, all of which satisfied the boundary conditions of the classical simple support. Again, a term-by-term comparison with the present analysis yielded analogous results.

Unfortunately, after an extensive literature search, no theoretical or experimental work was found which dealt with dynamic buckling of stiffened cylinders. The only dynamic studies were theoretical studies of unstiffened cylinders, and these are treated in the next section. However, to obtain an approximate comparison between the present dynamic buckling analysis and previously published static analyses, a dynamic buckling analysis was conducted using the shell parameters reported in references [21] and [38]. In these references the cylinder which was used had closely spaced stiffeners representative of the

large-diameter liquid rocket booster structures. Details of the structure and results of the comparison are contained in Fig. 3.1. The dynamic analysis was made using one circumferential and three axial terms. Since the dynamic loading consisted of a step pulse loading of infinite time duration, the predicted buckling load should roughly correspond to the predicted static buckling load. As observed from Fig. 3.1, except for the smeared static analysis, the dynamic load is generally above the corresponding static load. The difference can be attributed to the inclusion of the radial inertia and the nonlinear terms in the dynamic analysis.

### 3.2 Comparison with Dynamic Buckling

The only dynamic buckling analyses found in the literature were for unstiffened shells exclusively [46,48,49], and were not experimentally verified. Generally, a nonlinear buckling theory together with a stress function approach was used to reduce the problem to one equilibrium and one compatibility equation. These equations were solved by the Ritz-Galerkin method and then integrated numerically. Because of the sensitivity of the unstiffened cylinder to initial imperfections, the analyses concentrated on the influence of these imperfections on the buckling load. Since initial imperfections are not included in the present stiffened cylinder analysis, it was necessary to extend the unstiffened cylinder analyses for comparison purposes. In order to accomplish this, the equations of reference [49] were solved numerically for the case of zero imperfections, and plotted in Fig. 3.2. As a comparison, the same unstiffened cylinder was treated using the present analysis, and the results are shown in Fig. 3.2. Because of the

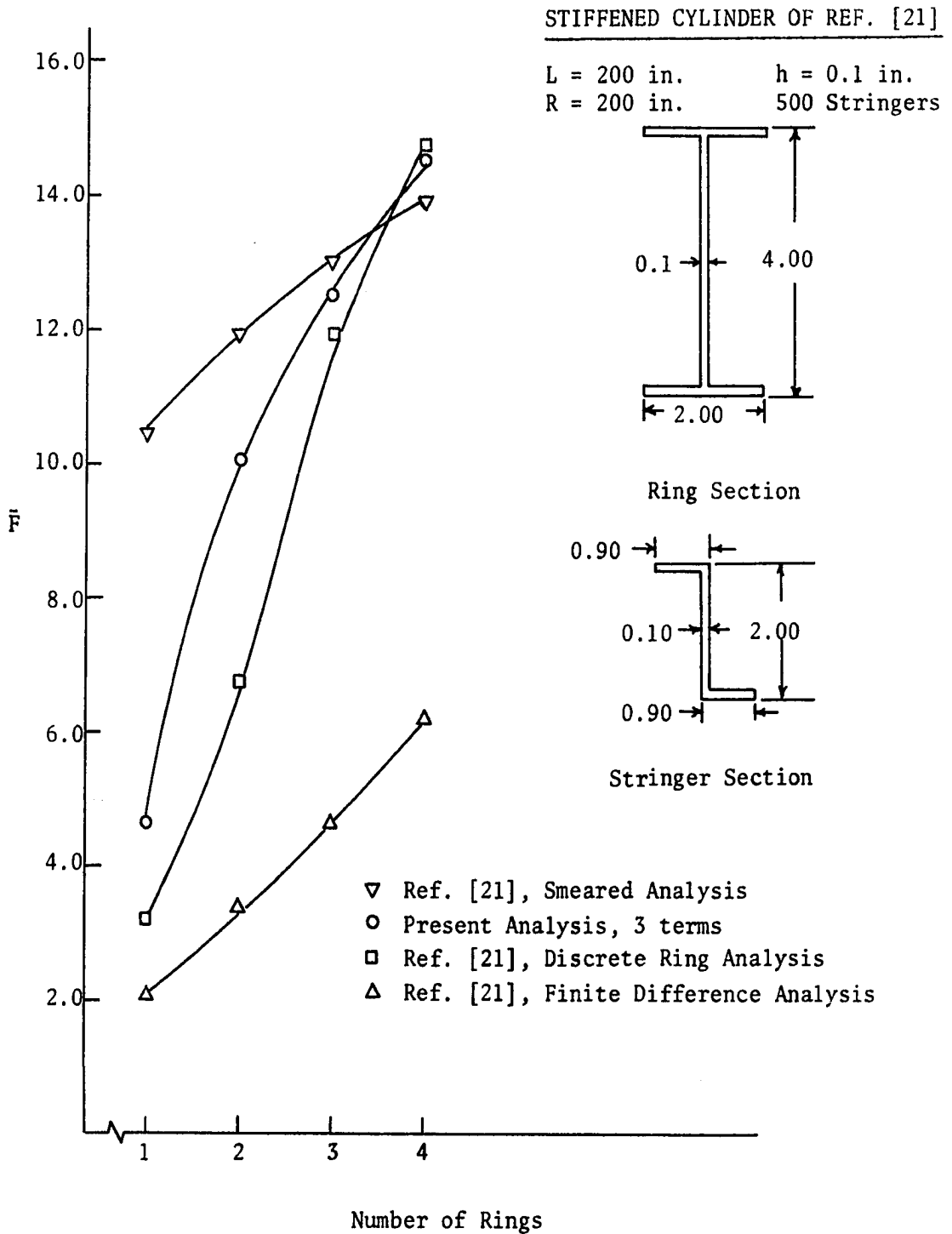


Figure 3.1 Static Buckling Comparison

different radial deflection functions used in reference [49], exact agreement would not be expected. However, the curves are in good agreement.

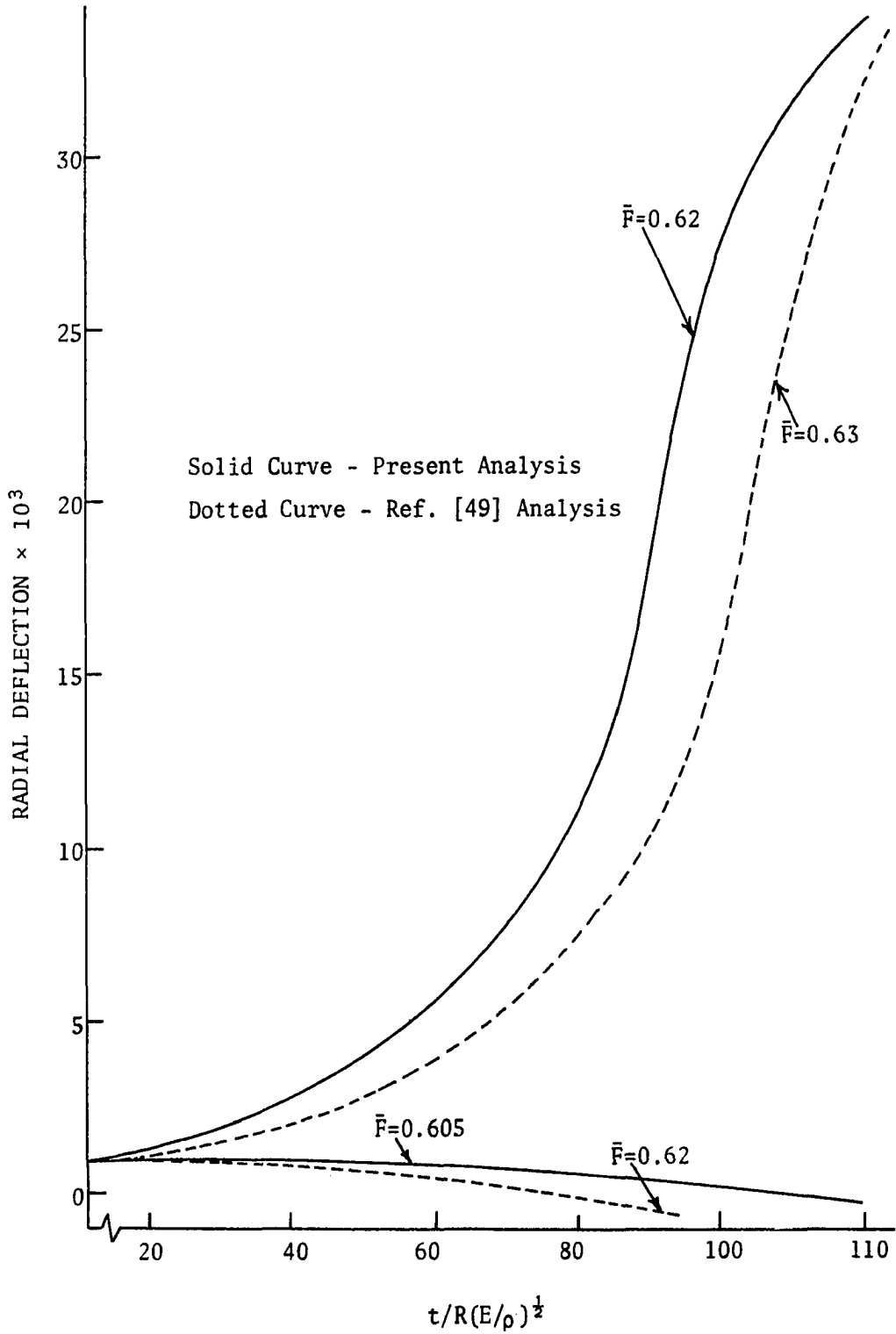


Figure 3.2 Dynamic Buckling Comparison, Unstiffened Shell

## CHAPTER IV

### RESULTS

#### 4.1 Representative Aircraft Structure

Because of the large number of geometric and physical parameters involved in this investigation, it is impractical to present results of a general nature. However, it is of value to present some computed results for stiffened cylinders which are representative of light aircraft fuselage structures. In order to determine the geometric parameters of a typical light aircraft structure, four light aircraft companies were contacted. Based on the data they provided, Table 4.1 was constructed. It must be mentioned that the data shown in Table 4.1 is approximate only. It reflects engineering judgment made by the author, and not by personnel of the respective aircraft companies. Many of the actual geometric configurations have been simplified for this analysis. For example, actual rings or bulkheads are seldom uniform, of constant thickness, or without "lightening" holes to conserve weight. In this analysis, all rings and stringers are considered uniform, of constant thickness, and evenly spaced along the inside of the cylinder. No provision has been made for cutouts in the shell for doors or windows. However, despite these limitations, it is felt that a useful first-order parametric study can be made based on the approximate quantities contained in Table 4.1.

Table 4.1 Representative Light Aircraft Geometry

Acft.	Type	Cabin Length (in.)	R (in.)	h (in.)	M	$A_s$ (in <sup>2</sup> )	$I_{os}$ (in <sup>4</sup> )	$J_s$ (in <sup>4</sup> )	$\bar{z}_s$ (in.)	$A_r$ (in <sup>2</sup> )	$I_{or}$ (in <sup>4</sup> )	$J_r$ (in <sup>4</sup> )	$\bar{z}_r$ (in.)
A	Single Engine	112	25	0.30	33	0.032	0.006	0.0049	0.308	0.094	0.088	0.039	0.763
B	Single Engine	110	25	0.25	22	0.065	0.015	0.0059	0.466	0.142	0.320	0.120	1.210
C	Twin Engine	168	34	0.30	27	0.046	0.013	0.0078	0.413	0.165	0.264	0.102	1.013
D	Twin Engine	217	31	0.34	30	0.035	0.003	0.0022	0.187	0.133	0.461	0.159	1.513

An inspection of Table 4.1 reveals that all four aircraft have approximately the same stiffener area, but that some of the other stiffener quantities vary by as much as 50 per cent. This is due to different geometrical shapes of the various stiffeners. For example, the stringers in aircraft C are channel-sections, while those in aircraft D are L-sections. However, the effect of variation of these parameters was shown to be small, as documented in Section 4.3.

Based on the data contained in Table 4.1, a representative set of stiffened cylinder parameters was chosen. To begin the study a 32-inch radius cylinder was used. The skin thickness was 0.04 inches and the largest spacing between rings was 32 inches. Thirty equally spaced stringers, together with the stiffener properties of aircraft C were used as a starting point. These various geometrical parameters were then varied, and the influence on the dynamic buckling behavior was noted.

In light of assumptions twelve and thirteen regarding the cylinder boundary conditions, the cylinder radius, thickness, and length were never such that the Batdorf parameter,  $Z$ , was less than 30. In fact, even if the stringers were smeared over the surface of the shortest cylinder, the smallest value of  $Z$  was 190. Thus, the expected buckling behavior of the stiffened cylinder would be that of a "long" cylinder.

Due to the relatively wide spacing between the rings on general-aviation light aircraft, it was felt that local buckling of the shell between the rings would be the mode of failure, rather than general instability. Local buckling between rings is defined as the buckling

mode in which the rings have little or no radial buckling deformation, and the cylinder buckles between the rings. General instability is defined as the buckling mode in which the rings deform radially and the cylinder wall and rings buckle as a composite wall. Since discreteness of the stiffeners has been accounted for, the present analysis can handle either type of instability.

Since an actual aircraft fuselage consists of a long cylinder with a number of repeating bays between the rings, it is reasonable to assume that buckling of the entire cylinder can be studied by considering a representative smaller portion or subshell of the cylinder. If this assumption is valid, fewer assumed mode terms in the deflection function would probably be needed to correctly model the dynamic behavior of the structure. Of course, fewer terms would mean a saving of computer time.

To validate the above assumption, the long cylinder shown in Fig. 4.1 was divided into three subshells. Subshell I consisted of one ring and an L/R of two. Subshell II consisted of two rings and an L/R of three. Subshell III consisted of the stringers between two rings and an L/R of one. A buckling analysis was performed on subshells I and II, and the results are shown on Fig. 4.2. Although the curves diverge somewhat for higher values of  $n$ , the lowest buckling load for both subshells was approximately the same and occurred for the same wave number, indicating the similarity of buckling shapes. As expected, subshell II required more terms than subshell I for convergence; subshell I required three terms while subshell II required five terms. It should be mentioned that the curves drawn through the calculated points on the various graphs are for ease in identifying the lowest buckling load.

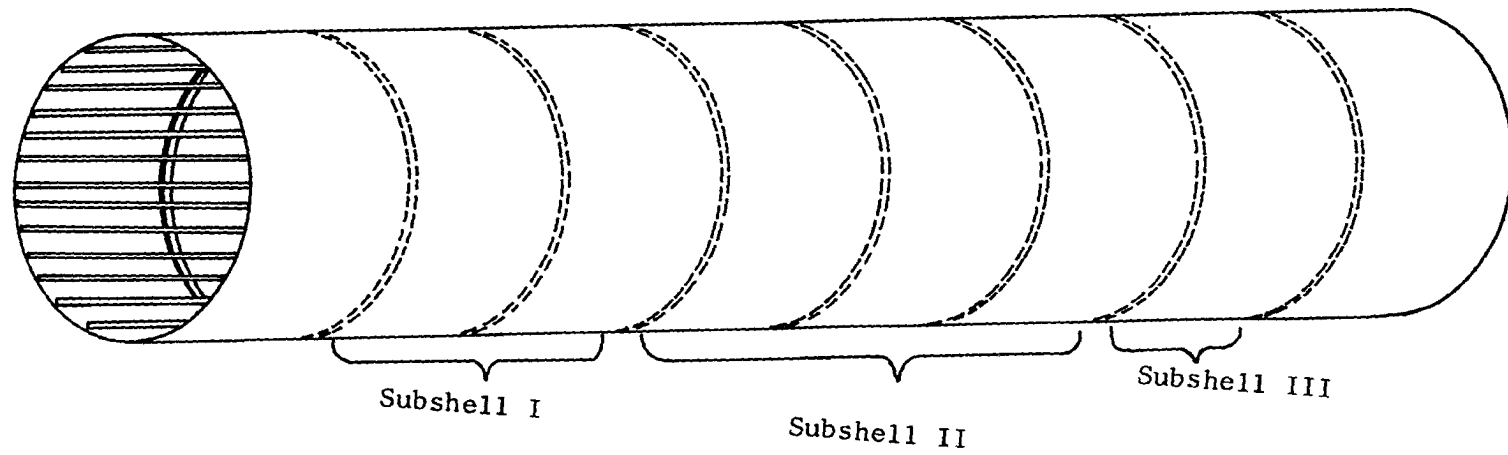


Figure 4.1 General Aircraft Structure

The curves are actually discrete points since  $n$  can take on integer values only.

Subshell III was used as a further check on the convergence of the curves presented in Fig. 4.2, and as a demonstration of local buckling of the subshell between the rings. When a stiffened cylinder undergoes local buckling between the rings, the rings can only exert a torsional restraint on the shell. Thus, a lower bound on the buckling load can be obtained by considering the stringer stiffened portion between the rings. This portion is shown as subshell III in Fig. 4.1, and the corresponding buckling curve is plotted on Fig. 4.2. The closeness of the subshell I and II curves to this lower bound curve demonstrates that local buckling between the rings is the mode of buckling for the representative cylinder considered in this analysis.

The effect of discreteness on the stringer stiffened shell can be seen in the region of  $n = 15$ . Since the shell consists of 30 stringers,  $n = 15$  represents the case of local buckling between the stringers. However, when rings are used in addition to stringers, the buckling at  $n = 15$  does not represent the lowest buckling load, as evidenced by the subshell I and II curves.

Based on this preliminary case, it is reasonable to assume that local buckling between the rings will be the dominant instability mode. Local buckling between the stringers will occur at some higher load and thus not be significant. Also, because of the great increase in computer running time and core space for each additional assumed mode term, the number of assumed mode terms in the circumferential direction will be limited to one. The number of terms in the axial direction will be

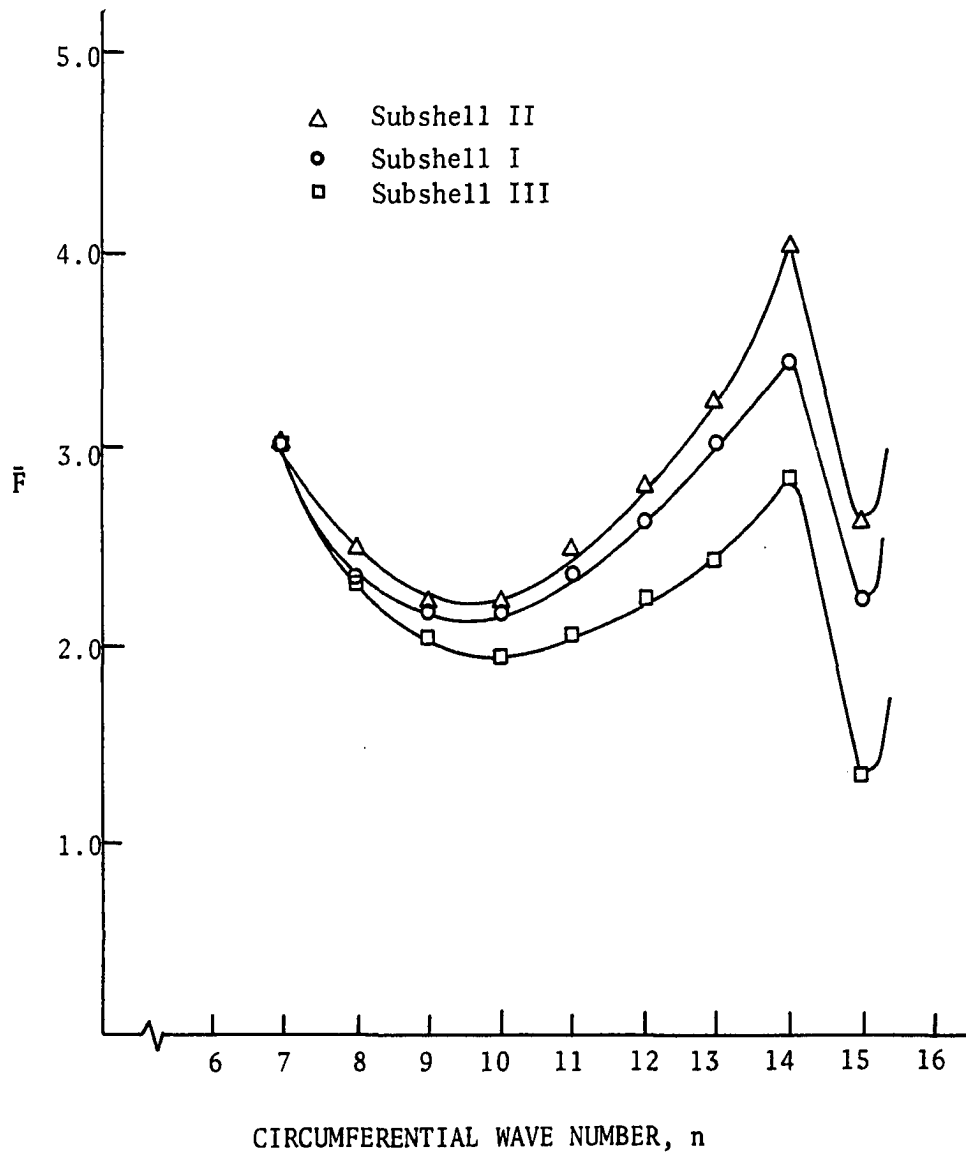


Figure 4.2 Comparison of Buckling Load for Different Cylinder Regions

increased until convergence is obtained.

#### 4.2 Dynamic Considerations

As stated in Section 1.2, it is believed that this study represents the first dynamic buckling analysis of a discretely stiffened cylinder. Because of the relative newness of the dynamic buckling field, general procedures and criteria for identifying dynamic buckling have not been generally established as they have been for static buckling. Consequently, the results presented in this and subsequent sections should be considered exploratory in nature. Unlike static buckling analyses, where the lowest buckling load results from the solution of an eigenvalue problem, the shell deflection-time history curves must be inspected to determine buckling. Next, the buckling load must be cross-plotted as a function of the wave number  $n$  to determine the lowest buckling load. Because of the many parameters that must be varied, and because of the large amount of computer time required for the analysis, the following general calculational procedure was adopted:

##### Computer Run #1

- a. Allow  $n$  to vary from one to twenty.
- b. Establish a best guess as an upper and lower bound on the load,  $\bar{F}$ .
- c. Establish an incrementing value for  $\bar{F}$ , usually beginning with 0.5.
- d. Begin with a Runge-Kutta step increment of 0.1 msec and terminate computation after  $t$  reaches 5.0 msec.

##### Computer Run #2

- a. Narrow region of  $n$  to those values yielding the lowest values of  $\bar{F}$ .

- b. Narrow the upper and lower bounds and reduce the size of the incrementing step.
- c. Examine the smoothness of the maximum deflection curves to determine whether the Runge-Kutta increment is adequate.

#### Computer Run #3

- a. Identify and input the critical value of  $n$  causing the lowest buckling load.
- b. Narrow the upper and lower bounds of  $\bar{F}$  and reduce the size of the incrementing step.
- c. Run the analysis for  $t > 50$  msec. to positively identify the lowest buckling load, and the time to the first maximum of the lowest buckling load.
- d. Repeat the entire procedure with more terms in the assumed deflection function to determine convergence of the results.

Although the analysis and computer program allows one to consider an axial end load varying arbitrarily with time, the present study has been limited to loads having a step function variation in time. Since actual crash load durations are on the order of 100 milliseconds [61], the step function time duration was at least 100 milliseconds.

In order to start the numerical analysis it was necessary to establish the initial displacement and velocity conditions on the radial assumed mode terms. It was decided to set the initial deflection of the lowest mode equal to 0.001 which represented an initial displacement of less than five per cent of the shell thickness. All other initial conditions were set equal to zero. This procedure was suggested by reference [49] for studying dynamic buckling of unstiffened cylinders.

The initial deflection was varied with no change in buckling behavior, thus indicating the insensitivity of buckling to initial conditions.

As mentioned in Section 2.6, the buckling load for a particular wave number is defined as the load at which a large increase in the amplitude of the deflection occurs. The actual buckling load for a particular structure can then be determined from a plot of load versus wave number, such as shown in Fig. 4.2.

By considering the behavior of the lowest mode only as a function of time, it can be seen from Fig. 4.3 that there are two types of shell response. If the load is below the critical buckling load, the shell oscillates around its original equilibrium position. Since damping is neglected in the analysis, this oscillation would rapidly damp out in an actual shell. If the load is at or above the critical buckling load, there is a radical increase in the maximum shell deflection. If the load is increased further, the maximum radial deflection increases, and the time to maximum deflection decreases. This type of behavior was previously observed and documented for dynamic buckling of unstiffened shells by Roth and Klosner [49]. They used the same instability criterion by investigating the response of the lowest mode only.

In order to distinguish the lowest buckling load between two values of  $n$ , it was often necessary to observe the dynamic behavior for durations of up to 100 milliseconds. For example, from Fig. 4.2 the buckling load occurred either at a wave number of nine or ten. To

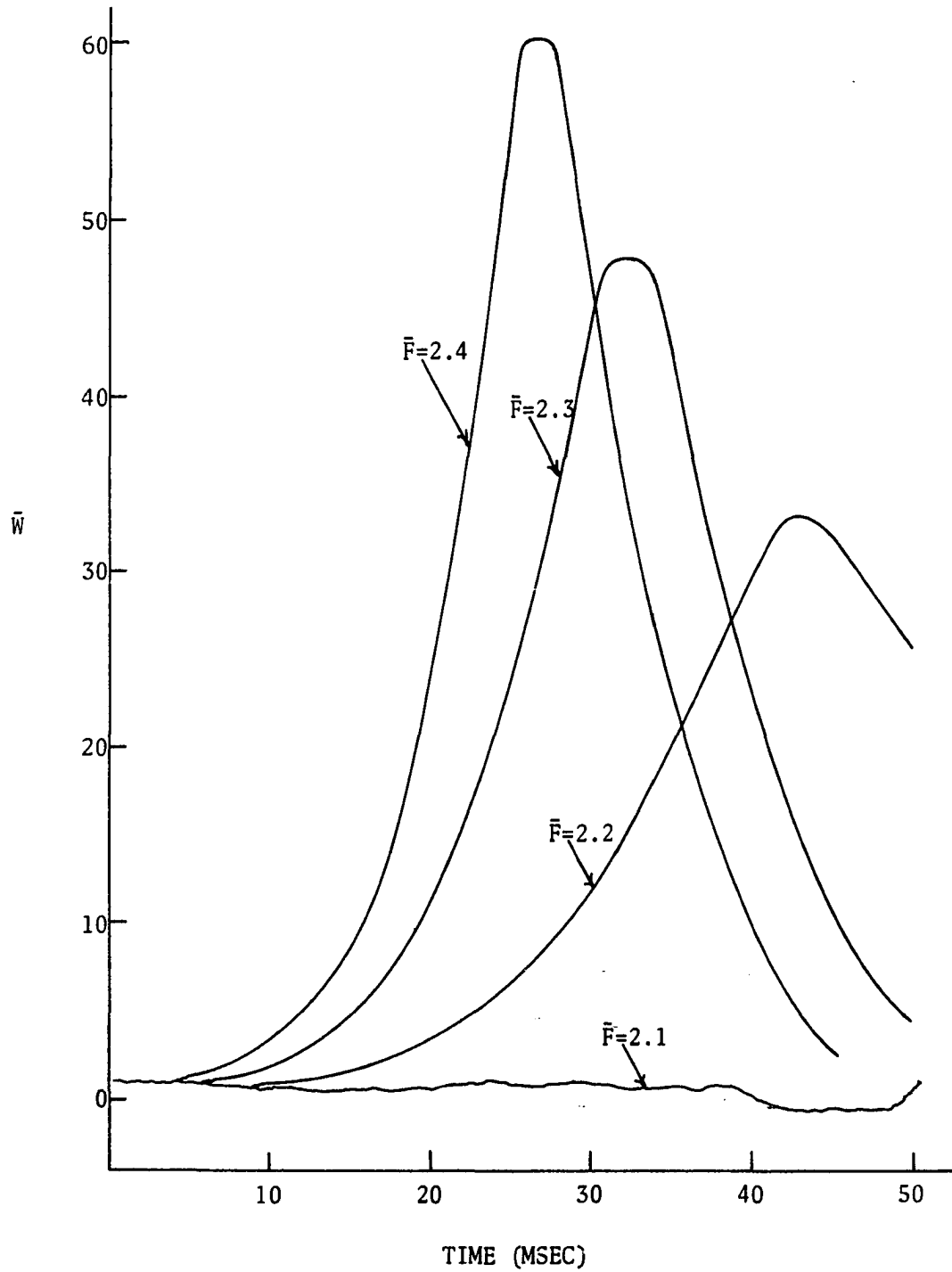


Figure 4.3 Maximum Radial Deflection Versus Time for Various End Loads,  $n = 9$

identify the exact buckling load and the corresponding wave number, it was necessary to study the behavior of the shell in greater detail for longer time durations. This illustrative study is shown in Figs. 4.3 and 4.4. Based on these figures, the representative cylinder would buckle at a wave number of nine rather than ten. The shell reaches a greater deflection in Fig. 4.3 than in Fig. 4.4 for the same applied load.

As mentioned previously, the time required for maximum deflection to occur decreases as the applied load is increased. This time can be classed as the critical time required for buckling. If the time duration of the axial loading is short enough, the shell should be able to withstand loads higher than the minimum buckling load. Although this fact has not been experimentally verified for dynamically loaded cylinders, the same conclusion was reached in reference [49]. Figure 4.5 depicts the time duration curve for the representative stiffened cylinder.

### 4.3 Geometric Considerations

In an attempt to suggest design improvements on current light aircraft, various parameters (such as number of stiffeners, stiffener area and stiffener eccentricity) were varied and the effects on the buckling load were noted. The results of this limited parametric study are shown in Figs. 4.6 through 4.11.

The influence of the number of stringers on the buckling load of subshell II are shown in Figs. 4.6 and 4.7. Since local buckling between the stringers was not the dominant mode of buckling, only the region of importance is shown on the respective figures. However, the

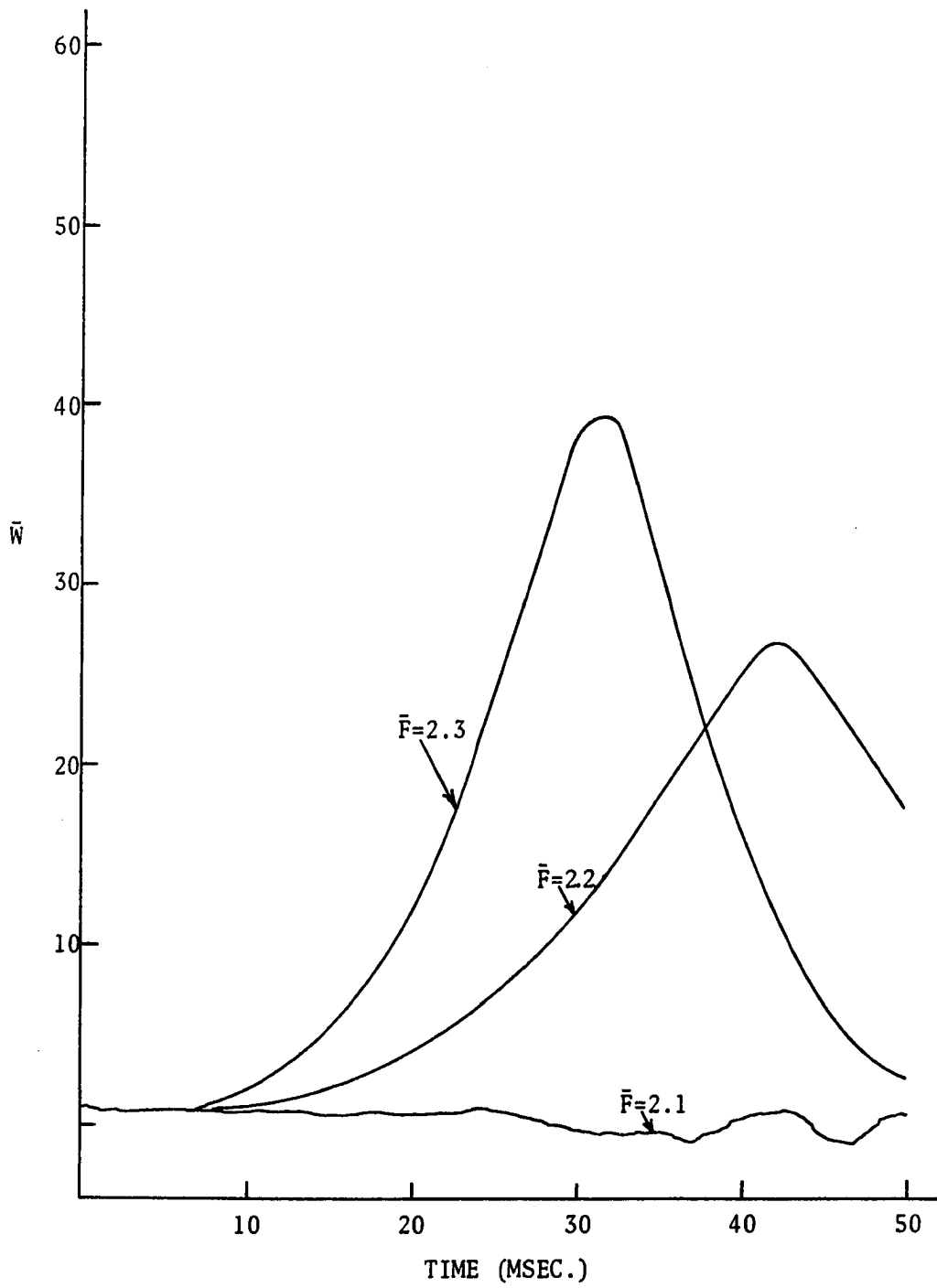


Figure 4.4 Maximum Radial Deflection Versus Time for Various End Loads,  $n = 10$

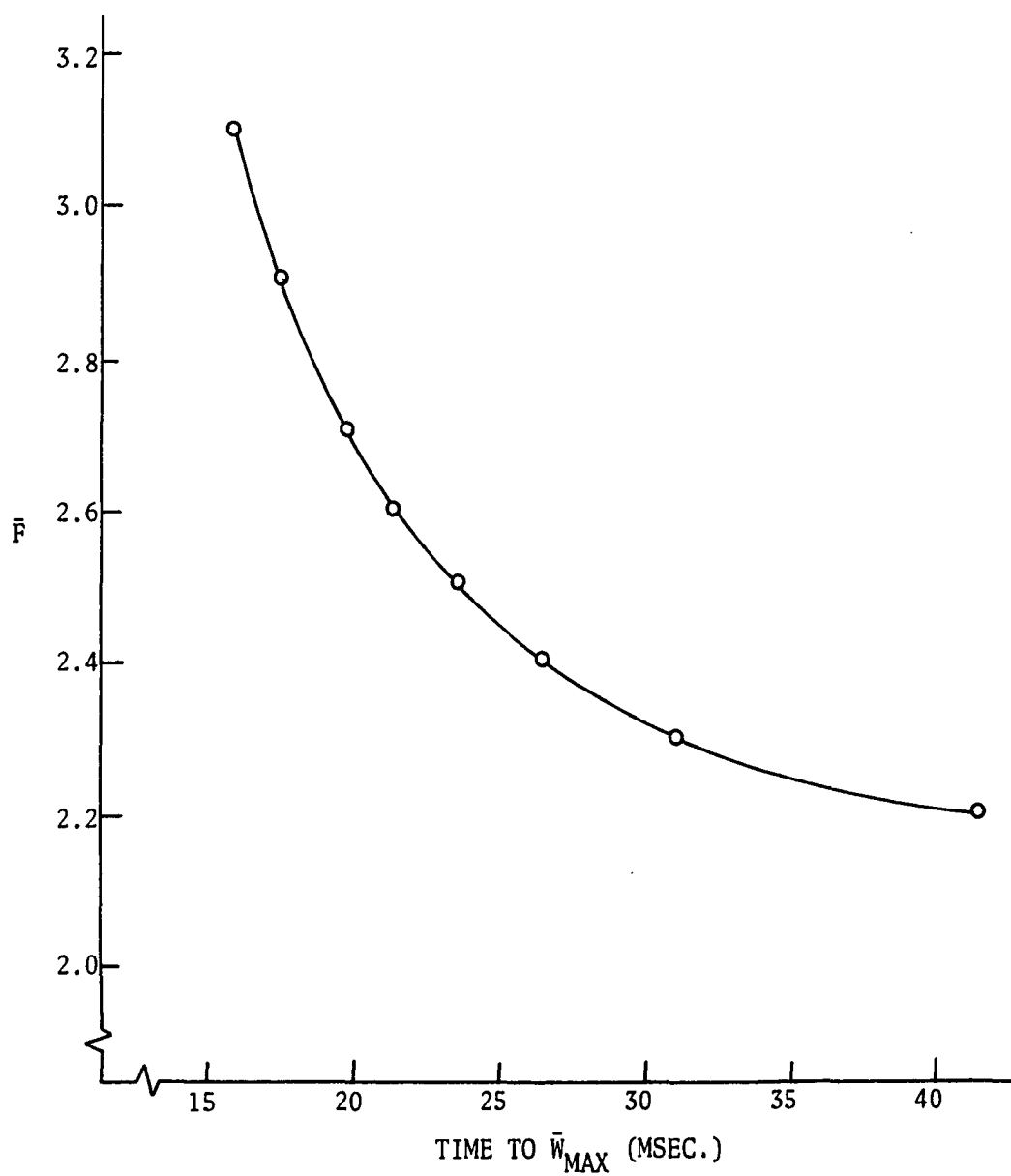


Figure 4.5 Buckling Load Versus Time Duration,  $n = 9$

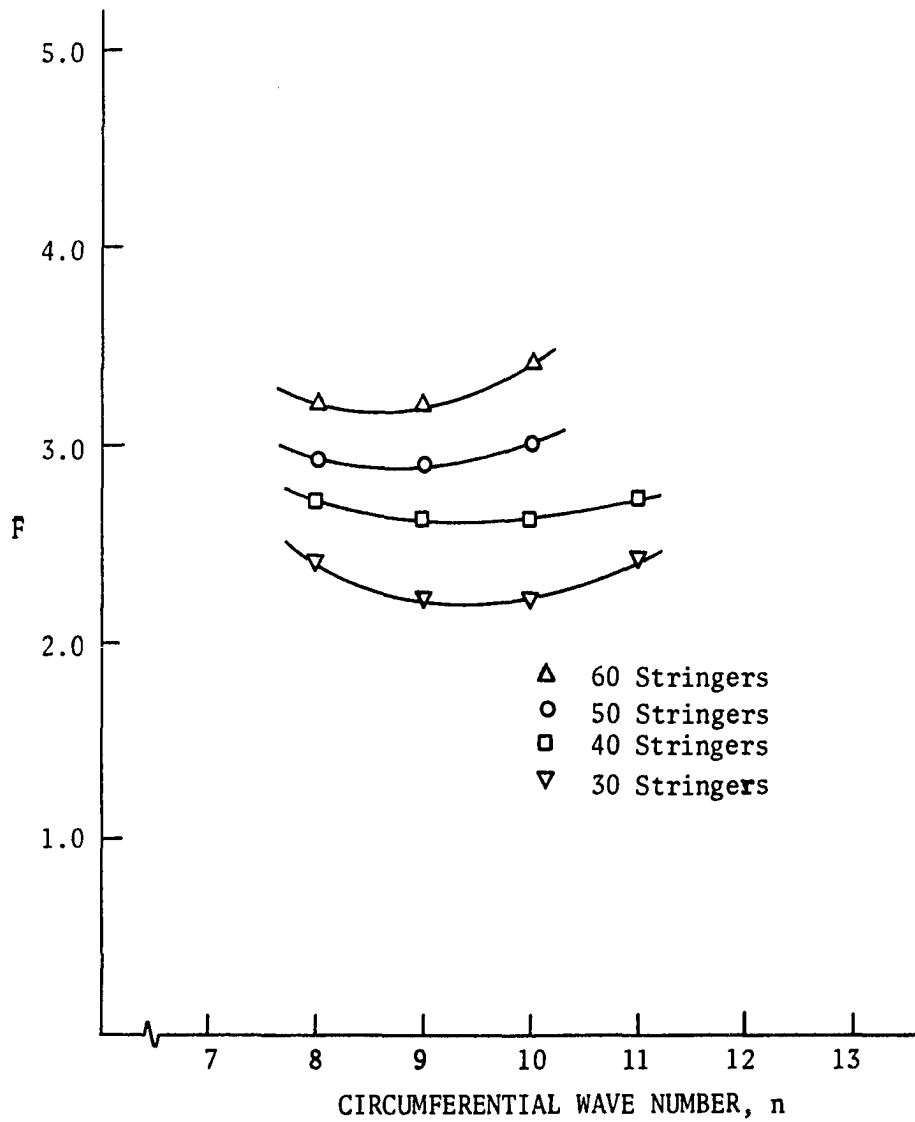


Figure 4.6 Axial Force Versus Wave Number with Increasing Number of Stringers

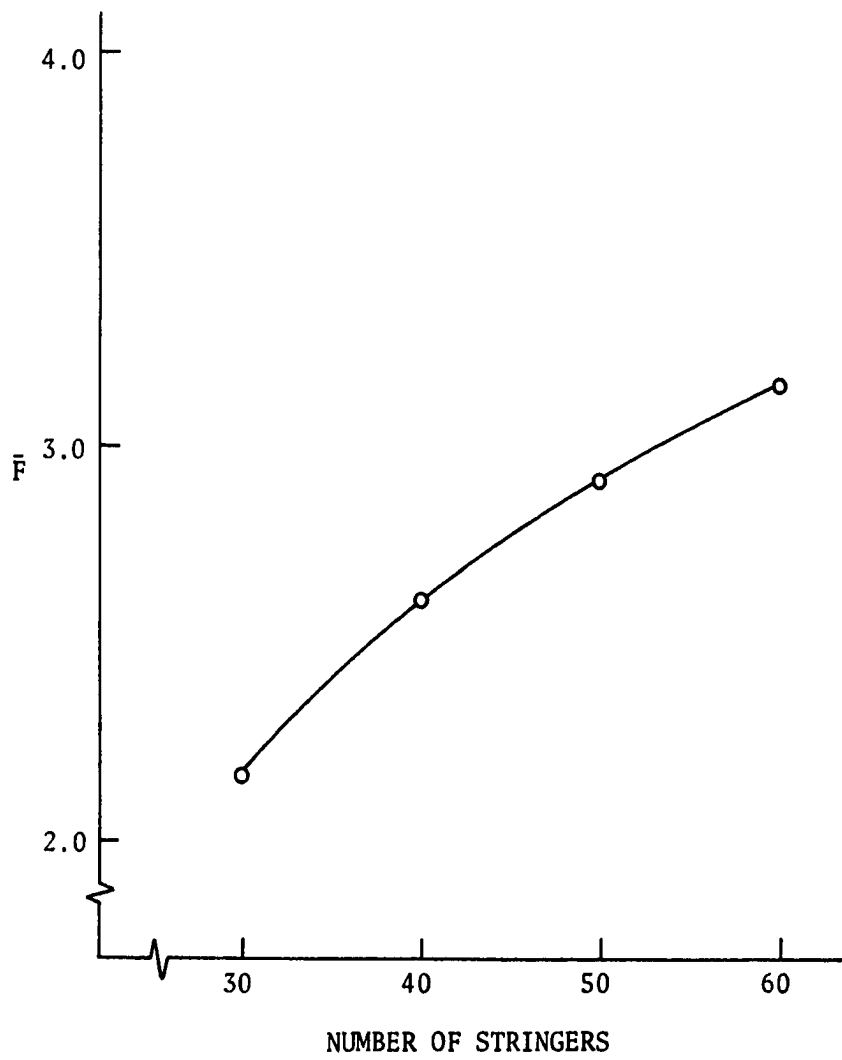


Figure 4.7 Influence of Number of Stringers on Buckling Load

calculations were also run for higher wave numbers to check this assumption. In performing the calculations all shell and stiffener parameters were held constant except for the number of stringers. It can be seen from Fig. 4.7, that if the number of stringers of the aircraft C type were doubled, the minimum dynamic buckling load would be increased by over 50 per cent. If the number of stringers was less than thirty, local buckling between the stringers would probably be the dominant mode of buckling, with a corresponding decrease in buckling load. This observation suggests a minimum weight design where the number of stringers was just enough to prevent local buckling between the stringers.

The influence of the number of rings on the buckling load is shown in Figs. 4.8 through 4.10. Figures 4.8 and 4.10 represent the lower bound on the calculations, since they were made using subshell III, which does not include the torsional rigidity of the rings. The calculations show the same trend previously observed when the number of stringers was increased. If the distance between rings is halved, the buckling load is increased by about 50 per cent. This same trend is also verified when the ring torsional rigidity is included, as shown in Fig. 4.9.

Finally, the ring and stringer cross-sectional areas and eccentricities were each varied independently and the analysis was repeated. No significant change in the buckling load was noted for increases of 25 to 50 per cent of each parameter. This somewhat surprising result was also observed by Singer, Baruch, and Harari [35] when they studied the static buckling of stiffened cylinders using a linear smeared

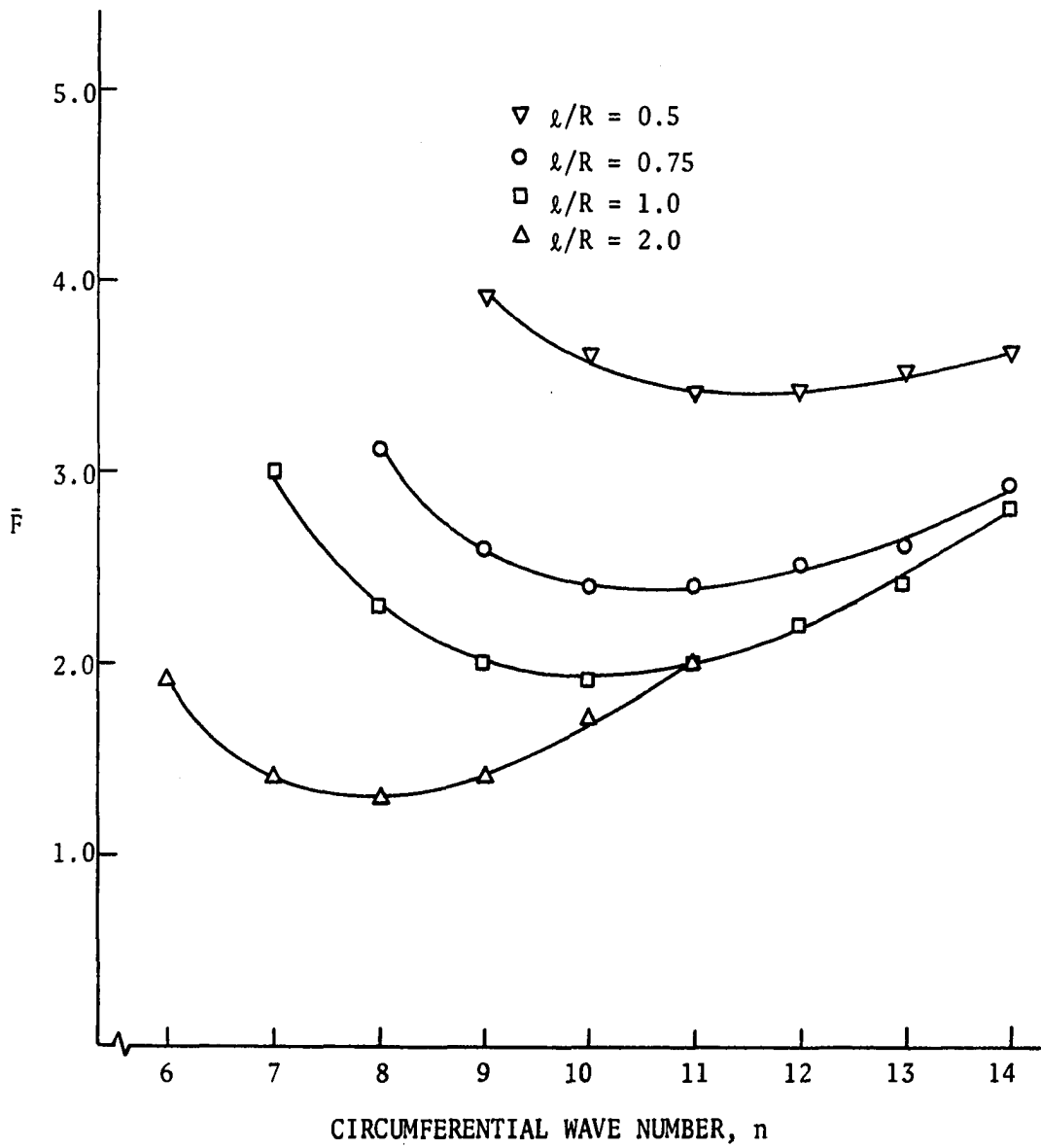


Figure 4.8 Axial Force Versus Wave Number for Different Ring Spacing, Subshell III

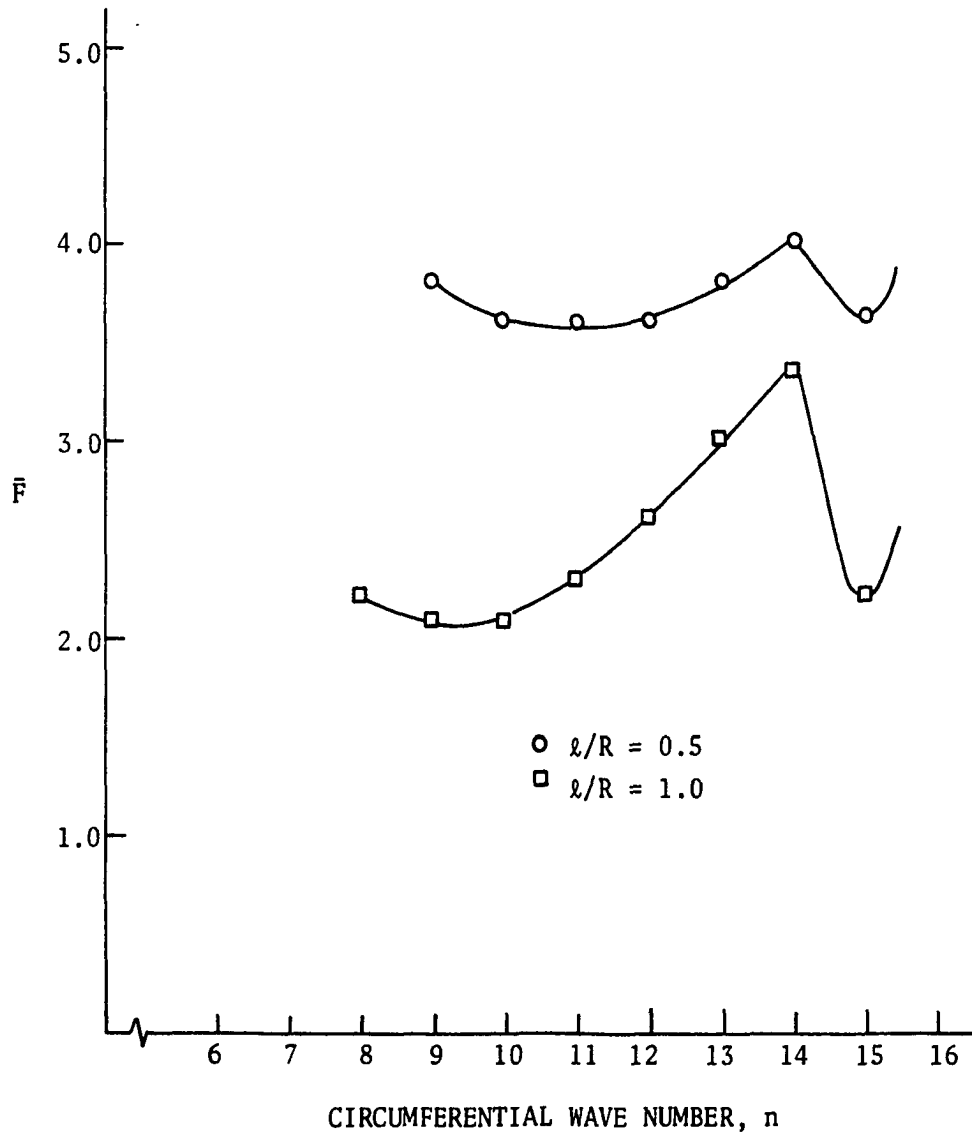


Figure 4.9 Axial Force Versus Wave Number for Different Ring Spacing, Subshell I

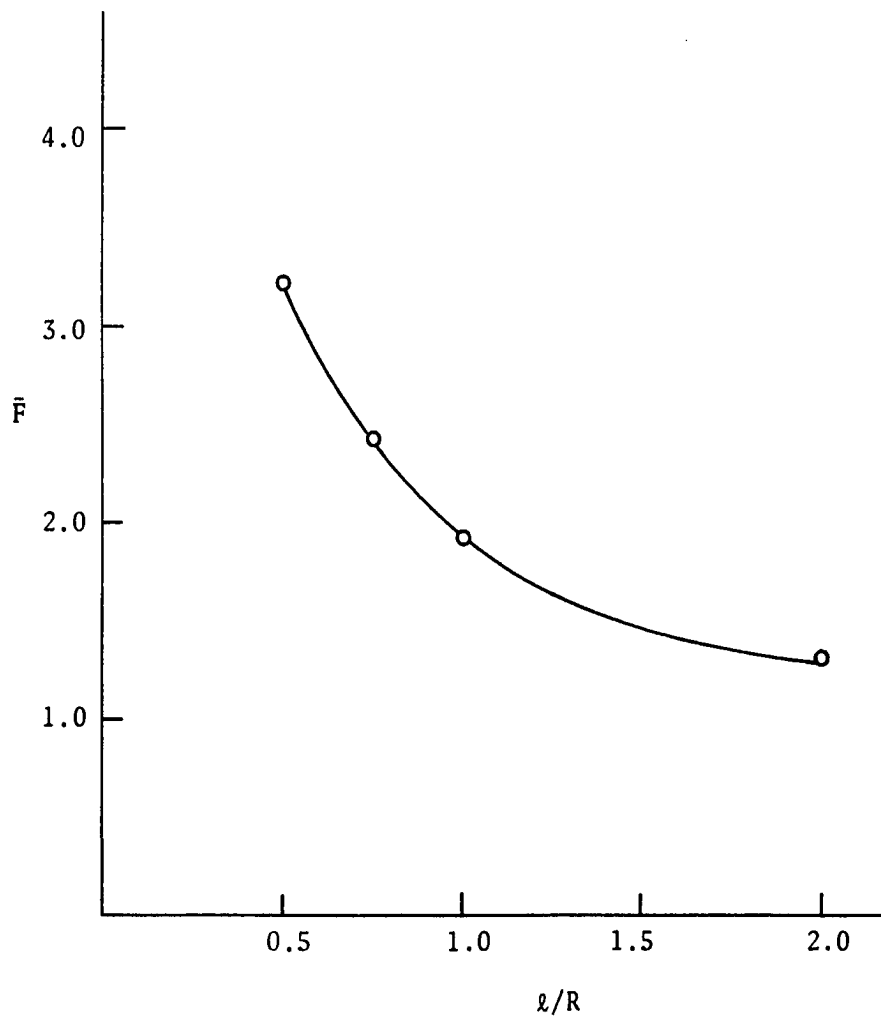


Figure 4.10 Influence of Number of Rings on Buckling Load

analysis. They stated that, except for very low values of the Batdorf parameters,  $Z$ , the buckling load was not increased appreciably by variation of stiffener area or eccentricity. Judging from the curves presented in reference [35], the value of  $Z$  had to be less than 25 for the variation to have any appreciable effect. As noted earlier, the smallest value of  $Z$  observed for any of the light aircraft structures was about 190.

The results of the parameter variation seem to suggest that stiffener eccentricity or one-sidedness need not be included in the analysis. This, however, is definitely not the case as shown in Fig. 4.11. If the stiffeners were placed on the outside rather than on the inside of the cylinder, the dynamic buckling load is increased. The effect of stiffener eccentricity on the buckling load was first demonstrated by Koiter [25]. Of course, from a practical standpoint, light aircraft normally would not be designed with the stiffeners outside the fuselage!

The results of this section demonstrate that the number rather than the geometric configuration of the stiffeners is the important design consideration. This is not surprising, especially due to the local buckling behavior observed previously. The stiffeners can only exert a torsional restraint in the local buckling mode. Consequently, "beefing up" the stiffeners will only effect the buckling load slightly. The results of this section also suggest an aircraft design where the stiffener cross-section is reduced until general instability would be on the verge of predominating over local buckling. Then the reduction in stiffener weight could be used to increase the total number of stiffeners. The final design should be a more crashworthy aircraft with no increase in weight.

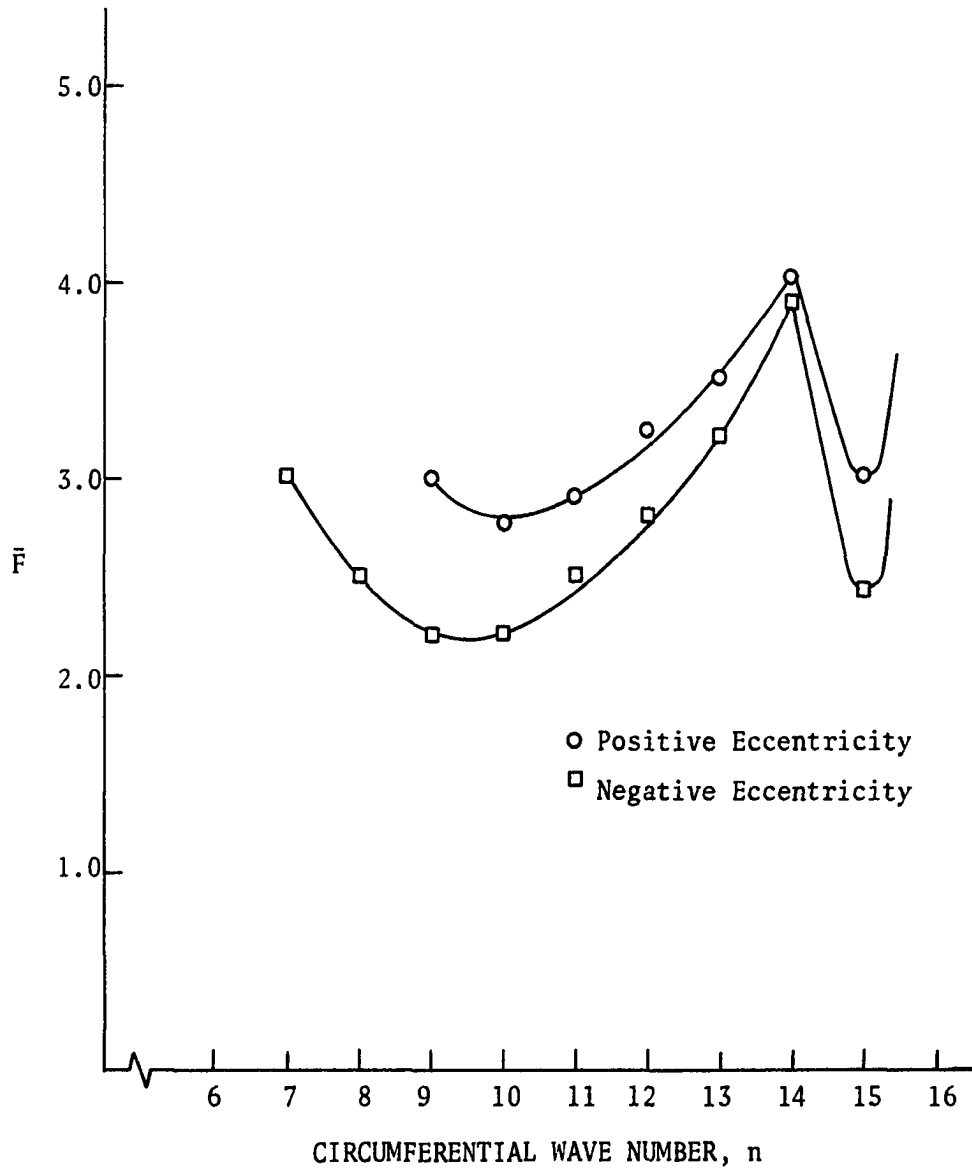


Figure 4.11 Influence of Stiffener Eccentricity on Buckling Load

#### 4.4 Discreteness Considerations

Because of the wide spacing between some stiffeners in light aircraft structures, the stiffeners were treated as discrete elements, by use of the Dirac delta representation. However, it was found that most light aircraft have relatively closely spaced stringers. An inspection of Table 4.1 reveals that the number of stringers varies from 33 on aircraft A, which has a 25-inch radius, to 22 on aircraft C, which also has a 25-inch radius. As noted in Section 4.1, a stringer spacing of 30 caused some discreteness effects to be apparent, but not enough to dominate the buckling mode. This was due in part to the large number of stringers and in part to the restraining effect of the rings, as was observed in Fig. 4.2. However, if light aircraft are designed with fewer stringers it is recommended that stringer discreteness be checked using the present analysis.

The discreteness effects of the rings were observed using a suggestion from reference [41], where it was shown that the first term, the first approximation, of the discrete solution is equal to the "smeared" solution, for the case of equal rings. This fact also applies to the present analysis. If the stiffeners are smeared in the analysis, and the buckling Equations (2-16) are solved by the Galerkin method, one sees that the terms corresponding to the unstiffened shell are the same as those in the discrete analysis. The ring terms in the smeared analysis yield terms of the type

$$(E_{\text{R}} A_{\text{R}} / \ell) \int_0^L \cos(i\pi x/L) \cos(\zeta\pi x/L) dx = \frac{1}{2} (E_{\text{R}} A_{\text{R}} L / \ell) \delta_{i\zeta} \quad (4-1)$$

The corresponding term for the discrete analysis would be

$$\int_0^L \sum_j E_{rj} A_{rj} \delta(x-j\ell) \cos(i\pi x/L) \cos(\zeta\pi x/L) dx = \sum_j E_{rj} A_{rj} \cos(i\pi x/L) \cos(\zeta\pi x/L) \quad (4-2)$$

In matrix form, Equation (4-1) would be an  $i\zeta$  diagonal matrix, whereas Equation (4-2) would also be an  $i\zeta$  matrix, but not necessarily diagonal. However, the diagonal terms of Equation (4-2) would be of the form

$$\sum_j E_{rj} A_{rj} \cos^2(i\pi x/L) = \frac{1}{2} (E_r A_r L/\ell) \quad (4-3)$$

Obviously Equation (4-3) is equal to Equation (4-1), demonstrating that the diagonal terms in the discrete case are equal to those of the smeared case.

Thus, instead of generating a smeared analysis to compare with the present analysis, it is only necessary to compare a one term solution with a multi-term solution to observe the discreteness effects.

The discreteness effects on subshell I are shown in Fig. 4.12. It is readily observed that a one-term solution was totally inadequate in predicting the buckling load, but that a three- or five-term solution rapidly converged to a lower bound answer. It is interesting to note that the three- and five-term solution predicted essentially the same critical buckling load at the same wave number, but differed somewhat at the higher wave numbers.

The discreteness effects on subshell II are shown in Fig. 4.13. They are of the same character as those for subshell I, but it took a five-term rather than a three-term solution to converge on the lowest buckling load. A seven-term solution is also shown in Fig. 4.13 which

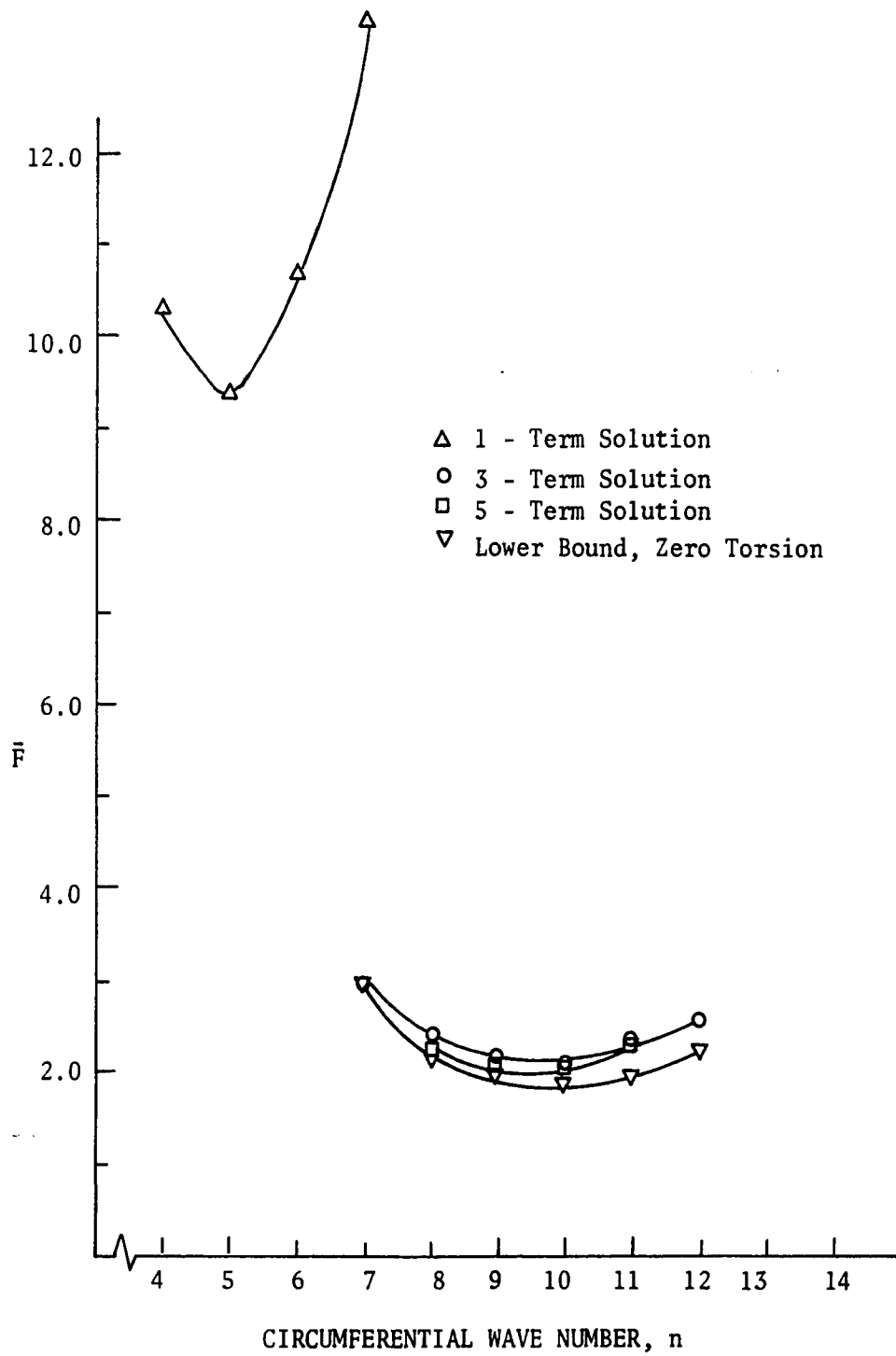


Figure 4.12 Convergence of Solution, Subshell I

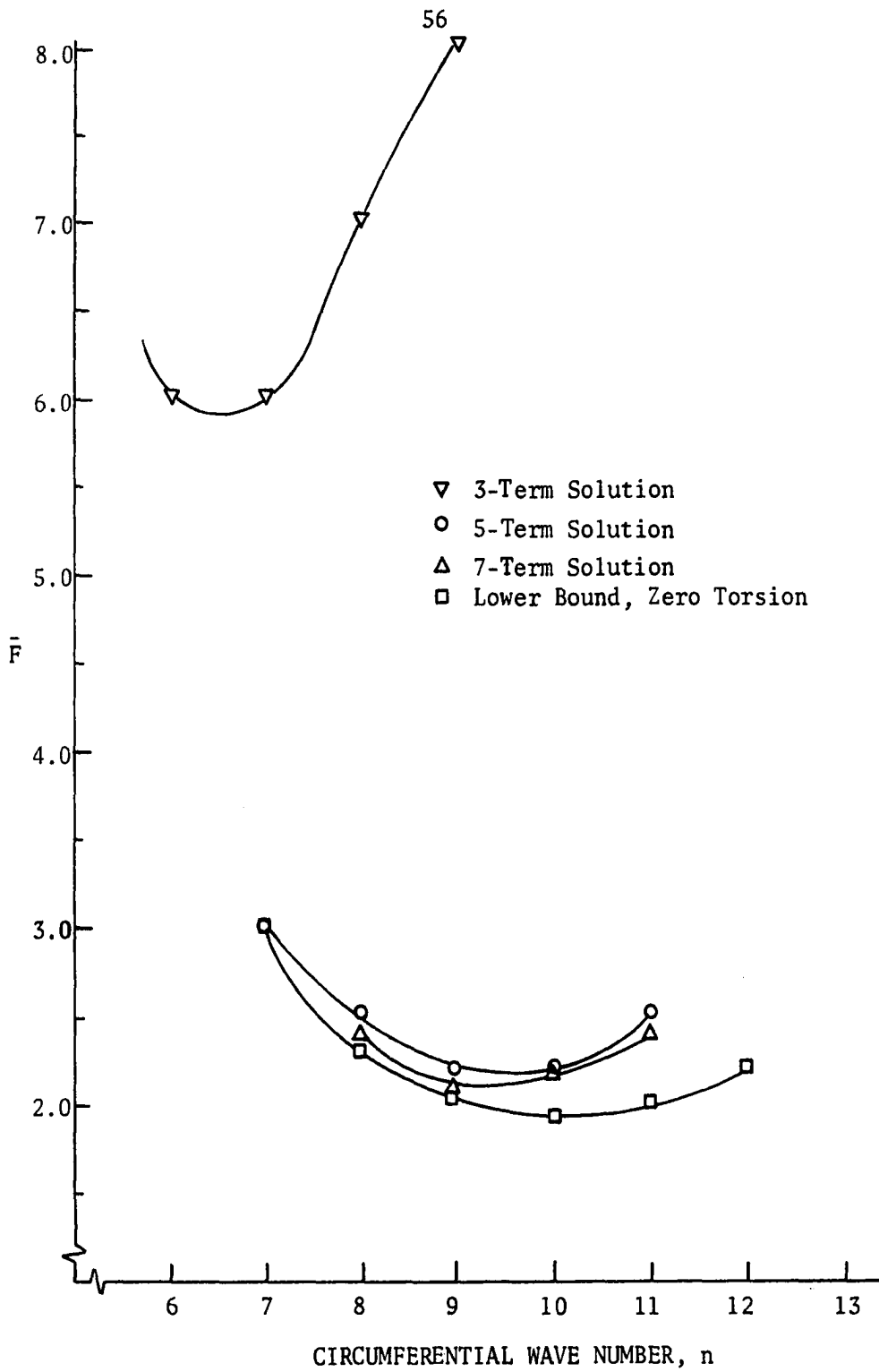


Figure 4.13 Convergence of Solution, Subshell II

further demonstrates the convergence. It is interesting to note that, for subshell I, only the third and fifth terms had a significant effect on the buckling load. Similarly, only the fifth and seventh terms had a significant effect on the subshell II buckling load. This behavior followed an empirical rule suggested by Dr. D. M. Egle for identifying the significant assumed mode terms. This rule can be deduced from Ref. [62] as:

1st term,  $(2n_b \pm m)$  term,  $(4n_b \pm m)$  term, etc.

where

$n_b$  = numbers of bays between rings

$m$  = axial wave number (normally 1)

This rule predicts the same important terms for subshell I and II as were actually observed.

Thus, as anticipated, the discreteness of the rings or bulkheads in light aircraft must be accounted for. The usual smeared analysis would calculate an incorrect wave number and a buckling load that could be an order of magnitude too high.

## CHAPTER V

### CLOSURE

The analysis developed in this dissertation can be applied to any light aircraft structure undergoing any dynamically varying axial compression loading. Since the stiffeners are treated as discrete elements, the analysis can be of great value in the design of new aircraft that can better withstand crash impact loads without any great increase in overall structural design weight. The computer program contained in the analysis can handle any dynamically varying load shape, such as ramp, exponential, or triangular. With minor modification, the program could handle stiffeners with varying geometric cross-sectional properties.

The present theory was compared with available dynamic unstiffened shell and static stiffened shell analyses, and good agreement was achieved. A limited parametric study was conducted on a stiffened cylinder which was representative of a present-day, light-aircraft cabin section. The results were presented primarily in graphical form, and the following general conclusions were obtained:

1. Since local buckling between bulkheads predominated over general shell instability in the test cases, the stiffeners in most aircraft are probably over-designed. A more efficient design could be achieved

by designing the stiffeners such that general instability buckling would be on the verge of predominating over local buckling.

2. The number of rings and stringers should be increased in preference to increasing the size or cross-sectional shape of the stiffeners in current aircraft design.
3. Stiffener discreteness must be included in a dynamic analysis of the type presented here in order to adequately model a light aircraft structure in a crash environment.

Finally, it is recommended that this analysis be complimented by a series of experiments in which representative cylinders are subjected to a carefully controlled dynamic buckling environment. No experiments were found in the current literature in which dynamic axial compression buckling of stiffened shells was studied. Experiments of this type could study phenomena such as time duration of loading (Section 4.2), the effect of stiffener discreteness (Section 4.4), and the effect of geometric variations of the stiffened shell on the buckling load (Section 4.3). The present theory would provide the analytical basis for designing such experiments to extract maximum useful information.

## REFERENCES

1. "Aviation. A Wing and a Subsidy", *Time*, Vol. 99, No. 9, Feb. 28, 1972, pp. 74-76.
2. Swearingen, J., "General Aviation Structures Directly Responsible for Trauma in Crash Decelerations", FAA-AM-71-3, Jan. 1971, Civil Aeromedical Institute, Oklahoma City, Oklahoma.
3. Hoff, N. J., "The Perplexing Behavior of Thin Cylindrical Shells in Axial Compression", *Israel J. Technol.*, Vol. 4, 1966, pp. 1-28.
4. Stein, M., "Some Recent Advances in the Investigation of Shell Buckling", *AIAA J.*, Vol. 6, No. 12, 1968, pp. 2339-2345.
5. Timoshenko, S. P. and Gere, J. M., *Theory of Elastic Stability*, 2d. ed. New York: McGraw-Hill Book Company, pp. 457-482, 1961.
6. Donnell, L. H., "A New Theory for the Buckling of Thin Cylinders under Axial Compression and Bending", *Trans. ASME*, Vol. 56, 1934, pp. 795-806.
7. von Kármán, T. and Tsien, H. S., "The Buckling of Thin Cylindrical Shells under Axial Compression", *J. Aero. Sci.*, Vol. 8, 1934, pp. 303-312.
8. Kempner, J., "Postbuckling Behavior of Axially Compressed Circular Cylindrical Shells", *J. Aero. Sci.*, Vol. 21, 1954, pp. 329-335.
9. Almroth, B. O., "Postbuckling Behavior of Orthotropic Cylinders under Axial Compression", *AIAA J.*, Vol. 2, No. 10, 1964, pp. 1795-1799.
10. Hoff, N. J., Madsen, W. A., and Mayers, J., "Postbuckling Equilibrium of Axially Compressed Circular Cylindrical Shells", *AIAA J.*, Vol. 4, No. 1, 1966, pp. 126-133.
11. von Kármán, T., Dunn, L. G., and Tsien, H.S., "The Influence of Curvature on the Buckling Characteristics of Structures", *J. Aero. Sci.*, Vol. 7, No. 7, 1940, pp. 276-289.
12. Batdorf, S. B., Schildcrout, M., and Stein, M., "Critical Stress of Thin-Walled Cylinders in Axial Compression", NACA TN 1343, June 1947, Langley Memorial Aero. Lab., Langley Field, Virginia.

13. Gerard, G. and Becker, H., "Handbook of Structural Stability - Part III Buckling of Curved Plates and Shells", NACA TN 3783, August 1957, New York University.
14. Stein, M., "The Influence of Prebuckling Deformations and Stresses on the Buckling of Perfect Cylinders", NASA TR R-190, Feb. 1964, Langley Research Center, Hampton, Virginia.
15. Almroth, B. O., "Influence of Edge Conditions on the Stability of Axially Compressed Cylindrical Shells", *AIAA J.*, Vol. 4, No. 1, 1966, pp. 134-140.
16. Weller, T., Baruch, M., Singer, J., "Influence of In-Plane Boundary Conditions on Buckling of Ring Stiffened Cylindrical Shells", *Israel J. Technol.*, Vol. 9, No. 4, 1971, pp. 397-410.
17. Hoff, N. J. and Rehfield, L. W., "Buckling of Axially Compressed Circular Cylindrical Shells at Stresses Smaller than Classical Critical Value", *J. Appl. Mech.*, Vol. 32, 1965, pp. 542-546.
18. Hoff, N. J., "Low Buckling Stresses of Axially Compressed Circular Cylindrical Shells of Finite Length", *J. Appl. Mech.*, Vol. 32, 1965, pp. 533-541.
19. Tennyson, R. C., "An Experimental Investigation of the Buckling of Circular Cylindrical Shells in Axial Compression Using the Photoelastic Technique", Institute for Aerospace Studies, University of Toronto, UTIAS Report No. 102, Nov. 1964.
20. Tennyson, R. C., "Analysis of the Buckling Process of Circular Cylindrical Shells under Axial Compression", UTIAS Report No. 129, Feb. 1968.
21. Block, D. L., "Influence of Discrete Ring Stiffeners and Prebuckling Deformations on the Buckling of Eccentrically Stiffened Orthotropic Cylinders", NASA TN D-4283, Jan. 1968, Langley Research Center, Hampton, Virginia.
22. Peterson, J. P., "Buckling of Stiffened Cylinders in Axial Compression and Bending, A Review of Test Data", NASA TN D-5561, Dec. 1969, Langley Research Center, Hampton, Virginia.
23. Almroth, B. O. and Bushnell, D., "Computer Analysis of Various Shells of Revolution", *AIAA J.*, Vol. 6, No. 10, 1968, pp. 1847-1855.
24. Singer, J., Arbocz, J., and Babcock, C. D., "Buckling of Imperfect Stiffened Cylindrical Shells under Axial Compression", *AIAA J.*, Vol. 9, No. 1, 1971, pp. 68-75.

25. Koiter, W. T., "On the Stability of Elastic Equilibrium", NASA TT F-10,833 (Translation of "Over de stabiliteit van het elastisch evenwicht", Thesis, Polytechnic Institute, Delft, H. J. Paris, Publisher, Amsterdam, 1945), March 1967.
26. Hutchinson, J. W., "Axial Buckling of Pressurized Imperfect Cylindrical Shells", *AIAA J.*, Vol. 3, No. 8, 1965, pp. 1461-1466.
27. Budiansky, B., and Hutchinson, J. W., "A Survey of Some Buckling Problems", *AIAA J.*, Vol. 4, No. 9, 1966, pp. 1505-1510.
28. Cohen, G. A., "Computer Analysis of Imperfection Sensitivity of Ring-Stiffened Orthotropic Shells of Revolution", *AIAA J.*, Vol. 9, No. 6, June 1971, pp. 1032-1039.
29. Hutchinson, J. W., and Frauenthal, J., "Elastic Post-buckling Behavior of Stiffened and Barreled Cylindrical Shells", *J. Appl. Mech.*, Vol. 36, No. 4, December 1969, pp. 784-790.
30. Hutchinson, J. W., and Amazigo, J. C., "Imperfection-Sensitivity of Eccentrically Stiffened Cylindrical Shells", *AIAA J.*, Vol. 5, No. 3, 1967, pp. 392-401.
31. Weller, T., Singer, J., and Nachmani, S., "Recent Experimental Studies on Buckling of Integrally Stiffened Cylindrical Shells under Axial Compression", TAE Report No. 100, Feb. 1970, Technion Research and Development Foundation, Haifa, Israel.
32. Peterson, J. P., and Anderson, T. K., "Bending Tests of Large-Diameter Ring-Stiffened Corrugated Cylinders", NASA TN D-3336, 1966, Langley Research Center, Hampton, Virginia.
33. Stuhlman, C., DeLuzio, A., and Almroth, B. O., "Influence of Stiffener Eccentricity and End Moment on Stability of Cylinders in Compression", *AIAA J.*, Vol. 4, No. 5, May 1966, pp. 872-877.
34. Singer, J., and Baruch, M., "Effect of Eccentricity of Stiffeners on the General Instability of Stiffened Cylindrical Shells under Hydrostatic Pressure", *J. Mech. Eng. Sci.*, Vol. 5, No. 1, 1963, pp. 23-27.
35. Singer, J., Baruch, M., and Harari, O., "On the Stability of Eccentrically Stiffened Cylindrical Shells under Axial Compression", *Intl. J. of Solids and Structures*, Vol. 3, 1967, pp. 445-470.
36. Singer, J., Baruch, M., and Harari, O., "Inversion of Eccentricity Effect in Stiffened Cylindrical Shell Buckling under External Pressure", *J. Mech. Eng. Sci.*, Vol. 8, 1966, pp. 363-373.

37. Simitzes, G., "Buckling of Eccentrically Stiffened Cylinders under Combined Loads", *AIAA J.*, Vol. 7, No. 2, Feb. 1969, pp. 335-336.
38. Block, D. L., Card, M. F., and Mikulas, M. M., "Buckling of Eccentrically Stiffened Orthotropic Cylinders", NASA TN D-2960, Aug. 1965, Langley Research Center, Hampton, Virginia.
39. McElman, J. A., Mikulas, M. M., and Stein, M., "Static and Dynamic Effects of Eccentric Stiffening of Plates and Cylindrical Shells", *AIAA J.*, Vol. 4, No. 5, May 1966, pp. 887-894.
40. Card, M. F., and Jones, R. M., "Experimental and Theoretical Results for Buckling of Eccentrically Stiffened Cylinders", NASA TN D-3639, Oct. 1966, Langley Research Center, Hampton, Virginia.
41. Singer, J., and Haftka, R., "Buckling of Discretely Ring Stiffened Cylindrical Shells", *Israel J. Technol.*, Vol. 6, No. 2, 1968, pp. 125-137.
42. Block, D. L., "Influence of Ring Stiffeners on Instability of Orthotropic Cylinders in Axial Compression", NASA TN D-2482, October 1964, Langley Research Center, Hampton, Virginia.
43. Singer, J., "The Influence of Stiffener Geometry and Spacing on the Buckling of Axially Compressed Cylindrical and Conical Shells", TAE Report No. 68, October 1967, Technion, Israel Institute of Technology, Haifa, Israel.
44. Schmidt, A. F., "Dynamic Buckling Tests of Aluminum Shells", *Aero. Eng. Review*, Vol. 15, No. 9, Sept. 1956, pp. 54-58.
45. Coppa, A. P., "The Buckling of Circular Cylindrical Shells Subject to Axial Impact", NASA TN D-1510, "Collected Papers on Instability of Shell Structures", pp. 361-400, Dec. 1962.
46. Volmir, A. S., "On the Stability of Dynamically Loaded Cylindrical Shells", *Soviet Physics Doklady*, Vol. 3, Jan.-Feb. 1958, pp. 1287-1289.
47. Agamirov, Y. L., and Volmir, A. S., "Behavior of Cylindrical Shells under Dynamic Loading by Hydrostatic Pressure or by Axial Compression", *Bulletin of the Academy of Sciences, USSR*, No. 3, 1959, pp. 78-83 (Translated in *J. of Amer. Rocket Society*, Vol. 31, No. 1, 1961, pp. 98-101).
48. Coppa, A. P., and Nash, W. A., "Dynamic Buckling of Shell Structures Subject to Longitudinal Impact", Report ASD-TDR-62-774, Aeronautical Systems Div., Wright-Patterson AFB, Ohio, Dec. 1962.

49. Roth, R. S., and Klosner, J. M., "Nonlinear Response of Cylindrical Shells Subjected to Dynamic Axial Loads", *AIAA J.*, Vol. 2, No. 10, Oct. 1964, pp. 1788-1794.
50. Lindberg, H. E., and Herbert, R. E., "Dynamic Buckling of a Thin Cylindrical Shell under Axial Impact", *J. Appl. Mech.*, Vol. 33, March 1966, pp. 105-112.
51. Howell, A. D., "An Analytical and Experimental Study of the Effects of Eccentric Longitudinal Stiffening on the Dynamic Response of Cylindrical Shells", unpublished Ph.D. dissertation, West Virginia University, Morgantown, West Virginia, 1970.
52. Tennyson, R. C., and Tash, J. D., "Dynamic Stability of Circular Cylindrical Shells" (abstract only), *Proc. 3rd Canadian Congress of Applied Mechanics*, P. G. Glockner, ed., Univ. of Calgary, Alberta, May 17-21, 1971, pp. 355-356.
53. Mescall, J., and Tsui, T., "Influence of Damping on the Dynamic Stability of Spherical Caps under Step Pressure Loading", *AIAA J.*, Vol. 9, No. 7, July 1971, pp. 1244-1247.
54. Donnell, L. H., "Stability of Thin-Walled Tubes under Torsion", NACA Rept. 479, 1934.
55. Kraus, H., *Thin Elastic Shells*. New York: John Wiley and Sons, Inc., pp. 200-204, 1967.
56. Singer, J., "On the Equivalence of the Galerkin and Rayleigh-Ritz Methods", *J. of the Royal Aero. Society*, Vol. 66, Sept. 1962, p. 592.
57. Batdorf, S. B., "On the Application of Inverse Differential Operators to the Solution of Cylinder Buckling and Other Problems", *AIAA/ASME 10th Structures, Structural Dynamics and Materials Conference*, pp. 386-391, April 14-16, 1969.
58. Carnahan, B., Luther, H., and Wilkes, J., *Applied Numerical Methods*. New York: John Wiley and Sons, Inc., p. 363, 1969.
59. Zweben, C., and Klosner, J. M., "Dynamic Instability of Circular Cylindrical Shells Having Viscoelastic Cores", *AIAA J.*, Vol. 5, No. 6, June 1967, pp. 1128-1134.
60. Egle, D. M., and Sewall, J. L., "An Analysis of Free Vibration of Orthogonally Stiffened Cylindrical Shells with Stiffeners Treated as Discrete Elements", *AIAA J.*, Vol. 6, No. 3, March 1966, pp. 518-526.

61. Turnbow, J. W., *et al.*, "Crash Survival Design Guide", USAAVLABS TR 70-22, August 1969, U. S. Army Aviation Materiel Labs., Fort Eustis, Virginia.
62. Egle, D. M., and Soder, K. E., "A Theoretical Analysis of the Free Vibration of Discretely Stiffened Cylindrical Shells with Arbitrary End Conditions", NASA CR-1316, June 1969, University of Oklahoma, Norman, Oklahoma.
63. Lighthill, M. J., *Fourier Analysis and Generalized Functions*. Cambridge University Press, pp. 19-20, 1958.

## APPENDIX A

### DERIVATION OF THE KINETIC AND POTENTIAL ENERGIES FOR A DISCRETELY STIFFENED CYLINDRICAL SHELL

#### A.1 Nonlinear Strain-Displacement Formulation

The Donnell [4] nonlinear strain-displacement relations for the shell mid-surface are

$$\begin{aligned}\epsilon_x &= u_{,x} + \frac{1}{2}(w_{,x})^2 \\ \epsilon_y &= v_{,y} + wR^{-1} + \frac{1}{2}(w_{,y})^2 \\ \gamma_{xy} &= u_{,y} + v_{,x} + w_{,x}w_{,y}\end{aligned}\tag{A-1}$$

It is assumed that the stiffeners behave as beam elements and that displacements vary linearly across the stringer depth. Therefore, to satisfy compatibility of displacements where shell and stringer are joined, we may write

$$\begin{aligned}\epsilon_{yr} &= \epsilon_y - zw_{,yy} \\ \epsilon_{xs} &= \epsilon_x - zw_{,xx}\end{aligned}\tag{A-2}$$

#### A.2 Unstiffened Cylinder Strain Energy

The strain energy of the unstiffened shell is found by considering a small element of a thin shell. Since plane stress is assumed to be a valid assumption for a thin shell and the shell material is homogeneous, isotropic, and linearly elastic, the following constitutive relations are appropriate

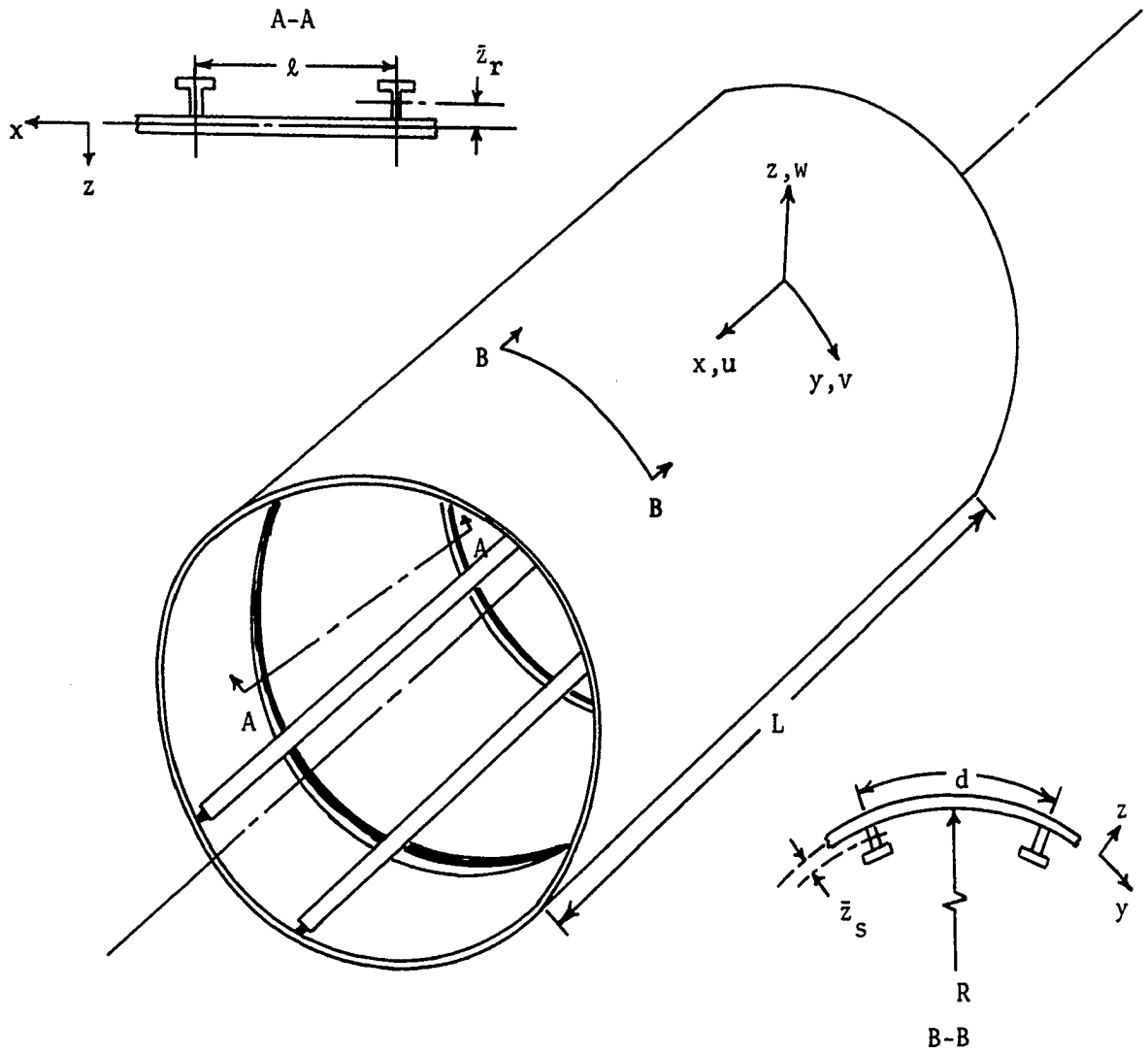


Figure A.1 Shell Geometry

$$\begin{aligned}\sigma_x &= E(1-\nu^2)^{-1}(\epsilon_x + \nu\epsilon_y) \\ \sigma_y &= E(1-\nu^2)^{-1}(\epsilon_y + \nu\epsilon_x) \\ \tau_{xy} &= G\gamma_{xy}\end{aligned}\tag{A-3}$$

The incremental change in strain energy per unit volume for the small element is

$$dU_{vol.} = \sigma_x d\epsilon_x + \sigma_y d\epsilon_y + \tau_{xy} d\gamma_{xy}\tag{A-4}$$

Substituting Equation (A-3) into (A-4) and integrating the result, one obtains the strain energy per unit volume

$$U_{vol.} = E(1-\nu^2)^{-1} \left[ \frac{1}{2}\epsilon_x^2 + \frac{1}{2}\epsilon_y^2 + \nu\epsilon_x\epsilon_y + \frac{1}{4}(1-\nu)\gamma_{xy}^2 \right]\tag{A-5}$$

If Equation (A-5) is integrated over the volume of the unstiffened cylinder, both the extensional and the bending strain energy will be found. This integration yields

$$\begin{aligned}U_{cylinder} &= \frac{1}{2} \int_0^{2\pi R} \int_0^L [Eh(1-\nu^2)^{-1} (\epsilon_x^2 + 2\nu\epsilon_x\epsilon_y + \epsilon_y^2 + \frac{1}{4}(1-\nu)\gamma_{xy}^2) \\ &\quad + D(w_{,xx} + w_{,yy})^2 - 2D(1-\nu)(w_{,xx}w_{,yy} - w_{,xy}^2)] dx dy\end{aligned}\tag{A-6}$$

If the strain displacement relations (A-1) are substituted into Equation (A-6), one obtains

$$\begin{aligned}U_c &= \int_0^{2\pi R} \int_0^L \left\{ Eh(1-\nu^2)^{-1} \left[ \frac{1}{2}u_{,x}^2 + \frac{1}{2}u_{,x}w_{,x}^2 + \left(\frac{1}{8}\right)w_{,x}^4 + \nu u_{,x}v_{,y} + \frac{1}{2}\nu R^{-1}ww_{,x}^2 \right. \right. \\ &\quad \left. \left. + \frac{1}{2}\nu u_{,x}w_{,y}^2 + \frac{1}{4}\nu w_{,x}^2w_{,y}^2 + \nu R^{-1}wu_{,x} + \frac{1}{2}\nu w_{,x}^2v_{,y} + R^{-1}wv_{,y} + \frac{1}{2}v_{,y}^2 + \frac{1}{2}v_{,y}w_{,y}^2 \right. \right. \\ &\quad \left. \left. + \frac{1}{2}R^{-1}ww_{,y}^2 + \left(\frac{1}{8}\right)w_{,y}^4 + \frac{1}{2}(w/R)^2 + \frac{1}{2}(1-\nu) \left( \frac{1}{2}u_{,y}^2 + \frac{1}{2}v_{,x}^2 + u_{,y}w_{,x}w_{,y} + v_{,x}w_{,x}w_{,y} \right) \right] \right\} dx dy\end{aligned}$$

$$+u, y v, x + \frac{1}{2} w, x^2 w, y^2] + D(w,_{xx} w,_{yy})^2 - 2D(1-\nu)(w,_{xx} w,_{yy} - w,_{xy}^2)] dx dy \quad (A-7)$$

### A.3 Ring Strain Energy

The rings are considered as thin curved beam elements, with the strain energy of an individual ring consisting of strain energy due to flexure, extension, and torsion. Thus

$$U_r = \frac{1}{2} \int_0^{2\pi R} \int_0^L (E_r A_r \epsilon_r^2 dA_r + G_r J_r w,_{xy}^2)_{x=j\ell} dy \quad (A-8)$$

Next, the ring strain-displacement relations (A-2) are substituted into Equation (A-8) and integrations are performed over the ring area. The strain energy of N rings becomes

$$U_r = \frac{1}{2} \int_0^{2\pi R} \int_0^L (E_r A_r \epsilon_r^2 - 2E_r A_r \bar{z}_r w,_{yy} \epsilon_r + E_r I_{or} w,_{yy}^2 + G_r J_r w,_{xy}^2) \delta(x-j\ell) dx dy \quad (A-9)$$

where  $\delta(x-j\ell)$  is a Dirac delta function defined by

$$\int_{-\infty}^{\infty} f(x) \delta(x-j\ell) dx = f(j\ell) \quad (x=j\ell) \\ \delta(x-j\ell) = 0 \quad (x \neq j\ell) \quad (A-10)$$

Now, Equation (A-9) is in terms of the strains of the shell middle surface. If the shell strain-displacement relations (A-1) are substituted into (A-9), one obtains

$$U_r = \sum_j \int_0^{2\pi R} \int_0^L \{ E_r A_r [ \frac{1}{2} v, y^2 + v, y R^{-1} w + \frac{1}{2} v, y w, y^2 + \frac{1}{2} R^{-1} w w, y^2 + (\frac{1}{8}) w, y^4 + \frac{1}{2} (w/R)^2 - \bar{z}_r w,_{yy} (v, y + R^{-1} w + \frac{1}{2} w, y^2) ] + \frac{1}{2} E_r I_{or} w,_{yy}^2 + \frac{1}{2} G_r J_r w,_{xy}^2 \} \delta(x-j\ell) dx dy \quad (A-11)$$

#### A.4 Stringer Strain Energy

In an analogous fashion to the derivation of the ring strain energy, the stringer strain energy can be found as

$$U_s = \frac{1}{2} \int_0^{2\pi R} \int_0^L (E_s A_s \epsilon_x^2 - 2E_s A_s \bar{z} w_{,x} \epsilon_x + E_s I_{os} w_{,xx}^2 + G_s J_s w_{,xy}^2) \delta(y-kd) dx dy \quad (A-12)$$

where

$$\int_{-\infty}^{\infty} f(y) \delta(y-kd) dy = f(kd) \quad (y=kd) \quad (A-13)$$

$$\delta(y-kd) = 0 \quad (y \neq kd)$$

As before, Equation (A-1) is substituted into Equation (A-12) to obtain

$$U_s = \sum_k \int_0^{2\pi R} \int_0^L \left\{ E_s A_s \left( \frac{1}{2} u_{,x}^2 + \frac{1}{2} u_{,x} w_{,x}^2 + \frac{1}{8} w_{,x}^4 - \bar{z} w_{,xx} u_{,x} - z w_{,xx} w_{,x}^2 \right) + \frac{1}{2} E_s I_{os} w_{,xx}^2 + \frac{1}{2} G_s J_s w_{,xy}^2 \right\} \delta(y-kd) dx dy \quad (A-14)$$

#### A.5 Potential Energy of External Load

The potential energy of the externally applied load on the end of the stiffened shell is the same as the negative of the work done on the shell. Thus it can be calculated as the product of the applied force and the change of length of the cylinder. Finally, the potential energy due to the load resultant  $\hat{N}_x$  applied at a distance  $\bar{e}$  from the shell middle surface is

$$U_{\text{external load}} = \int_0^{2\pi R} \hat{N}_x (u - \bar{e} w_{,x}) \Big|_0^L dy \quad (A-15)$$

### A.6 Total Potential Energy

The total potential energy is found by adding Equations (A-7), (A-11), (A-14) and (A-15) to obtain

$$\begin{aligned}
 U = & \int_0^{2\pi R} \int_0^L \left\{ Eh(1-\nu^2)^{-1} \left[ \frac{1}{2} u_{,x}^2 + \frac{1}{2} u_{,x} w_{,x}^2 + \frac{1}{8} w_{,x}^4 + \nu u_{,x} v_{,y} + \frac{1}{2} \nu R^{-1} w w_{,x}^2 \right. \right. \\
 & + \frac{1}{2} \nu u_{,x} w_{,y}^2 + \frac{1}{2} \nu w_{,x}^2 w_{,y}^2 + \nu R^{-1} w u_{,x} + \frac{1}{2} \nu w_{,x}^2 v_{,y} + R^{-1} w v_{,y} + \frac{1}{2} v_{,y}^2 + \frac{1}{2} v_{,y} w_{,y}^2 \\
 & + \frac{1}{2} R^{-1} w w_{,y}^2 + \frac{1}{8} w_{,y}^4 + \frac{1}{2} (w/R)^2 + \frac{1}{2} (1-\nu) \left( \frac{1}{2} u_{,y}^2 + \frac{1}{2} v_{,x}^2 + u_{,y} w_{,x} w_{,y} + v_{,x} w_{,x} w_{,y} \right. \\
 & \left. \left. + u_{,y} v_{,x} + \frac{1}{2} w_{,x}^2 w_{,y}^2 \right) \right] + D \left[ (w_{,xx} + w_{,yy})^2 - 2(1-\nu) (w_{,xx} w_{,yy} - w_{,xy}^2) \right] \\
 & + \sum_j \delta(x-j\ell) \left[ \frac{1}{2} E_r I_{or} w_{,yy}^2 + \frac{1}{2} G_r J_r w_{,xy}^2 + E_r A_r \left( \frac{1}{2} v_{,y}^2 + R^{-1} v_{,y} w_{,y} + \frac{1}{2} v_{,y} w_{,y}^2 \right. \right. \\
 & \left. \left. + \frac{1}{2} R^{-1} w w_{,y}^2 + \frac{1}{8} w_{,y}^4 + \frac{1}{2} (w/R)^2 - \bar{z}_r v_{,y} w_{,yy} - z_r R^{-1} w w_{,yy} - \frac{1}{2} \bar{z}_r w_{,yy} w_{,y}^2 \right) \right] \\
 & + \sum_k \delta(y-kd) \left[ \frac{1}{2} E_s I_{os} w_{,xx}^2 + \frac{1}{2} G_s J_s w_{,xy}^2 + E_s A_s \left( \frac{1}{2} u_{,x}^2 + \frac{1}{2} u_{,x} w_{,x}^2 + \frac{1}{8} w_{,x}^4 \right. \right. \\
 & \left. \left. - \bar{z}_s w_{,xx} u_{,x} - \bar{z}_s w_{,xx} w_{,x}^2 \right) \right] \right] dx dy + \int_0^{2\pi R} \hat{N}_x(u-\bar{e}w, x) \Big|_0^L dy \quad (A-16)
 \end{aligned}$$

### A.7 Total Kinetic Energy

Neglecting in-surface and rotatory inertia effects, one may write the kinetic energy of the unstiffened shell as

$$T_{\text{unstiffened shell}} = \frac{1}{2} \rho h \int_0^{2\pi R} \int_0^L w_{,t}^2 dx dy \quad (A-17)$$

In a like manner, the kinetic energy of rings and stringers (referenced to the shell middle surface) may be written as

$$\begin{aligned}
 T_r &= \frac{1}{2} \sum_j \int_0^{2\pi R} \int_0^L \delta(x-j\ell) \rho_r A_r w_{,t}^2 dx dy \\
 T_s &= \frac{1}{2} \sum_k \int_0^{2\pi R} \int_0^L \delta(y-kd) \rho_s A_s w_{,t}^2 dx dy \quad (A-18)
 \end{aligned}$$

APPENDIX B

APPLICATION OF HAMILTON'S PRINCIPLE TO DERIVE  
THE EQUATIONS OF MOTION

The governing equations of motion are obtained from Hamilton's principle, which requires that the first variation of the time-integrated difference between the potential and kinetic energies be zero.

$$\delta \int_{t_1}^{t_2} (U-T) dt = 0 \quad (B-1)$$

Substituting Equations (A-16), (A-17) and (A-18) into Equation (B-1) and performing the variational operation, one obtains

$$\begin{aligned} \delta \int_{t_1}^{t_2} (U-T) dt = & \int_0^t \int_0^{2\pi R} \int_0^L \left\{ Eh(1-\nu^2)^{-1} \left[ u_{,x} + \frac{1}{2} w_{,x}^2 + \nu v_{,y} + \frac{1}{2} \nu w_{,y}^2 + R^{-1} \nu w \right] \delta u_{,x} \right. \\ & + \frac{1}{2} [1-\nu] \left[ u_{,y} + w_{,x} w_{,y} + \nu v_{,x} \right] \delta u_{,y} + \frac{1}{2} [1-\nu] \left[ u_{,y} + w_{,x} w_{,y} + \nu v_{,x} \right] \delta v_{,x} \\ & + [\nu u_{,x} + \frac{1}{2} \nu w_{,x}^2 + \nu v_{,y} + R^{-1} w + \frac{1}{2} w_{,y}^2] \delta v_{,y} + [u_{,x} w_{,x} + \frac{1}{2} w_{,x}^3 + R^{-1} \nu w w_{,x} \\ & + \frac{1}{2} w_{,x} w_{,y}^2 + \nu w_{,x} v_{,y} + \frac{1}{2} (1-\nu) (u_{,y} w_{,y} + \nu v_{,x} w_{,y})] \delta w_{,x} + [\nu u_{,x} w_{,y} \\ & + \frac{1}{2} \nu w_{,x}^2 w_{,y} + \nu v_{,y} w_{,y} + R^{-1} w w_{,y} + \frac{1}{2} w_{,y}^3 + \frac{1}{2} (1-\nu) (u_{,y} w_{,x} + \nu v_{,x} w_{,x} \\ & + w_{,y} w_{,x}^2)] \delta w_{,y} + [\frac{1}{2} \nu R^{-1} w_{,x}^2 + R^{-1} \nu u_{,x} + R^{-1} \nu v_{,y} + \frac{1}{2} R^{-1} w_{,y}^2 \\ & + w(1/R)^2] \delta w \} + D \left\{ [\frac{1}{2} w_{,xx} + \frac{1}{2} \nu w_{,yy}] \delta w_{,xx} + [\frac{1}{2} w_{,y} + \frac{1}{2} \nu w_{,xx}] \right. \\ & \left. \cdot \delta w_{,yy} + [1-\nu] w_{,xy} \delta w_{,xy} \right\} + \sum_j \delta(x-j\ell) \{ E_r A_r [v_{,y} + R^{-1} w + \frac{1}{2} w_{,y}^2 \end{aligned}$$

$$\begin{aligned}
& -\bar{z}_r w_{,yy} \delta v_{,y} + E_r A_r [w_{,y} v_{,y} + R^{-1} w w_{,y} + \frac{1}{2} w_{,y}^3 - \bar{z}_r w_{,yy} w_{,y}] \delta w_{,y} + E_r A_r [R^{-1} v_{,y} \\
& + \frac{1}{2} R^{-1} w_{,y}^2 + w(1/R)^2 - \bar{z}_r R^{-1} w_{,yy}] \delta w + [E_r I_{or} w_{,yy} - E_r A_r \bar{z}_r (v_{,y} + R^{-1} w + \frac{1}{2} w_{,y}^2)] \\
& \cdot \delta w_{,yy} + G_r J_r w_{,xy} \delta w_{,xy} \Big] + \int_k \delta(y-kd) \{ E_s A_s [u_{,x} + \frac{1}{2} w_{,x}^2 - \bar{z}_s w_{,xx}] \delta u_{,x} + E_s A_s [w_{,x} u_{,x} \\
& + \frac{1}{2} w_{,x}^3 - \bar{z}_s w_{,xx} w_{,x}] \delta w_{,x} + [E_s I_{os} w_{,xx} - E_s A_s \bar{z}_s (u_{,x} + \frac{1}{2} w_{,x}^2)] \delta w_{,xx} + G_s J_s w_{,xy} \delta w_{,xy} \} \\
& - \rho h w_{,t} \delta w_{,t} - \int_j \delta(x-jl) \rho_r A_r w_{,t} \delta w_{,t} - \int_k \delta(y-kd) \rho_s A_s w_{,t} \delta w_{,t} \Big\} dx dy dt = 0
\end{aligned}$$

(B-2)

The following illustrations of integrations by parts operations will be performed on Equation (B-2).

$$\begin{aligned}
\int_0^t \int_0^L u_{,x} \delta u_{,x} dx dt &= \int_0^t \{ u_{,x} \delta u \Big|_0^L - \int_0^L u_{,xx} \delta u dx \} dt \\
\int_0^t \int_0^L w_{,x}^2 \delta u_{,x} dx dt &= \int_0^t \{ w_{,x}^2 \delta u \Big|_0^L - \int_0^L (w_{,x})^2_{,x} \delta u dx \} dt \\
\int_0^t \int_0^L v_{,y} \delta u_{,x} dx dt &= \int_0^t \{ v_{,y} \delta u \Big|_0^L - \int_0^L v_{,xy} \delta u dx \} dt \\
\int_0^t \int_0^L w_{,y}^2 \delta u_{,x} dx dt &= \int_0^t \{ w_{,y}^2 \delta u \Big|_0^L - \int_0^L (w_{,y})^2_{,x} \delta u dx \} dt \\
\int_0^t \int_0^{2\pi R} w_{,x} w_{,y} \delta u_{,y} dy dt &= \int_0^t \{ w_{,x} w_{,y} \delta u \Big|_0^{2\pi R} - \int_0^{2\pi R} (w_{,x} w_{,yy} + w_{,xy} w_{,y}) \delta u dx \} dt \\
\int_0^t \int_0^L w_{,xx} \delta w_{,xx} dx dt &= \int_0^t \{ w_{,xx} \delta w_{,x} \Big|_0^L - w_{,xxx} \delta w \Big|_0^L + \int_0^L w_{,xxxx} \delta w dx \} dt \\
\int_0^t \int_0^{2\pi R} \int_0^L w_{,xy} \delta w_{,xy} dx dy dt &= \int_0^t \{ \int_0^L w_{,xy} \delta w_{,x} \Big|_0^{2\pi R} dx - \int_0^{2\pi R} w_{,xyy} \delta w \Big|_0^L dy \\
& + \int_0^{2\pi R} \int_0^L w_{,xyy} \delta w dx dy \} dt
\end{aligned}$$

$$\int_0^t w_{,t} \delta w_{,t} dt = - \int_0^t w_{,tt} \delta w dt$$

Making use of the above integration by parts forms, and performing the indicated operations in Equation (B-2), one obtains the following equation

$$\begin{aligned} \delta \int_{t_1}^{t_2} (U-T) dt = & \int_0^t \left( - \int_0^{2\pi R} \int_0^L \{ Eh(1-\nu^2)^{-1} [u_{,xx} + w_{,x} w_{,xx} + \nu v_{,xy} + v w_{,y} w_{,xy} \right. \\ & + R^{-1} \nu w_{,x} + \frac{1}{2} (1-\nu) (u_{,yy} + w_{,xy} w_{,y} + w_{,x} w_{,yy} + v_{,xy}) \} \\ & + \int_k \delta(y-kd) E_s A_s [u_{,xx} + w_{,x} w_{,xx} - \bar{z} w_{,xxx}] \delta u dx dy \\ & + \int_0^{2\pi R} \{ Eh(1-\nu^2)^{-1} [u_{,x} + \frac{1}{2} w_{,x}^2 + \nu v_{,y} + \frac{1}{2} \nu w_{,y}^2 + R^{-1} \nu w \} \\ & + \int_k \delta(y-kd) E_s A_s [u_{,x} + \frac{1}{2} w_{,x}^2 - \bar{z} w_{,xxx}] + \hat{N}_x \} \delta u \Big|_0^L dy \\ & + \int_0^L \frac{1}{2} Eh(1+\nu)^{-1} \{ u_{,x} + w_{,x} w_{,y} + v_{,x} \} \delta u \Big|_0^{2\pi R} dx - \int_0^{2\pi R} \int_0^L \{ Eh(1-\nu^2)^{-1} \\ & \cdot [\nu u_{,xy} + \nu w_{,x} w_{,xy} + v_{,yy} + R^{-1} w_{,y} + w_{,y} w_{,yy} + \frac{1}{2} (1-\nu) (w_{,xx} w_{,y} \\ & + w_{,x} w_{,xy} + u_{,xy} + v_{,xx}) \} + \int_j \delta(x-j\ell) E_r A_r [v_{,yy} + R^{-1} w_{,y} + w_{,y} w_{,yy} \\ & - \bar{z} w_{,yyy}] \delta v dx dy + \int_0^{2\pi R} \frac{1}{2} Eh(1+\nu)^{-1} \{ w_{,x} w_{,y} + u_{,y} + v_{,x} \} \delta v \Big|_0^L dy \\ & + \int_0^L \{ Eh(1-\nu^2)^{-1} [\nu u_{,x} + \frac{1}{2} \nu w_{,x}^2 + v_{,y} + R^{-1} w_{,y} + \frac{1}{2} w_{,y}^2] + \int_j \delta(x-j\ell) E_r A_r \\ & \cdot [v_{,y} + R^{-1} w_{,y} + \frac{1}{2} w_{,y}^2 - \bar{z} w_{,yyy}] \delta v \Big|_0^{2\pi R} dx + \int_0^{2\pi R} \int_0^L \{ D\nabla^4 w + \rho h w_{,tt} \\ & + \int_j \delta(x-j\ell) \rho_r A_r w_{,tt} + \int_k \delta(y-kd) \rho_s A_s w_{,tt} \} \delta w dx dy \\ & - \int_0^{2\pi R} \int_0^L \{ Eh(1-\nu^2)^{-1} [u_{,xx} w_{,x} + u_{,x} w_{,xx} + 1.5 w_{,x}^2 w_{,xx} + R^{-1} \nu w_{,x}^2 + R^{-1} \nu w w_{,xx} \} \end{aligned}$$

$$\begin{aligned}
& +2w_{,x}w_{,y}w_{,xy} + \frac{1}{2}w_{,y}^2w_{,xx} + vw_{,xx}v_{,y} + vw_{,x}v_{,xy} + \frac{1}{2}vu_{,xy}w_{,y} + \frac{1}{2}u_{,xy}w_{,y} \\
& + vu_{,x}w_{,yy} + \frac{1}{2}vw_{,x}^2w_{,yy} + v_{,yy}w_{,y} + v_{,y}w_{,yy} + R^{-1}w_{,y}^2 + R^{-1}ww_{,yy} + 1.5w_{,y}^2w_{,yy} \\
& + (1-\nu)(u_{,y}w_{,xy} + \frac{1}{2}v_{,xx}w_{,y} + v_{,x}w_{,xy} + \frac{1}{2}u_{,yy}w_{,x} + \frac{1}{2}v_{,xy}w_{,x} \\
& + \frac{1}{2}w_{,yy}w_{,x}^2) - R^{-1}(v_{,y} + R^{-1}w_{,y} + \frac{1}{2}w_{,y}^2 + vu_{,x} + \frac{1}{2}vw_{,x}^2)] + \int_k \delta(y-kd) E_s A_s [w_{,xx}u_{,x} \\
& + w_{,x}u_{,xx} + 1.5w_{,x}^2w_{,xx} - \bar{z}_s w_{,xx}^2 - \bar{z}_s w_{,x}w_{,xx} + \bar{z}_s u_{,xxx} - \bar{z}_s w_{,xx}^2 - \bar{z}_s w_{,x}w_{,xxx} \\
& - (I_{os}/A_s)w_{,xxxx} - (G_s J_s/E_s A_s)w_{,xxyy}] + \int_j \delta(x-j\ell) E_r A_r [w_{,yy}v_{,y} \\
& + w_{,y}v_{,yy} + R^{-1}w_{,y}^2 + R^{-1}ww_{,yy} + 1.5w_{,y}^2w_{,yy} - \bar{z}_r w_{,yy}^2 - \bar{z}_r w_{,y}w_{,yyy} - R^{-1}v_{,y} \\
& - \frac{1}{2}R^{-1}w_{,y}^2 - w(1/R)^2 + \bar{z}_r R^{-1}w_{,yy} + \bar{z}_r v_{,yyy} + \bar{z}_r R^{-1}w_{,yy} - (I_{or}/A_r)w_{,yyyy} \\
& - (G_r J_r/E_r A_r)w_{,xxyy} + \bar{z}_r w_{,yy}^2 + \bar{z}_r w_{,y}w_{,yyy}] + \int_k \delta_y(y-kd) G_s J_s w_{,xxy} \\
& + \int_j \delta_x(x-j\ell) G_r J_r w_{,xxy} \} \delta w dx dy + \int_0^L \{ D[-w_{,yyy} - vw_{,xxy}] + Eh(1-\nu^2)^{-1} \\
& \cdot [vu_{,x}w_{,y} + \frac{1}{2}vw_{,x}^2w_{,y} + v_{,y}w_{,y} + R^{-1}ww_{,y} + \frac{1}{2}w_{,y}^3 + \frac{1}{2}(1-\nu)(u_{,y}w_{,x} + v_{,x}w_{,x} \\
& + w_{,y}w_{,x}^2)] + \int_j \delta(x-j\ell) E_r A_r [\bar{w}_{,y}v_{,y} + R^{-1}ww_{,y} + \frac{1}{2}w_{,y}^3 - \bar{z}_r w_{,yy}w_{,y} - (I_{or}/A_r) \\
& \cdot w_{,yyy} + \bar{z}_r v_{,yy} + \bar{z}_r R^{-1}w_{,y} + \bar{z}_r w_{,y}w_{,yy}] \} \delta w \int_0^{2\pi R} dx + \int_0^{2\pi R} \{ D[-w_{,xxx} - 2w_{,xxy} \\
& + vw_{,xxy}] + Eh(1-\nu^2)^{-1} [u_{,x}w_{,x} + \frac{1}{2}w_{,x}^3 + vR^{-1}ww_{,x} + \frac{1}{2}w_{,y}^2w_{,x} + vw_{,x}v_{,y} \\
& + \frac{1}{2}(1-\nu)(u_{,y}w_{,y} + v_{,x}w_{,y} + w_{,x}w_{,y}^2)] - \int_k \delta_y(y-kd) G_s J_s w_{,xy} - \int_j \delta_x(x-j\ell) \\
& \cdot G_r J_r w_{,xxy} + \int_k \delta(y-kd) E_s A_s [w_{,x}u_{,x} + \frac{1}{2}w_{,x}^3 + \bar{z}_s w_{,xx}w_{,x} + \bar{z}_s u_{,xx} - (I_{os}/A_s)
\end{aligned}$$

$$\begin{aligned}
& \cdot w_{,xxx} - (G_s J_s / E_s A_s) w_{,xyy} \} \delta w \Big|_0^L dy + \int_0^L \{ 2D(1-\nu) w_{,xy} + \sum_j \delta(x-j\ell) G_r J_r \\
& \cdot w_{,xy} + \sum_k \delta(y-kd) G_s J_s w_{,xy} \} \delta w_{,x} \Big|_0^{2\pi R} dx + \int_0^{2\pi R} \{ D[w_{,xx} + \nu w_{,yy}] \\
& - \sum_k \delta(y-kd) E_s A_s [\bar{z}_s u_{,x} + \bar{z}_s w_{,x}^2 - (I_{os}/A_s) w_{,xx}] - \hat{N}_x \bar{e} \} \delta w_{,x} \Big|_0^L dy \\
& + \int_0^L \{ D[w_{,yy} + \nu w_{,xx}] - \sum_j \delta(x-j\ell) E_r A_r [\bar{z}_r v_{,y} + \bar{z}_r R^{-1} w_{,y} + \frac{1}{2} \bar{z}_r w_{,y}^2 - (I_{or}/A_r) \\
& \cdot w_{,yy} \} \delta w_{,y} \Big|_0^{2\pi R} dx \} dt = 0 \tag{B-3}
\end{aligned}$$

Since the variation of the function with  $\theta$  is periodic, all of the terms in Equation (B-3) that are evaluated between zero and  $2\pi R$  reduce to zero. The three equations of motion ( $u, v, w$ ) and all relevant boundary conditions can now be extracted from Equation (B-3).

To simplify the governing equations, we make use of the notation advanced by Kraus [50], and define the following terms

$$\begin{aligned}
N_x = Eh(1-\nu^2)^{-1} [u_{,x} + \frac{1}{2} w_{,x}^2 + \nu (v_{,y} + R^{-1} w_{,y} + \frac{1}{2} w_{,y}^2)] + \sum_k \delta(y-kd) E_s A_s (u_{,x} + \frac{1}{2} w_{,x}^2 \\
- \bar{z}_s w_{,xx}) \tag{B-4}
\end{aligned}$$

$$\begin{aligned}
N_y = Eh(1-\nu^2)^{-1} [v_{,y} + R^{-1} w_{,y} + \frac{1}{2} w_{,y}^2 + \nu (u_{,x} + \frac{1}{2} w_{,x}^2)] + \sum_j \delta(x-j\ell) E_r A_r \\
(v_{,y} + R^{-1} w_{,y} + \frac{1}{2} w_{,y}^2 - \bar{z}_r w_{,yy}) \tag{B-5}
\end{aligned}$$

$$N_{xy} = \frac{1}{2} Eh(1+\nu)^{-1} (u_{,y} + \nu v_{,x} + w_{,x} w_{,y}) \tag{B-6}$$

$$M_x = -D(w_{,xx} + \nu w_{,yy}) - \sum_k \delta(y-kd) E_s A_s [(I_{os}/A_s) w_{,xx} - \bar{z}_s u_{,x} - \frac{1}{2} \bar{z}_s w_{,x}^2] \tag{B-7}$$

$$\begin{aligned}
M_y = -D(w_{,yy} + \nu w_{,xx}) - \sum_j \delta(x-j\ell) E_r A_r [(I_{or}/A_r) w_{,yy} - \bar{z}_r v_{,y} - \bar{z}_r R^{-1} w_{,y} \\
- \frac{1}{2} \bar{z}_r w_{,y}^2] \tag{B-8}
\end{aligned}$$

$$M_{xy} = -D(1-\nu) w_{,xy} - \frac{1}{2} \sum_k \delta(y-kd) G_s J_s w_{,xy} - \frac{1}{2} \sum_j \delta(x-j\ell) G_r J_r w_{,xy} \tag{B-9}$$

The three equations of motion (u,v,w) can now be extracted from Equation (B-3) and written as

$$N_{x,x} + N_{xy,y} = 0 \quad (\text{B-10a})$$

$$N_{y,y} + N_{xy,x} = 0 \quad (\text{B-10b})$$

$$\begin{aligned} & -M_{x,xx} - 2M_{xy,xy} - M_{y,yy} + R^{-1}N_y - N_x w_{,xx} - N_y w_{,yy} - 2N_{xy} w_{,xy} \\ & + \rho h w_{,tt} + \int_j \delta(x-j\ell) \rho_r A_r w_{,tt} + \int_k \delta(y-kd) \rho_s A_s w_{,tt} = 0 \end{aligned} \quad (\text{B-10c})$$

In a like manner, the boundary conditions which apply at the ends of the cylinder can be extracted from Equation (B-3) and written as

$$N_x + \hat{N}_x = 0 \quad \text{or} \quad u = 0 \quad (\text{B-11a})$$

$$N_{xy} = 0 \quad \text{or} \quad v = 0 \quad (\text{B-11b})$$

$$M_x + \hat{N}_x \bar{e} = 0 \quad \text{or} \quad w_{,x} = 0 \quad (\text{B-11c})$$

$$M_{x,x} + 2M_{xy,y} + N_x w_{,x} + N_{xy} w_{,y} = 0 \quad \text{or} \quad w = 0 \quad (\text{B-11d})$$

## APPENDIX C

### APPLICATION OF GALERKIN'S METHOD TO OBTAIN A SET OF ORDINARY NONLINEAR GOVERNING DIFFERENTIAL EQUATIONS

To correctly apply Galerkin's method, one must have the error functions  $Q_x$ ,  $Q_y$  and  $Q_z$  orthogonal to the assumed mode solutions. The error functions are formed by substituting the assumed displacement functions (2-18) into the buckling equations of motion (2-16). The orthogonalization equations are Equations (2-19), (2-20) and (2-21).

Obviously, a number of terms in each orthogonalization equation will integrate to zero. For ease in identifying and keeping track of the various terms, a table is constructed for each of the orthogonalization equations. In the following development, the B subscript is dropped as understood.

Table C.1 contains the final integrated results of Equation (2-19), which is repeated below for easy reference

$$\int_0^{2\pi R} \int_0^L Q_x(u, v, w) \sin(\zeta m \pi x / L) \cos(\xi n y / R) dx dy = 0 \quad \begin{matrix} \zeta = 1, 2, 3 \dots \\ \xi = 1, 2, 3 \dots \end{matrix} \quad (2-19)$$

Thus, after integration, Equation (2-19) becomes:

$$\delta_{i\zeta} \sum u_{ij} [ I_i^2 \delta_{j\xi} + \frac{1}{2} (1-\nu) J_j^2 \delta_{j\xi} + (1-\nu^2) (\pi R E h)^{-1} I_k^2 \sum_s E_s A_s \cos J_k \cos J_\xi ]$$

Table C.1. Integrated Terms from Axial Equation of Motion.

TERM	FINAL INTEGRATED RESULT
$u_{,xx}$	$-\frac{1}{2}\Delta_1 Eh\pi RL(1-\nu^2)^{-1} \Sigma \Sigma u_{ij} I_i^2$
$w_{,x} w_{,xx}$	$\Delta_5 (Eh\pi RL/8) (1-\nu^2)^{-1} \Sigma \Sigma w_{ij}^2 I_i^3$
$\nu v_{,xy}$	$-\frac{1}{2}\Delta_1 Eh\pi RL\nu(1-\nu^2)^{-1} \Sigma \Sigma v_{ij} I_i J_j$
$\nu R^{-1} w_{,x}$	$-\frac{1}{2}\Delta_1 Eh\pi L\nu(1-\nu^2)^{-1} \Sigma \Sigma w_{ij} I_i$
$\nu w_{,y} w_{,xy}$	$\Delta_5 (Eh\pi RL\nu/8) (1-\nu^2)^{-1} \Sigma \Sigma w_{ij}^2 I_i J_j^2$
$u_{,yy}$	$-\frac{1}{4}\Delta_1 Eh\pi RL(1+\nu)^{-1} \Sigma \Sigma u_{ij} J_j^2$
$v_{,xy}$	$-\frac{1}{4}\Delta_1 Eh\pi RL(1+\nu)^{-1} \Sigma \Sigma v_{ij} I_i J_j$
$w_{,xy} w_{,y}$	$\Delta_5 (Eh\pi RL/16) (1+\nu)^{-1} \Sigma \Sigma w_{ij}^2 I_i J_j^2$
$w_{,x} w_{,yy}$	$\Delta_5 (Eh\pi RL/16) (1+\nu)^{-1} \Sigma \Sigma w_{ij}^2 I_i J_j^2$
$u_{,xx}$	$-\frac{1}{2}\delta_{i\zeta} L \Sigma \Sigma u_{ij} I_i^2 \int_k^{\Gamma} E_s A_s \cos J_k \cos J_\xi$
$w_{,x} w_{,xx}$	$\frac{1}{4}\delta_{2i\zeta} L \Sigma \Sigma w_{ij}^2 I_i^3 \int_k^{\Gamma} E_s A_s \cos^2 J_k \cos J_\xi$
$-\bar{z}_s w_{,xxx}$	$-\frac{1}{2}\delta_{i\zeta} L \Sigma \Sigma w_{ij} I_i^3 \int_k^{\Gamma} E_s A_s \bar{z}_s \cos J_k \cos J_\xi$

$$\begin{aligned}
& + \Delta_1 \Sigma \Sigma v_{ij} \frac{1}{2} (1+v) I_{ij} J_j + \delta_{i\zeta} \Sigma \Sigma w_{ij} [R^{-1} v I_{ij} \delta_{j\xi} + (1-v^2) (\pi R E h)^{-1} I_{ik}^3 \Sigma E_s A_s \bar{z}_s \\
& \cdot \cos J_k \cos J_\xi] - \delta_{2i\zeta} \Sigma \Sigma w_{ij}^2 [\frac{1}{4} I_{ij} J_j^2 \delta_{2j\xi} + \frac{1}{4} I_i^3 \delta_{2j\xi} \\
& + (1-v^2) (2E\pi R)^{-1} I_{ik}^3 \Sigma E_s A_s \cos^2 J_k \cos J_\xi] = 0 \tag{C-1}
\end{aligned}$$

In a similar manner, Equation (2-20) may be evaluated. (The details of integration are contained in Table C.2.)

$$\int_0^{2\pi R} \int_0^L Q_y(u, v, w) \cos(\zeta \pi x / L) \sin(\xi \pi y / R) dx dy = 0 \quad \begin{array}{l} \zeta = 1, 2, 3, \dots \\ \xi = 1, 2, 3, \dots \end{array} \tag{2-20}$$

After integration, Equation (2-20) becomes

$$\begin{aligned}
& \Delta_1 \Sigma \Sigma u_{ij} \frac{1}{2} (1+v) I_{ij} J_j + \delta_{j\xi} \Sigma \Sigma v_{ij} [J_j^2 \delta_{i\zeta} + \frac{1}{2} (1-v) I_i^2 \delta_{i\zeta} + 2(1-v^2) (EhL)^{-1} \\
& \cdot J_j^2 \Sigma E_r A_r \cos I_j \cos I_\zeta] + \delta_{j\xi} \Sigma \Sigma w_{ij} [R^{-1} J_j \delta_{i\zeta} + 2(1-v^2) (EhL)^{-1}] \Sigma (R^{-1} J_j E_r A_r \\
& + J_j^3 E_r A_r \bar{z}_r) \cos I_j \cos I_\zeta - \delta_{2j\xi} \Sigma \Sigma w_{ij}^2 [\frac{1}{4} J_j^3 \delta_{2i\zeta} + \frac{1}{4} I_i^2 J_j \delta_{2i\zeta} + (1-v^2) (EhL)^{-1} \\
& \cdot J_j^3 \Sigma E_r A_r \cos^2 I_j \cos I_\zeta] = 0 \tag{C-2}
\end{aligned}$$

Finally, Equation (2-21) may be evaluated. Details of this integration are contained in Tables C.3, C.4 and C.5.

$$\int_0^{2\pi R} \int_0^L Q_z(u, v, w) \cos(\zeta \pi x / L) \cos(\xi \pi y / R) dx dy = 0 \quad \begin{array}{l} \zeta = 1, 2, 3, \dots \\ \xi = 1, 2, 3, \dots \end{array} \tag{2-21}$$

The last entries in Tables C.4 and C.5 are expanded here for clarity. They hinge on the definition of the derivative of a Dirac delta function found in reference [62].

$$\int_{-\infty}^{\infty} x(t) \delta^{(k)}(t-\psi) dt = (-1)^k x^{(k)}(\psi)$$

Table C.2. Integrated Terms from Circumferential Equation of Motion

TERM	FINAL INTEGRATED RESULT
$v_{,yy}$	$-\frac{1}{2}\Delta_1 Eh\pi RL(1-\nu^2)^{-1} \Sigma \Sigma v_{ij} J_j^2$
$R^{-1}w_{,y}$	$-\frac{1}{2}\Delta_1 Eh\pi L(1-\nu^2)^{-1} \Sigma \Sigma w_{ij} J_j$
$w_{,y}w_{,yy}$	$\Delta_5 (Eh\pi RL/8) (1-\nu^2)^{-1} \Sigma \Sigma w_{ij}^2 J_j^3$
$\nu u_{,xy}$	$-\frac{1}{2}\Delta_1 Eh\pi RL\nu(1-\nu^2)^{-1} \Sigma \Sigma u_{ij} I_i J_j$
$\nu w_{,x}w_{,xy}$	$\Delta_5 (Eh\pi RL\nu/8) (1-\nu^2)^{-1} \Sigma \Sigma w_{ij}^2 I_i J_j$
$u_{,xy}$	$-\frac{1}{4}\Delta_1 Eh\pi RL(1+\nu)^{-1} \Sigma \Sigma u_{ij} I_i J_j$
$v_{,xx}$	$-\frac{1}{4}\Delta_1 Eh\pi RL(1+\nu)^{-1} \Sigma \Sigma v_{ij} I_i^2$
$w_{,xx}w_{,y}$	$\Delta_5 (Eh\pi RL/16) (1+\nu)^{-1} \Sigma \Sigma w_{ij}^2 I_i^2 J_j$
$w_{,x}w_{,xy}$	$\Delta_5 (Eh\pi RL/16) (1+\nu)^{-1} \Sigma \Sigma w_{ij}^2 I_i^2 J_j$
$v_{,yy}$	$-\delta_{j\xi} \pi R \Sigma \Sigma v_{ij} J_j^2 \int_r^z E A_r \cos I_j \cos I_\zeta$
$R^{-1}w_{,y}$	$-\delta_{j\xi} \pi \Sigma \Sigma w_{ij} J_j \int_r^z E A_r \cos I_j \cos I_\zeta$
$w_{,y}w_{,yy}$	$\frac{1}{2}\delta_{2j\xi} \pi R \Sigma \Sigma w_{ij}^2 J_j^3 \int_r^z E A_r \cos^2 I_j \cos I_\zeta$
$-\bar{z}_r w_{,yyy}$	$-\delta_{j\xi} \pi R \Sigma \Sigma w_{ij} J_j^3 \int_r^z E A_r \bar{z}_r \cos I_j \cos I_\zeta$

**Table C.3** Unstiffened Cylinder Integrated Terms from Radial Equation of Motion

TERM	FINAL INTEGRATED RESULT
$-\frac{1}{2}w_x^2 w_{xx}$	$Eh(1-\nu^2)^{-1}(\pi RL/64)(3\Delta_1 + \Delta_2 - 3\Delta_3 - \Delta_4)\Sigma\Sigma w_{ij}^3 I_i^4$
$-\frac{1}{2}\nu w_y^2 w_{xx}$	$Eh(1-\nu^2)^{-1}(\nu\pi RL/64)(3\Delta_1 - 3\Delta_2 + \Delta_3 - \Delta_4)\Sigma\Sigma w_{ij}^3 I_i^2 J_j^2$
$-\frac{1}{2}w_y^2 w_{yy}$	$Eh(1-\nu^2)^{-1}(\pi RL/64)(3\Delta_1 - 3\Delta_2 + \Delta_3 - \Delta_4)\Sigma\Sigma w_{ij}^3 J_j^4$
$-\frac{1}{2}\nu w_x^2 w_{yy}$	$Eh(1-\nu^2)^{-1}(\nu\pi RL/64)(3\Delta_1 + \Delta_2 - 3\Delta_3 - \Delta_4)\Sigma\Sigma w_{ij}^3 I_i^2 J_j^2$
$-w_x w_y w_{xy}$	$Eh(1-\nu^2)^{-1}(\pi RL/32)(1-\nu)(-\Delta_1 + \Delta_2 + \Delta_3 - \Delta_4)\Sigma\Sigma w_{ij}^3 I_i^2 J_j^2$
$w_{xxxx}$	$\frac{1}{2}\Delta_1 D\pi RL\Sigma\Sigma w_{ij}^4 I_i^4$
$2w_{xxyy}$	$\Delta_1 D\pi RL\Sigma\Sigma w_{ij}^2 I_i^2 J_j^2$
$w_{yyyy}$	$\frac{1}{2}\Delta_1 D\pi RL\Sigma\Sigma w_{ij}^2 J_j^2$
$-u_x w_{xx}$	$\Delta_5 Eh\pi RL(1-\nu^2)^{-1} \frac{1}{8}\Sigma\Sigma u_{ij} w_{ij}^3 I_i^3$
$-\nu v_y w_{xx}$	$\Delta_5 Eh\nu\pi RL(1-\nu^2)^{-1} \frac{1}{8}\Sigma\Sigma v_{ij} w_{ij}^2 I_i^2 J_j$
$-\nu R^{-1} w w_{xx}$	$\Delta_5 Eh\nu\pi L(1-\nu^2)^{-1} \frac{1}{8}\Sigma\Sigma w_{ij}^2 I_i^2$
$-v_y w_{yy}$	$\Delta_5 Eh\pi RL(1-\nu^2)^{-1} \frac{1}{8}\Sigma\Sigma v_{ij} w_{ij}^3 J_j^3$
$-w R^{-1} w_{yy}$	$\Delta_5 Eh\pi L(1-\nu^2)^{-1} \frac{1}{8}\Sigma\Sigma w_{ij}^2 J_j^2$
$-\nu u_x w_{yy}$	$\Delta_5 Eh\nu\pi RL(1-\nu^2)^{-1} \frac{1}{8}\Sigma\Sigma u_{ij} w_{ij}^2 I_i J_j^2$
$-u_y w_{xy}$	$\Delta_5 Eh\pi RL(1+\nu)^{-1} \frac{1}{8}\Sigma\Sigma u_{ij} w_{ij}^2 I_i J_j^2$

Table C.3 Continued

Table C.3 (Cont'd.)

TERM	FINAL INTEGRATED RESULT
$-v_{,x} w_{,xy}$	$\Delta_5 E h \pi R L (1+v)^{-1} \frac{1}{8} \Sigma \Sigma v_{ij} w_{ij} I_i^2 J_j$
$v_{,y}$	$\frac{1}{2} \Delta_1 E h \pi L (1-v^2)^{-1} \Sigma \Sigma v_{ij} J_j$
$R^{-1} w$	$\frac{1}{2} \Delta_1 E h \pi L R^{-1} (1-v^2)^{-1} \Sigma \Sigma w_{ij}$
$\frac{1}{2} w_{,y}^2$	$-\Delta_5 E h \pi L (1-v^2)^{-1} (1/16) \Sigma \Sigma w_{ij}^2 J_j^2$
$v u_{,x}$	$\frac{1}{2} \Delta_1 E h \pi L v (1-v^2)^{-1} \Sigma \Sigma u_{ij} I_i$
$\frac{1}{2} v w_{,x}^2$	$-\Delta_5 E h v \pi L (1-v^2)^{-1} (1/16) \Sigma \Sigma w_{ij}^2 I_i^2$
$\rho h w_{,tt}$	$\frac{1}{2} \Delta_1 \rho h \pi R L \Sigma \Sigma \ddot{w}_{ij}$
$\hat{N}_x w_{,xx}$	$-\frac{1}{2} \Delta_1 \hat{N}_x \pi R L \Sigma \Sigma w_{ij} I_i^2$

Table C.4 Ring Integrated Terms from Radial Equation of Motion.

TERM	FINAL INTEGRATED RESULT
$(I_{or}/A_r)w,yyyy$	$\delta_{j\xi} \pi R \Sigma \Sigma w_{ij} J_j^4 \int_j^L E_r I_{or} \cos I_j \cos I_\zeta$
$-\bar{z}_r v,yyy$	$\delta_{j\xi} \pi R \Sigma \Sigma v_{ij} J_j^3 \int_j^L E_r A_r \bar{z}_r \cos I_j \cos I_\zeta$
$-2\bar{z}_r R^{-1}w,yy$	$2\delta_{j\xi} \pi \Sigma \Sigma w_{ij} J_j^2 \int_j^L E_r A_r \bar{z}_r \cos I_j \cos I_\zeta$
$-\bar{z}_r w,y^w,yyy$	$-\frac{1}{2}\delta_{2j\xi} \pi R \Sigma \Sigma w_{ij} J_j^4 \int_j^L E_r A_r \bar{z}_r \cos^2 I_j \cos I_\zeta$
$(G_{rr} J_{rr} / E_r A_r)w,xyy$	$\delta_{j\xi} \pi R \Sigma \Sigma w_{ij} J_j^2 I_j^2 \int_j^L G_{rr} J_{rr} \cos I_j \cos I_\zeta$
$-v,y^w,yy$	$\frac{1}{2}\delta_{2j\xi} \pi R \Sigma \Sigma v_{ij} w_{ij} J_j^3 \int_j^L E_r A_r \cos^2 I_j \cos I_\zeta$
$-wR^{-1}w,yy$	$\frac{1}{2}\delta_{2j\xi} \pi \Sigma \Sigma w_{ij} J_j^2 \int_j^L E_r A_r \cos^2 I_j \cos I_\zeta$
$-\frac{1}{2}w_y^2,yy$	$(\delta_{j\xi} - \delta_{3j\xi}) (\pi/8) \Sigma \Sigma w_{ij} J_j^4 \int_j^L E_r A_r \cos^3 I_j \cos I_\zeta$
$v,y$	$\delta_{j\xi} \pi \Sigma \Sigma v_{ij} J_j \int_j^L E_r A_r \cos I_j \cos I_\zeta$
$R^{-1}w$	$\delta_{j\xi} \pi R^{-1} \Sigma \Sigma w_{ij} \int_j^L E_r A_r \cos I_j \cos I_\zeta$
$\frac{1}{2}w_y^2$	$-\frac{1}{4}\delta_{2j\xi} \pi \Sigma \Sigma w_{ij} J_j^2 \int_j^L E_r A_r \cos^2 I_j \cos I_\zeta$
$\rho_{rr} A_r w,tt$	$\delta_{j\xi} \rho_{rr} A_r \pi R \Sigma \Sigma \dot{w}_{ij} \int_j^L \cos I_j \cos I_\zeta$
$G_{rr} J_{rr} w,xyy \delta_x(x-jl)$	$\delta_{j\xi} \pi R \Sigma \Sigma w_{ij} J_j^2 I_j \int_j^L G_{rr} J_{rr} (\zeta \pi L^{-1} \sin I_j \sin I_\zeta - I_j \cos I_j \cos I_\zeta)$

Table C.5 Stringer Integrated Terms from Radial Equation of Motion.

TERM	FINAL INTEGRATED RESULT
$(I_{os}/A_s)w_{,xxxx}$	$\frac{1}{2}\delta_{i\zeta} L\Sigma\Sigma w_{,ij} I_k^4 \int E I_{os} \cos J_k \cos J_\xi$
$-\bar{z}_s u_{,xxx}$	$\frac{1}{2}\delta_{i\zeta} L\Sigma\Sigma u_{,ij} I_k^3 \int E A_s \bar{z}_s \cos J_k \cos J_\xi$
$-\bar{z}_s w_{,x} w_{,xxx}$	$-\frac{1}{4}\delta_{2i\zeta} L\Sigma\Sigma w_{,ij} I_k^2 \int E A_s \bar{z}_s \cos^2 J_k \cos J_\xi$
$(G_{s's'}^j/E_{s's'})w_{,xxyy}$	$\frac{1}{2}\delta_{i\zeta} L\Sigma\Sigma w_{,ij} I_k^2 \int G_{s's'}^j \cos J_k \cos J_\xi$
$-u_{,x} w_{,xx}$	$\frac{1}{4}\delta_{2i\zeta} L\Sigma\Sigma u_{,ij} w_{,ij} I_k^3 \int E A_s \cos^2 J_k \cos J_\xi$
$-\frac{1}{2}w_{,x}^2 w_{,xx}$	$(\delta_{i\zeta} - \delta_{3i\zeta})L/16\Sigma\Sigma w_{,ij} I_k^4 \int E A_s \cos^3 J_k \cos J_\xi$
$\rho_{s's'} A_s w_{,tt}$	$\frac{1}{2}\delta_{i\zeta} \rho_{s's'} A_s L\Sigma\Sigma \ddot{w}_{,ij} \int \cos J_k \cos J_\xi$
$G_{s's'}^j w_{,xxy} \delta_{,y}(y-kd)$	$\frac{1}{2}\delta_{i\zeta} L\Sigma\Sigma w_{,ij} I_k^2 \int G_{s's'}^j (\xi n R^{-1} \sin J_k \sin J_\xi - J_j \cos J_k \cos J_\xi)$

Applying the above equation to the last term in Table C.5, one obtains the following results:

$$\int_0^{2\pi R} \int_0^L [\Sigma \Sigma w_{ij} G_{ij} J_s^2 I_i^2 J_j^2 \delta_{ij} (y-kd) \cos(\frac{\pi x}{L}) \cos(\zeta \pi x/L) \sin(J_j y) \cos(\xi n y/R)] dx dy$$

$$= \Sigma \Sigma w_{ij} \frac{1}{2} G_{ij} J_s^2 I_i^2 J_j^2 \left[ -J_j \cos(J_j y) \cos(\xi n y/R) \Big|_{y=kd} + (\xi n/R) \sin(J_j y) \sin(\xi n y/R) \Big|_{y=kd} \right]$$

Thus, after integration of Equation (2-21), one obtains the following expression:

$$\begin{aligned} & Eh(1-\nu^2)^{-1} \frac{1}{32} \Sigma \Sigma w_{ij}^3 [I_i^4 (3\Delta_1 + \Delta_2 - 3\Delta_3 - \Delta_4) + 2I_i^2 J_j^2 (-\Delta_1 + \Delta_2 + \Delta_3 - \Delta_4 + 4\nu\Delta_1 - 2\nu\Delta_2 \\ & - 2\nu\Delta_3) + J_j^4 (3\Delta_1 - 3\Delta_2 + \Delta_3 - \Delta_4)] + (2/L) \Sigma \Sigma w_{ij}^3 (\delta_{ij} \xi - \delta_{3j} \xi) \frac{1}{8} J_j^4 \int E_r A_r \cos^3 I_j \cos I_\zeta \\ & + (1/\pi R) \Sigma \Sigma w_{ij}^3 (\delta_{i\zeta} - \delta_{3i\zeta}) \frac{1}{8} I_i^4 \int E_s A_s \cos^3 J_k \cos J_\xi + \Delta_5 Eh(1-\nu^2)^{-1} (\nu/8R) \\ & \cdot \Sigma \Sigma w_{ij} (I_i^2 + J_j^2) + \delta_{2j} \xi (2/L) \Sigma \Sigma w_{ij}^2 (\frac{1}{4} R^{-1} J_j^2 - \frac{1}{2} J_j^4 z_r) \int E_r A_r \cos^2 I_j \cos I_\zeta - \delta_{2i\zeta} \\ & \cdot (1/\pi R) \Sigma \Sigma w_{ij}^2 \frac{1}{2} I_i^4 \int E_s A_s \bar{z}_s \cos^2 J_k \cos J_\xi + \Delta_1 Eh(1-\nu^2)^{-1} \Sigma \Sigma w_{ij} [(h^2/12) I_i^4 \\ & + (h^2/6) I_i^2 J_j^2 + (h^2/12) J_j^4 + (1/R^2) - \hat{N}_x (1-\nu^2) I_i^2 (Eh)^{-1}] + \delta_{j\xi} (2/L) \Sigma \Sigma w_{ij} \\ & \cdot [J_j^4 E_r I_{or} + 2R^{-1} J_j^2 E_r A_r \bar{z}_r + (1/R^2) E_r A_r] \int \cos I_j \cos I_\zeta + \delta_{j\xi} (2/L) \Sigma \Sigma w_{ij} \\ & \cdot J_j^2 I_i \int G_r J_r \zeta \pi L^{-1} \sin I_j \sin I_\zeta + \delta_{i\zeta} (1/\pi R) \Sigma \Sigma w_{ij} I_i^4 \int E_s I_{os} \cos J_k \cos J_\xi \\ & + \delta_{i\zeta} (1/\pi R) \Sigma \Sigma w_{ij} I_i^2 J_j \int G_s J_s \xi n R^{-1} \sin J_k \sin J_\xi + \Delta_1 Eh(1-\nu^2)^{-1} \nu R^{-1} \Sigma \Sigma u_{ij} I_i \\ & + \delta_{i\zeta} (1/\pi R) \Sigma \Sigma u_{ij} I_i^3 \int E_s A_s \bar{z}_s \cos J_k \cos J_\xi + \Delta_1 Eh(1-\nu^2)^{-1} R^{-1} \Sigma \Sigma v_{ij} J_j \end{aligned}$$

$$\begin{aligned}
& +\delta_{j\xi} (2/L) \Sigma \Sigma v_{ij} (J_j^3 \bar{z}_R + J_j R^{-1}) \int_j E_r A_r \cos I_j \cos I_\zeta + \Delta \frac{1}{5} E h (1-v^2)^{-1} \Sigma \Sigma u_{ij} w_{ij} \\
& \cdot (I_i^3 + I_i J_j^2) + \delta_{2i\zeta} (1/\pi R) \Sigma \Sigma u_{ij} w_{ij} \frac{1}{2} I_k^3 \int_k E_s A_s \cos^2 J_k \cos J_\xi + \Delta \frac{1}{5} E h (1-v^2)^{-1} \\
& \cdot \Sigma \Sigma v_{ij} w_{ij} (J_j^3 + I_i^2 J_j) + \delta_{2j\xi} L^{-1} \Sigma \Sigma v_{ij} w_{ij} J_j^3 \int_j E_r A_r \cos^2 I_j \cos I_\zeta + \Sigma \Sigma \ddot{w}_{ij} \\
& \cdot [\Delta_1 \rho h + \delta_{j\xi} \rho A_r (2/L) \int_j \cos I_j \cos I_\zeta + \delta_{i\zeta} \rho A_s (1/\pi R) \int_k \cos J_k \cos J_\xi] = 0
\end{aligned}$$

(C-3)

## APPENDIX D

### COMPUTER PROGRAM DOCUMENTATION

The program was written in FORTRAN IV, and was run using an IBM System 360, Model 50 computer. The core storage required for the program was dependent upon the number of terms in the assumed mode function. The maximum number of terms run was ten, which required E-level system operation.

The flow of the program can be observed in Fig. D.1 and is summarized as follows: The main program reads the input data which defines the various material and geometric parameters, the number of assumed modal functions, the range of the circumferential wave number, the range of the applied axial load, the Runge-Kutta step size, and the maximum time duration. The main program then calls Subroutines UVCOF and WCOEF in succession. These general subroutines calculate the coefficients for the required number of  $u$ ,  $v$ , and  $w$  equations of motion. (The number of equations is dependent upon the number of assumed modal functions,  $k$ . The two subroutines will generate coefficients for any number of equations. This number is limited only by the available computer core space. Subroutine UVCOF generates the coefficients for  $k$  algebraic  $u$  equations and  $k$  algebraic  $v$  equations. Subroutine WCOEF generates the coefficients for  $k$  nonlinear differential  $w$  equations.) The main program then calculates the terms in the  $w$

equation of motion containing the nondimensional load as a parameter. Subroutine RUNGE is called to solve the set of nonlinear differential equations. Subroutine RUNGE also uses subroutine FCT to solve the two sets of algebraic equations. For each step in the Runge-Kutta procedure, subroutine FCT must be called four times to solve the two sets of algebraic equations. The results are displayed in the form of shell displacement as a function of time for a particular axial end load and circumferential wave number. The output can be punched on cards for use in plotting the data.

The input data deck is set up as follows:

1. Title card identifying case being run.
2. Number of axial and circumferential assumed mode terms being used.
3. Maximum and minimum values of  $n$  being run.
4. Unstiffened shell parameters.
5. Ring parameters.
6. Stringer parameters.
7. Dynamic parameters.
8. Dynamic parameters (Cont.)
9. Maximum value of time and Runge-Kutta step size.
10. Maximum and minimum values of axial load, and load step size.

The program is set up so that cases may be stacked, and all parameters may be varied.

The formats for the above cards are:

1. (80A1)

All eighty columns are available to assign a descriptive title to the problem being run.

2. (2I4) ISTAR, JSTAR

ISTAR = maximum number of assumed mode terms in the axial direction,  $i$ .

JSTAR = maximum number of assumed mode terms in the circumferential direction,  $j$ .

3. (2I4) NCRG, NCRS

NCRG = 1 + minimum value of the circumferential wave number,  $n$ .

NCRS = 1 + maximum value of  $n$ .

4. (5E15.8) ESHEL, HSHEL, PNU, RSHEL, SHLT

ESHEL = Young's modulus of shell,  $E$ . (psi)

HSHEL = Thickness of shell,  $h$ . (in.)

PNU = Poisson's ratio,  $\nu$ . (dimensionless)

RSHEL = Radius of Shell,  $R$  (in.)

SHLT = Length of shell,  $L$ . (in.)

5. (I15,3E15.8) NRNG, ARING, ERING, ZRING

NRNG = Number of Rings,  $N$ .

ARING = Cross-sectional area of one ring,  $A_r$ . (in.<sup>2</sup>)

ERING = Young's modulus of rings,  $E_r$ . (psi)

ZRING = Distance from ring centroid to shell mid-surface,  $\bar{z}_r$  (in.)

6. (I15,3E15.8) MSTR, ASTR, ESTR, ZSTR  
 MSTR = Number of Stringers, M.  
 ASTR = Cross-sectional area of one stringer,  $A_S$ . (in.<sup>2</sup>)  
 ESTR = Young's modulus of stringers,  $E_S$ . (psi)  
 ZSTR = Distance from stringer centroid to shell mid-surface,  $Z_S$ . (in.)
7. (5E15.8) SHDEN, RGDEN, STDEN, RGMI, STMI  
 SHDEN = Unstiffened cylinder density,  $\rho$ . (lb-sec<sup>2</sup>/in.<sup>4</sup>)  
 RGDEN = Ring density,  $\rho_R$ . (lb-sec<sup>2</sup>/in.<sup>4</sup>)  
 STDEN = Stringer density,  $\rho_S$ . (lb-sec<sup>2</sup>/in.<sup>4</sup>)  
 RGMI = Moment of inertia of one ring about shell mid-surface,  $I_{OR}$ . (in.<sup>4</sup>)  
 STMI = Moment of inertia of the stringer about shell mid-surface,  $I_{OS}$ . (in.<sup>4</sup>)
8. (4E15.8) GRING, GSTR, RGJ, STJ  
 GRING = Modulus of rigidity of ring,  $G_R$ . (psi)  
 GSTR = Modulus of rigidity of stringer,  $G_S$ . (psi)  
 RGJ = Polar moment of inertia of ring,  $J_R$ . (in.<sup>4</sup>)  
 STJ = Polar moment of inertia of stringer,  $J_S$ . (in.<sup>4</sup>)
9. (3E15.8) X, XMAX, H  
 X = Starting value of independent variable, t. (sec.)  
 XMAX = Maximum value of independent variable, t. (sec.)  
 H = Runge-Kutta increment size.
10. (3I10) ILOAD, ISTOP, INT  
 ILOAD = Smallest value of load,  $\bar{F}_{min}$  (dimensionless)  
 ISTOP = Largest value of load,  $\bar{F}_{max}$  (dimensionless)  
 INT = Increment for increasing load value.

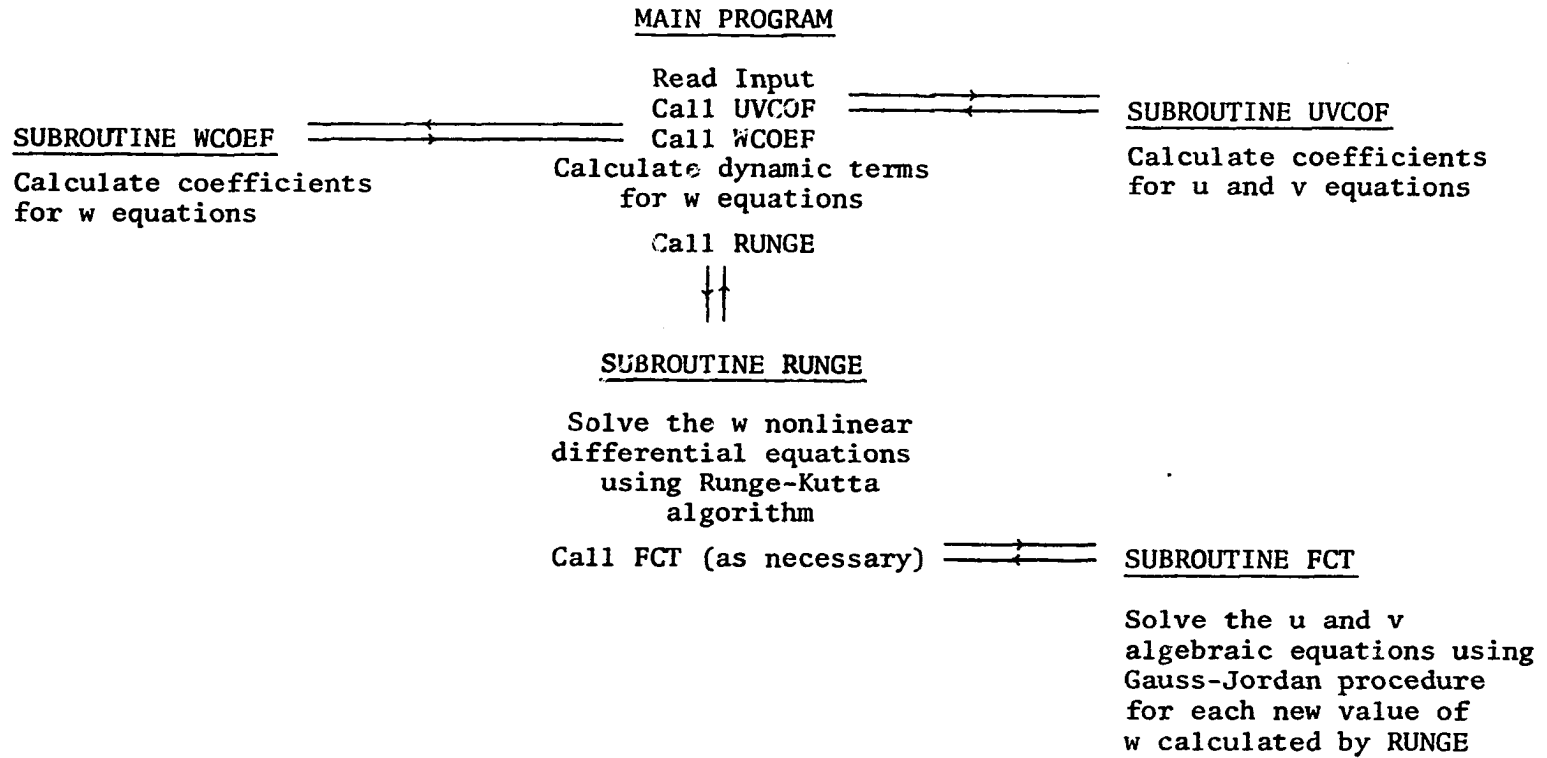


Figure D.1 Computer Program Flow Chart

APPENDIX E

COMPUTER PROGRAM LISTING

C	MAIN PROGRAM	MAIN 1
	EXTERNAL FCT	MAIN 2
	INTEGER P,Q	MAIN 3
C		MAIN 4
	DIMENSION Y(10),DERY(10),B(5,40),D(5,40)	MAIN 5
	DIMENSION PRMT(3),ICASE(80)	MAIN 6
C		MAIN 7
C	THE DIMENSION SIZE FOR WCOF(II,NN) MUST BE EQUAL TO	MAIN 8
C	OR LARGER THAN ISIZE FOR THE FIRST SUBSCRIPT AND EQUAL TO OR	MAIN 9
C	LARGER THAN 8*ISIZE FOR THE SECOND SUBSCRIPT.	MAIN 10
C	THE DIMENSION SIZE FOR C(II,NN) MUST BE EQUAL TO	MAIN 11
C	OR LARGER THAN 2*ISIZE FOR THE FIRST SUBSCRIPT AND EQUAL TO	MAIN 12
C	OR LARGER THAN 4*ISIZE FOR THE SECOND SUBSCRIPT.	MAIN 13
	COMMON WCOF(5,40),C(10,20),ISTAR,JSTAR,MAX,NCIR,ESHE3,HSHEL,PNU,	MAIN 14
	1NRNG,ARING,ERING,ZRING,MSTR,ASTR,ESTR,ZSTR,ISIZE,PI,DRING,DSTR,	MAIN 15
	2FN1,FN2,FM1,FM2,SHDEN,RGDEN,STDEN,RGMI,STMI,GRING,GSTR,RGJ,STJ,	MAIN 16
	3PLOAD,RSHEL,SHLT,IFLAG,NDOT	MAIN 17
C		MAIN 18
C	ISTAR=MAX. VALUE OF I . JSTAR=MAX. VALUE OF J	MAIN 19
C	ARING=RING CROSS-SECT. AREA, ASTR=STRINGER CROSS-SECT. AREA	MAIN 20
C	ERING = YOUNGS MODULUS OF RING, ESTR=YOUNGS MODULUS OF STRINGER	MAIN 21
C	DRING=DISTANCE BETWEEN RINGS, DSTR=DISTANCE BETWEEN STRINGERS	MAIN 22
C	ZRING=DISTANCE FROM RING CONTROID TO SHELL MID SURFACE	MAIN 23
C	ZSTR=DISTANCE FROM STRINGER CENTROID TO SHELL MID SURFACE	MAIN 24
C	NRNG=NUMBER OF RINGS, MSTR=NUMBER OF STRINGERS	MAIN 25
C	ESHEL=YOUNGS MODULUS OF SHELL	MAIN 26
C	HSHEL=SHELL THICKNESS, RSHEL=SHELL RADIUS	MAIN 27
C	PNU=POISSONS RATIO	MAIN 28
C	NCIR=NUMBER OF CIRCUMFERENTIAL WAVES (INTEGER)	MAIN 29
C	MAX=NUMBER OF AXIAL HALF WAVES(INTEGER)	MAIN 30
C	SHLT=SHELL LENGTH	MAIN 31
C	N1=NCIR/RSHEL (COMPUTED)...FN1	MAIN 32
C	N2=N1*N1 (COMPUTED)...FN2	MAIN 33
C	M1=MAX*3.14/SHLT (COMPUTED)...FM1	MAIN 34
C	M2=M1*M1(COMPUTED)...FM2	MAIN 35

C	SHDEN=MASS DENSITY OF SHELL	MAIN 36
C	RGDEN=MASS DENSITY OF RING, STDEN=MASS DENSITY OF STRINGER	MAIN 37
C	RGMI=MOMENT OF INERTIA OF RING, STMI=MOMENT OF INERTIA OF STRINGER	MAIN 38
C	GSTR=MODULUS OF RIGIDITY OF STRINGER	MAIN 39
C	GRING=MODULUS OF RIGIDITY OF RING	MAIN 40
C	RGJ=RING POLAR MOMENT OF INERTIA, STJ=STRINGER POLAR MOMENT	MAIN 41
C	PLOAD=AXIAL COMPRESSIVE FORCE	MAIN 42
C		MAIN 43
C	READ AND WRITE CASE IDENTIFICATION PARAMETERS	MAIN 44
C		MAIN 45
	900 FORMAT(1H1,80A1)	MAIN 46
	999 FORMAT(' ')	MAIN 47
	1000 FORMAT(80A1)	MAIN 48
	1001 FORMAT(2I4)	MAIN 49
	1002 FORMAT(1H ,8H1STAR = ,I4,5X,8HJSTAR = ,I4/)	MAIN 50
	1003 FORMAT(5E15.8)	MAIN 51
	1005 FORMAT(1I5,3E15.8)	MAIN 52
	1007 FORMAT(5E15.8)	MAIN 53
	1008 FORMAT(3I10)	MAIN 54
	1009 FORMAT(5X,1I5,3E15.8)	MAIN 55
	1012 FORMAT(5X,5E15.8)	MAIN 56
	1013 FORMAT(' PRMT VALUES ARE...PRMT(1)=X,PRMT(2)=X MAX,PRMT(3)=H ')	MAIN 57
	1018 FORMAT(' SHELL INPUT-ESHEL,HSHEL,PNU,RSHEL,SHLT ')	MAIN 58
	1019 FORMAT(' RING INPUT-NRNG,ARNG,ERING,ZRING ')	MAIN 59
	1020 FORMAT(' STRINGER INPUT-MSTR,ASTR,ESTR,ZSTR ')	MAIN 60
	1021 FORMAT(' DYNAMIC-SHDEN,RGDEN,STDEN,RGMI,STMI ')	MAIN 61
	1022 FORMAT(' DYNAMIC-GRING,GSTR,RGJ,STJ ')	MAIN 62
	1035 FORMAT(' RANGE OF BUCKLING LOAD...ILOAD,ISTOP,INT ')	MAIN 63
	1040 FORMAT(1X,3I10)	MAIN 64
	1045 FORMAT(' BUCKLING DID NOT OCCUR UNTIL AFTER MAX. LOAD WAS REACHED	MAIN 65
	1*****SORRY ')	MAIN 66
	1055 FORMAT(/30H NUMBER OF AXIAL HALF-WAVES = ,I4,5X,39HNUMBER OF CIRC	MAIN 67
	1UMFERENTIAL FULL WAVES = ,I4/)	MAIN 68
5	READ(5,1000)ICASE	MAIN 69
	WRITE(6,900)ICASE	MAIN 70
	READ(5,1001)ISTAR,JSTAR	MAIN 71

	IF(ISTAR-100)6,15,15	MAIN 72
6	WRITE(6,1002)ISTAR,JSTAR	MAIN 73
C		MAIN73A
C	READ IN NCRG,NCRS	MAIN73B
C		MAIN73C
	READ(5,1001)NCRG,NCRS	MAIN73D
C		MAIN 74
C	READ AND WRITE SHELL INPUT PARAMETERS	MAIN 75
C		MAIN 76
	READ(5,1003)ESHEL,HSHEL,PNU,RSHEL,SHLT	MAIN 77
	WRITE(6,1018)	MAIN 78
	WRITE(6,1007)ESHEL,HSHEL,PNU,RSHEL,SHLT	MAIN 79
C		MAIN 80
C	READ AND WRITE RING INPUT PARAMETERS	MAIN 81
C		MAIN 82
	READ(5,1005)NRNG,ARING,ERING,ZRING	MAIN 83
	WRITE(6,1019)	MAIN 84
	WRITE(6,1009)NRNG,ARING,ERING,ZRING	MAIN 85
C		MAIN 86
C	READ AND WRITE STRINGER INPUT PARAMETERS	MAIN 87
C		MAIN 88
	READ(5,1005)MSTR,ASTR,ESTR,ZSTR	MAIN 89
	WRITE(6,1020)	MAIN 90
	WRITE(6,1009)MSTR,ASTR,ESTR,ZSTR	MAIN 91
C		MAIN 92
C	READ AND WRITE DYNAMIC INPUT PARAMETERS	MAIN 93
C		MAIN 94
	READ(5,1007)SHDEN,RGDEN,STDEN,RGMI,STMI,GRING,GSTR,RGJ,STJ	MAIN 95
	WRITE(6,1021)	MAIN 96
	WRITE(6,1012)SHDEN,RGDEN,STDEN,RGMI,STMI	MAIN 97
	WRITE(6,1022)	MAIN 98
	WRITE(6,1012)GRING,GSTR,RGJ,STJ	MAIN 99
	NSIZE=2*ISTAR*JSTAR	MAIN100
C		MAIN101
C	READ AND WRITE VALUES OF PRMT AND DERY	MAIN102
C		MAIN103

	READ(5,1007)PRMT	MAIN104
	DO 4 J2=1,NSIZE	MAIN105
4	DERY(J2)=1.00	MAIN106
	WRITE(6,1013)	MAIN107
	WRITE(6,1012)PRMT	MAIN108
C		MAIN109
C	CALCULATE INTERMEDIATE VALUES	MAIN110
C		MAIN111
	MAX=1	MAIN112
	ISIZE=ISTAR*JSTAR	MAIN113
	PI=3.1415926535892	MAIN114
	DRING=SHLT/(NRNG+1.0)	MAIN115
	DSTR=2.0*PI*RSHEL/MSTR	MAIN116
C		MAIN117
C	READ INITIAL EXTERNAL LOAD, MAX LOAD, LOAD STEP SIZE	MAIN118
C	EXAMPLE LOAD VALUES...PLOAD=.610, ILOAD=610	MAIN119
C		MAIN120
	READ(5,1008)ILOAD,ISTOP,INT	MAIN121
	WRITE(6,999)	MAIN122
	WRITE(6,1035)	MAIN123
	WRITE(6,1040)ILOAD,ISTOP,INT	MAIN124
	DO 10 NCR=NCRG,NCRS	MAIN125
	NCIR=NCR-1	MAIN127
C		MAIN128
C	WRITE AXIAL AND CIRCUMFERENTIAL WAVE NUMBERS	MAIN129
C		MAIN130
	WRITE(6,1055)MAX,NCIR	MAIN131
	FNCIR=NCIR	MAIN132
	FN1=FNCIR/RSHEL	MAIN133
	FN2=FN1*FN1	MAIN134
	FMAX=MAX	MAIN135
	FM1=FMAX*PI/SHLT	MAIN136
	FM2=FM1*FM1	MAIN137
	CALL UVCOF	MAIN138
C		MAIN139
	CALL WCOEF	MAIN140

```

17 JX95=ILOAD
18 AJ=JX95
   NDOT=0
   PLOAD=AJ/1000.0
   PLOAD=PLLOAD*HSHEL*HSHEL*ESHSEL/RSHEL
C
C COMPUTE DYNAMIC TERMS OF WCOEF SUBROUTINE MATRIX
C
C SET WORKING MATRICES EQUAL TO ZERO
C
   KOLX=3*ISIZE
   KOL=2*ISIZE+1
   DO 9 J4=KOL,KOLX
   DO 8 I4=1,ISIZE
   B(I4,J4)=0.0
   D(I4,J4)=0.0
   WCOF(I4,J4)=0.0
8 CONTINUE
9
   II=0
   DO 190 Q=1,ISIZE
   II=II+1
   INTGQ=(Q-1)/ISTAR
   IZETA=Q-INTGQ*ISTAR
   IXI=INTGQ+1
   FZETA=IZETA
   FXI=IXI
   NN=2*ISIZE
   DOI20P=1,ISIZE
   NN=NN+1
   INTGP=(P-1)/ISTAR
   I=P-INTGP*ISTAR
   J=INTGP+1
   FI=I
   FJ=J
C
C COMPUTE STRINGER TERMS
MAIN145
MAIN146
MAIN146A
MAIN147
MAIN148
MAIN149
MAIN150
MAIN151
MAIN152
MAIN153
MAIN154
MAIN155
MAIN156
MAIN157
MAIN158
MAIN159
MAIN160
MAIN161
MAIN162
MAIN163
MAIN164
MAIN165
MAIN166
MAIN167
MAIN168
MAIN169
MAIN170
MAIN171
MAIN172
MAIN173
MAIN174
MAIN175
MAIN176
MAIN177
MAIN178
MAIN179

```



```
120 CONTINUE
190 CONTINUE
    Y(1)=0.001
    DO 3 L=2,NSIZE
3     Y(L)=0.00
    CALL RUNGE(PRMT,Y,DERY,NDIM,IHLF,FCT,OUTP,AUX)
    IF(NDOT)22,22,10
22    JX95=JX95+INT
    IF(JX95-ISTOP)18,18,10
10    CONTINUE
    GO TO 5
15    CALL EXIT
    STOP
    END
```

```
MAIN216
MAIN217
MAIN218
MAIN219
MAIN220
MAIN221
MAIN222
MAIN227
MAIN228
MAIN230
MAIN231
MAIN232
MAIN233
MAIN234
```

C	SUBROUTINE UVCOF	UVCF 1
C	THIS SUBROUTINE CALCULATES THE U,V,W,W**2 COEFFICIENTS FOR THE	UVCF 2
C	U AND V EQUATIONS.	UVCF 3
C		UVCF 4
C	INTEGER P,Q	UVCF 5
C	THE DIMENSION SIZE FOR THE NEXT STATEMENT MUST BE EQUAL TO OR	UVCF 6
C	LARGER THAN 2*ISIZE FOR THE FIRST SUBSCRIPT AND EQUAL TO OR	UVCF 7
C	LARGER THAN 4*ISIZE FOR THE SECOND SUBSCRIPT.	UVCF 8
C		UVCF 9
C	DIMENSION B(10,20)	UVCF 10
C	COMMON WCOF(5,40),C(10,20),ISTAR,JSTAR,MAX,NCIR,ESHE3,HSHEL,PNU,	UVCF 11
C	1NRNG,ARING,ERING,ZRING,MSTR,ASTR,ESTR,ZSTR,ISIZE,PI,DRING,DSTR,	UVCF 12
C	2FN1,FM2,FM1,FM2,SHDEN,RGDEN,STDEN,RGMI,STMI,GRING,GSTR,RGJ,STJ,	UVCF 13
C	3PLOAD,RSHEL,SHLT,IFLAG,NDOT	UVCF 14
C		UVCF 15
C	SET WORKING MATRICES EQUAL TO ZERO	UVCF 16
C		UVCF 17
C		UVCF 18
C	NSIZE=2*ISIZE	UVCF 19
C	MSIZE=4*ISIZE	UVCF 20
C	DO 2 J=1,MSIZE	UVCF 21
C	DO 1 I=1,NSIZE	UVCF 22
C	B(I,J)=0.00	UVCF 23
1	C(I,J)=0.00	UVCF 24
2	CONTINUE	UVCF 25
C	COMPUTE COMPOSITE U-V EQUATION COEFFICIENT MATRIX	UVCF 26
C		UVCF 27
C	II=0	UVCF 28
C		UVCF 29
C	COMPUTE U EQUATION MATRIX	UVCF 30
C		UVCF 31
C	DO 130 Q=1,ISIZE	UVCF 32
C	II=II+1	UVCF 33
C	INTGQ=(Q-1)/ISTAR	UVCF 34
C	IZETA=Q-INTGQ*ISTAR	UVCF 35
C	IXI=INTGQ+1	UVCF 36



```

INTGP=(P-1)/ISTAR
I=P-INTGP*ISTAR
J=INTGP+1
FI=I
FJ=J
C
C COMPUTE SHELL TERMS
C
IF(I-IZETA)110,106,110
IF(J-IXI)110,107,110
106 C(II,NN)=FI*FM1*FJ*FNI*(1.0+PNU)/2.0
107 CONTINUE
110
C
C SUBMATRIX W...U EQUATION
C
DO 115 P=1,ISIZE
NN=NN+1
INTGP=(P-1)/ISTAR
I=P-INTGP*ISTAR
J=INTGP+1
FI=I
FJ=J
C
C COMPUTE STRINGER TERMS
C
IF(I-IZETA)115,111,115
111 SUM2=0.00
DO 112 K=1,MSTR
FK=K
112 SUM2=SUM2+COS(FJ*FNI*FK*DSTR)*COS(FXI*FNI*FK*DSTR)
B(II,NN)=(1.0-PNU*PNU)*FI**3*FM2*FM1*ESTR*ASTR*ZSTR*SUM2/
1PI*RSHEL*ESHSEL*HSHEL)
C
C COMPUTE SHELL TERMS
C
IF(J-IXI)113,114,113
UVCF 73
UVCF 74
UVCF 75
UVCF 76
UVCF 77
UVCF 78
UVCF 79
UVCF 80
UVCF 81
UVCF 82
UVCF 83
UVCF 84
UVCF 85
UVCF 86
UVCF 87
UVCF 88
UVCF 89
UVCF 90
UVCF 91
UVCF 92
UVCF 93
UVCF 94
UVCF 95
UVCF 96
UVCF 97
UVCF 98
UVCF 99
UVCF100
UVCF101
UVCF102
UVCF103
UVCF104
UVCF105
UVCF106
UVCF107
UVCF108

```

```

113 C(II,NN)=B(II,NN)                                UVCF109
GO TO 115                                            UVCF110
114 C(II,NN)=B(II,NN)+PNU*FI*FM1/RSHEL             UVCF111
115 CONTINUE                                         UVCF112
C                                                    UVCF113
C SUBMATRIX W**2.,.U EQUATION                      UVCF114
C                                                    UVCF115
C DO 120 P=1,ISIZE                                  UVCF116
C NN=NN+1                                           UVCF117
C INTGP=(P-1)/ISTAR                                UVCF118
C I=P-INTGP#ISTAR                                  UVCF119
C J=INTGP+1                                         UVCF120
C FI=I                                              UVCF121
C FJ=J                                              UVCF122
C                                                    UVCF123
C COMPUTE STRINGER TERMS                           UVCF124
C                                                    UVCF125
C IF(2*I-IZETA)120,116,120                          UVCF126
116 SUM2=0.00                                       UVCF127
DO 117 K=1,MSTR                                    UVCF128
FK=K                                               UVCF129
117 SUM2=SUM2+COS(FJ*FN1*FK*DSTR)**2*COS(FX I*FN1*FK*DSTR)
B(II,NN)=(1.0-PNU*PNU)*(FI*FM1)**3*SUM2*ESTR*ASTR/(2.0*PI*
1RSHEL*ESHSEL*HSHEL)
C                                                    UVCF132
C COMPUTE SHELL TERMS                               UVCF133
C                                                    UVCF134
C IF(2*J-IXI)118,119,118                            UVCF135
118 C(II,NN)=-B(II,NN)                             UVCF136
GO TO 120                                          UVCF137
119 C(II,NN)=-FI*FM1*FJ*FJ*FN2/4.0-FI**3*FM2*FM1/4.0-B(II,NN)
120 CONTINUE                                         UVCF139
130 CONTINUE                                         UVCF140
C                                                    UVCF141
C COMPUTE V EQUATION MATRIX                         UVCF142
C                                                    UVCF143
C                                                    UVCF144

```



```

C      COMPUTE RING TERMS
C
136   IF(J-IXI)140,136,140
      SUM2=0.00
      DO 137 K=1,NRNG
      FK=K
137   SUM2=SUM2+COS(FI*FM1*FK*DRING)*COS(FZETA*FM1*FK*DRING)
      B(II,NN)=2.0*(1.0-PNU*PNU)*FJ*FJ*FN2*ERING*ARING*SUM2/(ESHELL
      I*HSHELL*SHLTI)
C
C      COMPUTE SHELL TERMS
C
138   IF(1-IZETA)138,139,138
      C(II,NN)=B(II,NN)
      GO TO 140
139   C(II,NN)=B(II,NN)+FJ*FJ*FN2+FI*FI*FM2*(1.0-PNU)/2.0
140   CONTINUE
C
C      SUBMATRIX W...V EQUATION
C
      DO 145 P=1,ISIZE
      NN=NN+1
      INTGP=(P-1)/ISTAR
      I=P-INTGP*ISTAR
      J=INTGP+1
      FI=I
      FJ=J
C
C      COMPUTE RING TERMS
C
      IF(J-IXI)145,141,145
141   SUM2=0.00
      DO 142 K=1,NRNG
      FK=K
142   SUM2=SUM2+COS(FI*FM1*FK*DRING)*COS(FZETA*FM1*FK*DRING)

```

```

UVCF181
UVCF182
UVCF183
UVCF184
UVCF185
UVCF186
UVCF187
UVCF188
UVCF189
UVCF190
UVCF191
UVCF192
UVCF193
UVCF194
UVCF195
UVCF196
UVCF197
UVCF198
UVCF199
UVCF200
UVCF201
UVCF202
UVCF203
UVCF204
UVCF205
UVCF206
UVCF207
UVCF208
UVCF209
UVCF210
UVCF211
UVCF212
UVCF213
UVCF214
UVCF215
UVCF216

```



GO TO 150  
149 C(II,NN)=-B(II,NN)-(FJ\*FN1)\*\*3/4.0-FI\*FI\*FJ\*FM2\*FN1/4.0  
150 CONTINUE  
160 CONTINUE  
RETURN  
END

UVCF253  
UVCF254  
UVCF255  
UVCF256  
UVCF257  
UVCF258

	SUBROUTINE WCOEF	WCOF 1
C		WCOF 2
C	THIS SUBROUTINE CALCULATES THE W EQUATION COEFFICIENTS	WCOF 3
C	(U,V,W,W**2,W**3,U*W,V*W,D2W/DT2) AND PLACES THEM	WCOF 4
C	IN A MATRIX CALLED WCOF	WCOF 5
C		WCOF 6
	INTEGER P,Q	WCOF 7
C		WCOF 8
C	THE DIMENSION SIZE FOR THE SUBSCRIPTED VARIABLES MUST BE EQUAL TO	WCOF 9
C	OR LARGER THAN ISIZE FOR THE FIRST SUBSCRIPT AND EQUAL TO OR	WCOF 10
C	LARGER THAN 8*ISIZE FOR THE SECOND SUBSCRIPT.	WCOF 11
C		WCOF 12
	DIMENSION B(5,40),D(5,40)	WCOF 13
	COMMON WCOF(5,40),C(10,20),ISTAR,JSTAR,MAX,NCIR,ESHE3,HSHEL,PNU,	WCOF 14
	1NRNG,ARING,ERING,ZRING,MSTR,ASTR,ESTR,ZSTR,ISIZE,PI,DRING,DSTR,	WCOF 15
	2FN1,FN2,FM1,FM2,SHDEN,RGDEN,SDEN,RGMI,STMI,GRING,GSTR,RGJ,STJ,	WCOF 16
	3PLOAD,RSHEL,SHLT,IFLAG,NDOT	WCOF 17
C		WCOF 18
C	SET WORKING MATRICES EQUAL TO ZERO	WCOF 19
C		WCOF 20
	MSIZE=8*ISIZE	WCOF 21
	DO 2 J=1,MSIZE	WCOF 22
	DO 1 I=1,ISIZE	WCOF 23
	B(I,J)=0.00	WCOF 24
	D(I,J)=0.00	WCOF 25
1	WCOF(I,J)=0.00	WCOF 26
2	CONTINUE	WCOF 27
C		WCOF 28
C	COMPUTE COMPLETE W EQUATION MATRIX	WCOF 29
C		WCOF 30
	II=0	WCOF 31
	DO 190 Q=1,ISIZE	WCOF 32
	II=II+1	WCOF 33
	INTGQ=(Q-1)/ISTAR	WCOF 34
	IZETA=Q-INTGQ*ISTAR	WCOF 35
	IXI=INTGQ+1	WCOF 36

	FZETA=IZETA	WCOF 37
	FXI=IXI	WCOF 38
C		WCOF 39
C	SUBMATRIX U...W EQUATION	WCOF 40
C		WCOF 41
	NN=0	WCOF 42
	DO 105 P=1,ISIZE	WCOF 43
	NN=NN+1	WCOF 44
	INTGP=(P-1)/ISTAR	WCOF 45
	I=P-INTGP*ISTAR	WCOF 46
	J=INTGP+1	WCOF 47
	FI=I	WCOF 48
	FJ=J	WCOF 49
C		WCOF 50
C	COMPUTE STRINGER TERMS	WCOF 51
C		WCOF 52
	IF(I-IZETA)105,101,105	WCOF 53
101	SUM2=0.00	WCOF 54
	DO 102 K=1,MSTR	WCOF 55
	FK=K	WCOF 56
102	SUM2=SUM2+COS(FJ*FN1*FK*DSTR)*COS(FXI*FN1*FK*DSTR)	WCOF 57
	B(II,NN)=(FI*FM1)**3*ESTR*ASTR*ZSTR*SUM2/(PI*RSHEL)	WCOF 58
C		WCOF 59
C	COMPUTE SHELL TERMS	WCOF 60
C		WCOF 61
	IF(J-IXI)103,104,103	WCOF 62
103	WCOF(II,NN)=B(II,NN)	WCOF 63
	GO TO 105	WCOF 64
104	WCOF(II,NN)=B(II,NN)+ESHEL*HSHEL*PNU*FI*FM1/(RSHEL*(1.0-PNU*PNU))	WCOF 65
105	CONTINUE	WCOF 66
C		WCOF 67
C	SUBMATRIX V...W EQUATION	WCOF 68
C		WCOF 69
	DO 110 P=1,ISIZE	WCOF 70
	NN=NN+1	WCOF 71
	INTGP=(P-1)/ISTAR	WCOF 72

	I=P-INTGP*ISTAR	WCOF 73
	J=INTGP+1	WCOF 74
	FI=I	WCOF 75
	FJ=J	WCOF 76
C		WCOF 77
C	COMPUTE RING TERMS	WCOF 78
C		WCOF 79
	IF(J-IXI)110,106,110	WCOF 80
106	SUM2=0.00	WCOF 81
	DO 107 K=1,NRNG	WCOF 82
	FK=K	WCOF 83
107	SUM2=SUM2+COS(FI*FM1*FK*DRING)*COS(FZETA*FM1*FK*DRING)	WCOF 84
	B(II,NN)=2*ERING*ARING*SUM2*((FJ*FN1)**3*ZRING+FJ*FN1/RSHEL)/SHLT	WCOF 85
C		WCOF 86
C	COMPUTE SHELL TERMS	WCOF 87
C		WCOF 88
	IF(I-IZETA)108,109,108	WCOF 89
108	WCOF(II,NN)=B(II,NN)	WCOF 90
	GO TO 110	WCOF 91
109	WCOF(II,NN)=B(II,NN)+ESHEL*HSHEL*FJ*FN1/(RSHEL*(1.0-PNU*PNU))	WCOF 92
110	CONTINUE	WCOF 93
C		WCOF 94
C	SUBMATRIX W...W EQUATION	WCOF 95
C		WCOF 96
	DO120P=1,ISIZE	WCOF 97
	NN=NN+1	WCOF 98
120	CONTINUE	WCOF 99
C		WCOF100
C	SUBMATRIX W**2...W EQUATION	WCOF101
C		WCOF102
	DO 130 P=1,ISIZE	WCOF103
	NN=NN+1	WCOF104
	INTGP=(P-1)/ISTAR	WCOF105
	I=P-INTGP*ISTAR	WCOF106
	J=INTGP+1	WCOF107
	FI=I	WCOF108

```

      FJ=J
C
C   COMPUTE STRINGER TERMS
C
121   IF(2*I-IZETA)126,121,126
      SUM1=0.00
      DO 122 K=1,MSTR
         FK=K
122   SUM1=SUM1+COS(FJ*FN1*FK*DSTR)**2*COS(FX I*FN1*FK*DSTR)
      B(I I,NN)=(F I*FM1)**4*ESTR*ASTR*ZSTR*SUM1/(PI*RSHEL*2.0)
C
C   COMPUTE RING TERMS
C
123   IF(2*J-IXI)127,124,127
124   SUM1=0.00
      DO 125 K=1,NRNG
         FK=K
125   SUM1=SUM1+COS(FI*FM1*FK*DRING)**2*COS(FZETA*FM1*FK*DRING)
      D(I I,NN)=2.0*SUM1*(FJ*FJ*FN2/(4.0*RSHEL)-(FJ*FN1)**4*FZETA/2.0)*
      IERING*ARING/SHLT
126   IF(2*I-IZETA)128,129,128
127   WCOF(I I,NN)=-B(I I,NN)
      GO TO 130
128   WCOF(I I,NN)=D(I I,NN)
      GO TO 130
C
C   COMPUTE SHELL TERMS
C
129   WCOF(I I,NN)=-B(I I,NN)+D(I I,NN)+ESHEL*HSHEL*PNU*(F I*F I*
      IFM2+FJ*FJ*FN2)/(8.0*RSHEL*(1.0-PNU*PNU))
130   CONTINUE
C
C   SUBMATRIX W**3...W EQUATION
C
      DO 160 P=1,ISIZE

```

```

WCOF109
WCOF110
WCOF111
WCOF112
WCOF113
WCOF114
WCOF115
WCOF116
WCOF117
WCOF118
WCOF119
WCOF120
WCOF121
WCOF122
WCOF123
WCOF124
WCOF125
WCOF126
WCOF127
WCOF128
WCOF129
WCOF130
WCOF131
WCOF132
WCOF133
WCOF134
WCOF135
WCOF136
WCOF137
WCOF138
WCOF139
WCOF140
WCOF141
WCOF142
WCOF143
WCOF144

```

	NN=NN+1	WCOF145
	INTGP=(P-1)/ISTAR	WCOF146
	I=P-INTGP*ISTAR	WCOF147
	J=INTGP+1	WCOF148
	FI=I	WCOF149
	FJ=J	WCOF150
C		WCOF151
C	COMPUTE STRINGER TERMS	WCOF152
C		WCOF153
	DEL1=0.00	WCOF154
	DEL2=0.00	WCOF155
	IF(I-IZETA)134,131,134	WCOF156
131	DEL1=+1.0	WCOF157
132	SUM1=0.00	WCOF158
	DO 133 K=1,MSTR	WCOF159
	FK=K	WCOF160
133	SUM1=SUM1+COS(FJ*FN1*FK*DSTR)**3*COS(FXI*FN1*FK*DSTR)	WCOF161
	B(II,NN)=DEL1*SUM1*ESTR*ASTR*(FI*FM1)**4/(PI*RSHEL*8.0)	WCOF162
	GO TO 136	WCOF163
134	IF(3*I-IZETA)136,135,136	WCOF164
135	DEL1=-1.0	WCOF165
	GO TO 132	WCOF166
136	IF(J-IXI)147,137,147	WCOF167
137	DEL2=+1.0	WCOF168
C		WCOF169
C	COMPUTE RING TERMS	WCOF170
C		WCOF171
138	SUM1=0.00	WCOF172
	DO 139 K=1,NRNG	WCOF173
139	SUM1=SUM1+COS(FI*FM1*FK*DRING)**3*COS(FZETA*FM1*FK*DRING)	WCOF174
	D(II,NN)=DEL2*2.0*SUM1*(FJ*FN1)**4*ERING*ARING/(8.0*SHLT)	WCOF175
	IF(DEL1)140,151,140	WCOF176
C		WCOF177
C	COMPUTE SHELL TERMS	WCOF178
C		WCOF179
140	IF(DEL1*DEL2)141,141,144	WCOF180

```

141 IF(DELI)142,142,143
142 WCOF(II,NN)=B(II,NN)+D(II,NN)+(ESHEL*HSHEL)*(-3.0*(FI*FM1)**4+
12.0*FI*FI*FM2*FJ*FJ*FN2*(1.0-2*PNU)+(FJ*FN1)**4)/
2(32.0*(1.0-PNU*PNU))
GO TO 160
143 WCOF(II,NN)=B(II,NN)+D(II,NN)+(ESHEL*HSHEL)*((FI*FM1)**4
1+2.0*FI*FI*FM2*FJ*FJ*FN2*(1.0-2.0*PNU)-3.0*(FJ*FN1)**4)/
2(32.0*(1-PNU*PNU))
GO TO 160
144 IF(DELI)145,145,146
145 WCOF(II,NN)=B(II,NN)+D(II,NN)+(ESHEL*HSHEL)*(-(FI*FM1)**4
1-2.0*FI*FI*FM2*FJ*FJ*FN2-(FJ*FN1)**4)/(32.0*(1.0-PNU*PNU))
GO TO 160
146 WCOF(II,NN)=B(II,NN)+D(II,NN)+(ESHEL*HSHEL)*((3.0*(FI*FM1)**4
1-2.0*FI*FI*FM2*FJ*FJ*FN2*(1.0-4.0*PNU)+3*(FJ*FN1)**4)/(32.0
2*(1.0-PNU*PNU))
GO TO 160
147 IF(3*J-IXI)149,148,149
148 DEL2=-1.0
GO TO 138
149 IF(DELI)150,160,150
150 WCOF(II,NN)=B(II,NN)
GO TO 160
151 WCOF(II,NN)=D(II,NN)
160 CONTINUE
C
C SUBMATRIX U*W...W EQUATION
C
DO 165 P=1,ISIZE
NN=NN+1
INTGP=(P-1)/ISTAR
I=P-INTGP*ISTAR
J=INTGP+1
FI=I
FJ=J
WCOF181
WCOF182
WCOF183
WCOF184
WCOF185
WCOF186
WCOF187
WCOF188
WCOF189
WCOF190
WCOF191
WCOF192
WCOF193
WCOF194
WCOF195
WCOF196
WCOF197
WCOF198
WCOF199
WCOF200
WCOF201
WCOF202
WCOF203
WCOF204
WCOF205
WCOF206
WCOF207
WCOF208
WCOF209
WCOF210
WCOF211
WCOF212
WCOF213
WCOF214
WCOF215
WCOF216

```

```

C      COMPUTE STRINGER TERMS
C
      IF(2*I-IZETA)165,161,165
      SUM1=0.00
      DO 162 K=1,MSTR
      FK=K
      162 SUM1=SUM1+COS(FJ*FN1*FK*DSTR)**2*COS(FX I*FN1*FK *DSTR)
C
C      COMPUTE SHELL TERMS
C
      B(II,NN)=(FI*FM1)**3*SUM1*ESTR*ASTR/(2.0*PI*RSHEL)
      IF(2*J-IXI)163,164,163
      WCOF(II,NN)=B(II,NN)
      GO TO 165
      163 WCOF(II,NN)=B(II,NN)+ESHEL*HSHEL*((FI*FM1)**3+FI*FM1*FJ*FJ*FN2)/
      1(4.0*(1.0-PNU*PNU))
      165 CONTINUE
C
C      SUBMATRIX V*W...W EQUATION
C
      DO 170 P=1,ISIZE
      NN=NN+1
      INTGP=(P-1)/ISTAR
      I=P-INTGP*ISTAR
      J=INTGP+1
      FI=I
      FJ=J
C
C      COMPUTE RING TERMS
C
      IF(2*J-IXI)170,166,170
      SUM1=0.00
      DO 167 K=1,NRNG
      FK=K
      167 SUM1=SUM1+COS(FI*FM1*FK*DRING)**2*COS(FZETA*FM1*FK*DRING)
      B(II,NN)=SUM1*ERING*ARING*(FJ*FN1)**3/SHLT
      WCOF217
      WCOF218
      WCOF219
      WCOF220
      WCOF221
      WCOF222
      WCOF223
      WCOF224
      WCOF225
      WCOF226
      WCOF227
      WCOF228
      WCOF229
      WCOF230
      WCOF231
      WCOF232
      WCOF233
      WCOF234
      WCOF235
      WCOF236
      WCOF237
      WCOF238
      WCOF239
      WCOF240
      WCOF241
      WCOF242
      WCOF243
      WCOF244
      WCOF245
      WCOF246
      WCOF247
      WCOF248
      WCOF249
      WCOF250
      WCOF251
      WCOF252

```

C		WCOF253
C	COMPUTE SHELL TERMS	WCOF254
C		WCOF255
	IF(2*I-IZETA)168,169,168	WCOF256
168	WCOF(II,NN)=B(II,NN)	WCOF257
	GO TO 170	WCOF258
169	WCOF(II,NN)=B(II,NN)+ESHEL*HSHEL*((FJ*FN1)**3+FI*FI*FM2* 1FJ*FN1)/(4.0*(1-PNU*PNU))	WCOF259
170	CONTINUE	WCOF260
C		WCOF261
C	SUBMATRIX D2W/DT2...W EQUATION	WCOF262
C		WCOF263
	DO 180 P=1,ISIZE	WCOF264
	NN=NN+1	WCOF265
	INTGP=(P-1)/ISTAR	WCOF266
	I=P-INTGP*ISTAR	WCOF267
	J=INTGP+1	WCOF268
	FI=I	WCOF269
	FJ=J	WCOF270
C		WCOF271
C	COMPUTE STRINGER TERMS	WCOF272
C		WCOF273
C		WCOF274
	IF(I-IZETA)176,171,176	WCOF275
171	SUM1=0.00	WCOF276
	DO 172 K=1,MSTR	WCOF277
	FK=K	WCOF278
172	SUM1=SUM1+COS(FJ*FN1*FK*DSTR)*COS(FXI*FN1*FK*DSTR) B(II,NN)=SUM1*STDEN*ASTR/(PI*RSHEL)	WCOF279
C		WCOF280
C	COMPUTE RING TERMS	WCOF281
C		WCOF282
173	IF(J-IXI)177,174,177	WCOF283
174	SUM1=0.00	WCOF284
	DO 175 K=1,NRNG	WCOF285
	FK=K	WCOF286
175	SUM1=SUM1+COS(FI*FM1*FK*DRING)*COS(FZETA*FM1*FK*DRING)	WCOF287
		WCOF288

	D(II,NN)=SUM1*RGDEN*ARING*2.0/SHLT	WCOF289
	IF(I-IZETA)178,179,178	WCOF290
176	IF(J-IXI)180,173,180	WCOF291
177	WCOF(II,NN)=B(II,NN)	WCOF292
	GO TO 180	WCOF293
178	WCOF(II,NN)=D(II,NN)	WCOF294
	GO TO 180	WCOF295
C		WCOF296
C	COMPUTE SHELL TERMS	WCOF297
C		WCOF298
179	WCOF(II,NN)=B(II,NN)+D(II,NN)+SHDEN*HSHEL	WCOF299
180	CONTINUE	WCOF300
190	CONTINUE	WCOF301
	RETURN	WCOF302
	END	WCOF303

	SUBROUTINE RUNGE(PRMT,Y,DERY,NDIM,IHLF,FCT,OUTP,AUX)	RUNG 1
C		RUNG 2
C	THIS SUBROUTINE TAKES THE PLACE OF SUBROUTINE RKGS CONTAINED IN	RUNG 3
C	THE IBM SCIENTIFIC SUBROUTINE PACKAGE.	RUNG 4
C	FOR A DESCRIPTION OF THE VARIABLES CONTAINED IN THIS SUBROUTINE,	RUNG 5
C	SEE THE IBM SUBROUTINE RKGS WRITEUP.	RUNG 6
C		RUNG 7
C	THE DIMENSION SIZE FOR THE NEXT STATEMENT MUST BE EQUAL TO OR	RUNG 8
C	GREATER THAN 2*ISIZE	RUNG 9
C		RUNG 10
	DIMENSION Y(10),DERY(10),PHI(10),SAVEY(10),SDATA(4,2),PRMT(3)	RUNG 11
	COMMON WCOF(5,40),C(10,20),ISTAR,JSTAR,MAX,NCIR,ESHE3,HSHEL,PNU,	RUNG 12
	1NRNG,ARING,ERING,ZRING,MSTR,ASTR,ESTR,ZSTR,ISIZE,PI,DRING,DSTR,	RUNG 13
	2FN1,FN2,FM1,FM2,SHDEN,RGDEN,STDEN,RGMI,STMI,GRING,GSTR,RGJ,STJ,	RUNG 14
	3PLOAD,RSHEL,SHLT,IFLAG,NDOT	RUNG 15
1000	FORMAT(1X,E15.8)	RUNG 16
1005	FORMAT('*****BUCKLING HAS OCCURRED...MAX,NCIR,PLOAD*****')	RUNG 17
	1*****')	RUNG 18
1010	FORMAT(1X,2I5,2X,E15.8)	RUNG 19
1015	FORMAT(' PLOAD =')	RUNG 20
1020	FORMAT(10(2X,E11.5))	RUNG 21
1025	FORMAT(' EXPONENT OVERFLOW WILL PROBABLY OCCUR BECAUSE OF RUNGE-	RUNG21A
	1KUTTA STEP BEING TOO BIG.....CASE TERMINATED')	RUNG21B
	X=PRMT(1)	RUNG 22
	XMAX=PRMT(2)	RUNG 23
	H=PRMT(3)	RUNG 24
	N=2*ISIZE	RUNG 25
	PNX=PLOAD*RSHEL/(HSHEL*HSHEL*ESHEL)	RUNG 26
	WRITE(6,1015)	RUNG 27
	WRITE(6,1000)PNX	RUNG 28
10	CALL FCT(X,Y,DERY)	RUNG 29
	DO 22 J=1,N	RUNG 30
	SAVEY(J)=Y(J)	RUNG 31
	PHI(J)=DERY(J)	RUNG 32
22	Y(J)=SAVEY(J)+0.5*H*DERY(J)	RUNG 33
	X=X+0.5*H	RUNG 34

	CALL FCT(X,Y,DERY)	RUNG 35
	DO 33 J=1,N	RUNG 36
	PHI(J)=PHI(J)+2.0*DERY(J)	RUNG 37
33	Y(J)=SAVEY(J)+0.5*H*DERY(J)	RUNG 38
	CALL FCT(X,Y,DERY)	RUNG 39
	DO 44 J=1,N	RUNG 40
	PHI(J)=PHI(J)+2.0*DERY(J)	RUNG 41
44	Y(J)=SAVEY(J)+H*DERY(J)	RUNG 42
	X=X+0.5*H	RUNG 43
	CALL FCT(X,Y,DERY)	RUNG 44
	DO 55 J=1,N	RUNG 45
55	Y(J)=SAVEY(J)+(PHI(J)+DERY(J))*H/6.0	RUNG 46
	N9=N-1	RUNG 47
	WRITE(6,1020)X,(Y(J),J=1,N9,2)	RUNG 48
	IF(ABS(Y(1))-0.5)56,57,57	RUNG 49
56	IF (X-XMAX)10,60,60	RUNG49A
57	WRITE(6,1025)	RUNG49B
	NDOT=1	RUNG49C
	GO TO 80	RUNG49D
60	IF(Y(1)-0.001)80,70,70	RUNG 50
70	WRITE(6,1005)	RUNG 51
	WRITE(6,1010)MAX,NCIR,PNX	RUNG 52
80	RETURN	RUNG 54
	END	RUNG 55

	SUBROUTINE FCT(X,Y,DERY)	FNCT 1
C		FNCT 2
C	THIS SUBROUTINE CONTAINS NO READ AND WRITE STATEMENTS.	FNCT 3
C		FNCT 4
C	THE DIMENSION SIZE FOR THE NEXT STATEMENT MUST BE EQUAL TO OR	FNCT 5
C	GREATER THAN 2*ISIZE, WHERE ISIZE=ISTAR*JSTAR	FNCT 6
C		FNCT 7
	DIMENSION Y(10),DERY(10),A(10,10),R(10),T(10),Z(10)	FNCT 8
C		FNCT 9
C	THE DIMENSION SIZE FOR C(II,NN) MUST BE EQUAL TO OR GREATER	FNCT 10
C	THAN 2*ISIZE FOR THE FIRST SUBSCRIPT AND EQUAL TO OR GREATER	FNCT 11
C	THAN 4*ISIZE FOR THE SECOND SUBSCRIPT.	FNCT 12
C	THE DIMENSION SIZE FOR WCOF(II,NN) MUST BE EQUAL TO OR GREATER	FNCT 13
C	THAN ISIZE FOR THE FIRST SUBSCRIPT AND EQUAL TO OR GREATER THAN	FNCT 14
C	8*ISIZE FOR THE SECOND SUBSCRIPT.	FNCT 15
C		FNCT 16
	COMMON WCOF(5,40),C(10,20),ISTAR,JSTAR,MAX,NCIR,ESHE3,HSHEL,PNU,	FNCT 17
	1NRNG,ARING,ERING,ZRING,MSTR,ASTR,ESTR,ZSTR,ISIZE,PI,DRING,DSTR,	FNCT 18
	2FN1,FN2,FM1,FM2,SHDEN,RGDEN,STDEN,RGMI,STMI,GRING,GSTR,RGJ,STJ,	FNCT 19
	3PLOAD,RSHEL,SHLT,IFLAG,NDOT	FNCT 20
C		FNCT 21
C	PLACE U AND V COEFFICIENTS INTO THE GAUSS-JORDAN MATRIX A(N)	FNCT 22
C		FNCT 23
	MARK=0	FNCT 24
	NSIZE=2*ISIZE	FNCT 25
	DO 16 J=1,NSIZE	FNCT 26
	DO 15 I=1,NSIZE	FNCT 27
15	A(I,J)=C(I,J)	FNCT 28
16	CONTINUE	FNCT 29
C		FNCT 30
C	PLACE PROPER U AND V COEFFICIENTS INTO R(N) MATRIX	FNCT 31
C		FNCT 32
	DO 19 K=1,NSIZE	FNCT 33
19	R(K)=0.00	FNCT 34
	DO 21 K=1,NSIZE	FNCT 35
	DO 20 J=1,ISIZE	FNCT 36

	J1=J+2*ISIZE	FNCT 37
	J2=J+3*ISIZE	FNCT 38
20	R(K)=R(K)+C(K,J1)*Y(2*J-1)+C(K,J2)*Y(2*J-1)*Y(2*J-1)	FNCT 39
21	CONTINUE	FNCT 40
C		FNCT 41
C	CHANGE SIGN OF R(I) MATRIX	FNCT 42
C		FNCT 43
	DO 35 I=1,NSIZE	FNCT 44
35	R(I)=-R(I)	FNCT 45
22	N=NSIZE	FNCT 46
C		FNCT 47
C	SOLVES N SIMULTANEOUS LINEAR ALGEBRAIC EQUATIONS BY A GAUSS-JORDAN	FNCT 48
C	REDUCTION. A IS THE COEFFICIENT MATRIX, R IS THE CONSTANT	FNCT 49
C	VECTOR. A IS DESTROYED AND R IS REPLACED BY THE SOLUTION	FNCT 50
	DO 11 J=1,N	FNCT 51
11	T(J)=1.0	FNCT 52
	M=N-1	FNCT 60
	DO 1 J=1,M	FNCT 61
	AD=A(J,J)	FNCT 62
	DO 3 K=J,N	FNCT 63
3	A(J,K)=A(J,K)/AD	FNCT 64
	R(J)=R(J)/AD	FNCT 65
	L=N-J	FNCT 66
	NN=0	FNCT 67
	DO 1 I=1,L	FNCT 68
	NN=J+I	FNCT 69
	DA=A(NN,J)	FNCT 70
	DO 2 K=J,N	FNCT 71
2	A(NN,K)=A(NN,K)-A(J,K)*DA	FNCT 72
1	R(NN)=R(NN)-R(J)*DA	FNCT 73
	DO 4 J=1,N	FNCT 74
	K=N+1-J	FNCT 75
	S=0.0	FNCT 76
	IF(K-N)9,4,9	FNCT 77
9	L=K+1	FNCT 78
	DO 5 I=L,N	FNCT 79

5	S=A(K,I)*T(I)+S	FNCT 80
4	T(K)=(R(K)-S)/A(K,K)	FNCT 81
	DO 6 J=1,N	FNCT 82
6	R(J)=T(J)	FNCT 83
C		FNCT 84
	IF(MARK-1)23,30,30	FNCT 85
C		FNCT 86
C	SET A(N,N) EQUAL TO ZERO	FNCT 87
C		FNCT 88
23	DO 32 I=1,NSIZE	FNCT 89
	DO 33 J=1,NSIZE	FNCT 90
33	A(I,J)=0.00	FNCT 91
32	CONTINUE	FNCT 92
C		FNCT 93
C	MAKE A(N,N) INTO AN IDENTITY MATRIX	FNCT 94
C		FNCT 95
	DO 34 IJ=1,NSIZE	FNCT 96
34	A(IJ,IJ)=1.00	FNCT 97
C		FNCT 98
C	PLACE W COEFFICIENTS INTO GAUSS-JORDAN MATRIX A(N)	FNCT 99
C		FNCT100
	DO 25 J=1,ISIZE	FNCT101
	DO 24 I=1,ISIZE	FNCT102
	JN=J+7*ISIZE	FNCT103
24	A(2*I,2*J)=WCOF(I,JN)	FNCT104
25	CONTINUE	FNCT105
C		FNCT106
C	SET Z(N)=ZERO	FNCT107
C		FNCT108
	DO 26 I=1,NSIZE	FNCT109
26	Z(I)=0.00	FNCT110
C		FNCT111
C	PLACE PROPER W COEFFICIENTS INTO R(N)	FNCT112
C		FNCT113
	DO 28 K=1,ISIZE	FNCT114
	Z(2*K-1)=Y(2*K)	FNCT115

```

DO 27 J=1,ISIZE
J1=J+ISIZE
J2=J+2*ISIZE
J3=J+3*ISIZE
J4=J+4*ISIZE
J5=J+5*ISIZE
J6=J+6*ISIZE
27 Z(2*K)=Z(2*K)+WCDF(K,J)*R(J)+WCDF(K,J1)*R(J1)
1+WCDF(K,J2)*Y(2*J-1)+WCDF(K,J3)*Y(2*J-1)*Y(2*J-1)
2+WCDF(K,J4)*Y(2*J-1)**3+WCDF(K,J5)*R(J)*Y(2*J-1)
3+WCDF(K,J6)*R(J1)*Y(2*J-1)
28 CONTINUE
C
C SET R(N)=Z(N)
C
C DO 29 I=1,NSIZE
29 R(I)=Z(I)
MARK =1
C
C CHANGE SIGN OF R(2*K)
C
C DO 36 K=1,ISIZE
36 R(2*K)=-R(2*K)
GO TO 22
C
C PLACE R(N) RESULTS IN DERY
C
C DO 31 I=1,NSIZE
30 DERY(I)=R(I)
31 RETURN
END

```

```

FNCT116
FNCT117
FNCT118
FNCT119
FNCT120
FNCT121
FNCT122
FNCT123
FNCT124
FNCT125
FNCT126
FNCT127
FNCT128
FNCT129
FNCT130
FNCT131
FNCT132
FNCT133
FNCT134
FNCT135
FNCT136
FNCT137
FNCT138
FNCT139
FNCT140
FNCT141
FNCT142
FNCT143
FNCT144
FNCT145
FNCT146

```